

STATE OF CALIFORNIA DEPARTMENT OF TRANSPORTATION
TECHNICAL REPORT DOCUMENTATION PAGE
 TR0003 (REV. 10/98)

1. REPORT NUMBER CA12-1741	2. GOVERNMENT ASSOCIATION NUMBER	3. RECIPIENT'S CATALOG NUMBER
4. TITLE AND SUBTITLE WATER JETTING FOR THE MITIGATION OF DEFECTS IN DRILLED SHAFTS - A LABORATORY INVESTIGATION OF JETTING EFFECTIVENESS IN DIFFERENT DELETERIOUS MATERIALS	5. REPORT DATE September 2012	
	6. PERFORMING ORGANIZATION CODE	
7. AUTHOR(S) Gregg L. Fiegel, Daniel C. Jansen, Jay S. DeNatale	8. PERFORMING ORGANIZATION REPORT NO. CA12-1741	
9. PERFORMING ORGANIZATION NAME AND ADDRESS Department of Civil and Environmental Engineering California Polytechnic State University San Luis Obispo, CA 93407-0353	10. WORK UNIT NUMBER	
	11. CONTRACT OR GRANT NUMBER Task ID 1741	
12. SPONSORING AGENCY AND ADDRESS California Department of Transportation Division of Research & Innovation Sacramento, CA 95814	13. TYPE OF REPORT AND PERIOD COVERED Final Report	
	14. SPONSORING AGENCY CODE	

15. SUPPLEMENTAL NOTES

16. ABSTRACT

Presented in this report are results of a laboratory investigation designed to examine the effectiveness of water jetting as a means for mitigating defects in drilled shaft foundations. The primary objective of this research was to establish an empirical relationship between water jetting pressure and the removal of deleterious materials from drilled shaft defects (e.g. low strength concrete, slurry mix concrete, semi-cemented sand, loose soil, etc.). The principal research activities conducted as part of this study included: a search of the existing literature and interviews with foundation contractors to identify the current state of water jet technology; and, a parametric laboratory investigation to examine water jetting effectiveness in relation to jetting pressure, standoff distance, jetting time, and characteristics of deleterious materials.

17. KEY WORDS Water jetting, drilled shafts, bridge foundations,	18. DISTRIBUTION STATEMENT No restrictions. This document is available to the public through the National Technical Information Service, Springfield, VA 22161	
19. SECURITY CLASSIFICATION (of this report) Unclassified	20. NUMBER OF PAGES 93	21. PRICE



Division of Research
& Innovation

WATER JETTING FOR THE MITIGATION OF DEFECTS IN DRILLED SHAFTS - A LABORATORY INVESTIGATION OF JETTING EFFECTIVENESS IN DIFFERENT DELETERIOUS MATERIALS

Final Report



DISCLAIMER STATEMENT

This document is disseminated in the interest of information exchange. The contents of this report reflect the views of the authors who are responsible for the facts and accuracy of the data presented herein. The contents do not necessarily reflect the official views or policies of the State of California or the Federal Highway Administration. This publication does not constitute a standard, specification or regulation. This report does not constitute an endorsement by the Department of any product described herein.

For individuals with sensory disabilities, this document is available in Braille, large print, audiocassette, or compact disk. To obtain a copy of this document in one of these alternate formats, please contact: the Division of Research and Innovation, MS-83, California Department of Transportation, P.O. Box 942873, Sacramento, CA 94273-0001.

**WATER JETTING FOR THE MITIGATION OF DEFECTS IN DRILLED SHAFTS -
A LABORATORY INVESTIGATION OF JETTING EFFECTIVENESS IN
DIFFERENT DELETERIOUS MATERIALS**

Submitted to

California Department of Transportation
Attn: Douglas Brittsan, Branch Chief
Office of Geotechnical Support
Foundation Testing Branch
5900 Folsom Blvd
Sacramento, CA 95819

Submitted by:

Gregg L. Fiegel, PhD, PE, Professor
Daniel C. Jansen, PhD, PE, Professor
Jay S. DeNatale, PhD, PE, Professor Emeritus

Department of Civil and Environmental Engineering
California Polytechnic State University
San Luis Obispo, CA 93407-0353

September 2012

ACKNOWLEDGMENTS

The following report summarizes the results of a study titled "Water Jetting for the Mitigation of Defects in Drilled Shafts - A Laboratory Investigation of Jetting Effectiveness in Different Deleterious Materials." Researchers from the Department of Civil and Environmental Engineering at California Polytechnic State University, San Luis Obispo completed the study in cooperation with the California Department of Transportation (Caltrans) and the West Coast Chapter of the International Association of Foundation Drilling (ADSC). The authors appreciate the assistance, insight, and technical support provided by members of the Foundation Testing Branch and the Office of Geotechnical Support at Caltrans. The authors also gratefully acknowledge the assistance of the Case Pacific Company. Case Pacific employees Will Smith, Randy Verdell, and Matt Schlotterbeck were especially helpful in providing insight into the practice of water jetting. Finally, the authors also appreciate the support provided by the following graduate and undergraduate student researchers who worked on this project: Joseph Heavin, Matthew Schaffer, Clayton Proto, Roshani Patel, Stefanie Gille, and Jonathan Lund. Each of these students provided valuable assistance during the laboratory investigation and helped to prepare several of the written sections and figures included in this final report.

DISCLAIMER

The following report is based upon work supported by Caltrans (Contract No. 65A0299) and the West Coast Chapter of the International Association of Foundation Drilling (ADSC). Any opinions, findings, conclusions, or recommendations expressed in this report are those of the authors and do not necessarily reflect the views of these organizations. Please note that the following report does not constitute a standard, specification, or regulation.

ABSTRACT

Presented in this report are results of a laboratory investigation designed to examine the effectiveness of water jetting as a means for mitigating defects in drilled shaft foundations. The primary objective of this research was to establish an empirical relationship between water jetting pressure and the removal of deleterious materials from drilled shaft defects (e.g. low strength concrete, slurry mix concrete, semi-cemented sand, loose soil, etc.). The principal research activities conducted as part of this study included: a search of the existing literature and interviews with foundation contractors to identify the current state of water jet technology; and, a parametric laboratory investigation to examine water jetting effectiveness in relation to jetting pressure, standoff distance, jetting time, and characteristics of deleterious materials. The following report summarizes the research approach, results, and conclusions.

The experimental work consisted primarily of water blasting thirty (30) test specimens of different materials using rotary jets, nozzles, pumping equipment, and testing procedures currently employed in construction practice. The tested materials included concrete, low strength concrete, slurry mix concrete, sand-cement grout, and bentonite-cement grout. During testing, erosion levels and rates were measured as a function of jetting pressure and standoff distance for specimens with compressive strengths ranging between 5 psi (bentonite-cement grout) and 6,600 psi (concrete). The results of these experiments were consistent with one another and generally repeatable. Erosion levels, erosion rates, and water jetting effectiveness were found to correlate primarily with material compressive strength, standoff distance, and jetting pressure. Using typical water jetting equipment and jetting pressures between 10,000 and 11,000 pounds per square inch, significant erosion was observed up to 13 inches from the water jet for the weakest material specimens. Materials with the lowest compressive strengths exhibited the greatest tendency to erode.

When examining jetted surfaces in the concrete samples, it was observed that larger aggregates often created small shadow zones where jetting effectiveness was reduced and binder materials were less easily eroded. These shadow zones have been observed adjacent to reinforcing steel bars during water jetting of drilled shafts in the field. In experiments conducted as part of this study, shadow zones of deleterious material were observed behind reinforcing steel bars. Rebar were found to influence erosion levels and water jetting effectiveness by interfering with the jet path. The most pronounced shadow effects occurred behind bars with larger diameters and behind longitudinal-transverse bar arrangements with tight spacings. Shadow effects were more prominent the farther the rebar were positioned from the water jet.

TABLE OF CONTENTS

CHAPTER	PAGE
1. OVERVIEW	1
1.1 INTRODUCTION	1
1.2 RESEARCH OBJECTIVES	1
1.3 REPORT ORGANIZATION	2
2. BACKGROUND	3
2.1 ANOMALIES IN DRILLED SHAFTS	3
2.2 ANOMALY DETECTION AND DEFECT ANALYSIS	3
2.2.1 Anomaly Detection Methods and Access Tubes	3
2.2.2 Anomaly and Defect Analysis	5
2.3 CASE HISTORIES OF DEFECTS IN DRILLED SHAFTS	6
2.3.1 Trabuco Creek Bridge	6
2.3.2 Muddy River Bridge	6
2.3.3 Thomes Creek Bridge	8
2.3.4 West Sylmar Overhead	9
2.3.5 Jacklin Road Undercrossing	10
2.3.5.1 <i>Observations of Core Sections</i>	12
2.3.5.2 <i>Strength Test Results of Core Samples</i>	13
2.4 MITIGATION OF DRILLED SHAFT DEFECTS USING WATER JETTING	15
2.4.1 Procedures and Equipment	15
2.4.2 Standard Mitigation Plan	19
2.4.2.1 <i>Plan A - Basic Repair</i>	19
2.4.2.2 <i>Plan B - Grout Repair</i>	20
3. PROJECT APPROACH	21
3.1 INTRODUCTION	21
3.2 LABORATORY TEST SPECIMENS	21
3.2.1 Ring Specimens	21
3.2.2 Cylindrical Specimens	24
3.2.3 Ring Specimens with Reinforcing Steel Bars	27
3.2.4 PVC Access Tube Specimens	31
3.3 LABORATORY WATER JETTING PROCEDURES	32
3.3.1 Equipment	32
3.3.2 Ring Sample Testing Procedure	34
3.3.3 Cylindrical Sample Testing Procedure	37
3.3.4 Ring Sample with Reinforcing Steel Bars Testing Procedure	39
3.3.5 PVC Access Tube Specimen Testing Procedure	39

TABLE OF CONTENTS (CONTINUED)

CHAPTER	PAGE
3.4 CONCRETE AND DELETERIOUS MATERIALS	40
3.4.1 Caltrans Practice	40
3.4.2 Deleterious Materials in Drilled Shafts	40
3.4.3 Material Mix Designs	41
3.4.3.1 Objectives	41
3.4.3.2 Low Strength Concrete (SCM)	42
3.4.3.3 Concrete (CON)	42
3.4.3.4 Slurry Mix Concrete (SMX)	43
3.4.3.5 Sand-Cement Grout (GRT)	43
3.4.3.6 Bentonite-Cement Grout (CLY)	44
3.4.4 Sample Preparation and Quality Control Testing	44
3.5 WATER JETTING TEST MATRIX	45
3.6 SAMPLES NOT WATER JETTED	45
4. TEST RESULTS	48
4.1 RING SAMPLES	48
4.1.1 Initial Ring Tests	48
4.1.2 Subsequent Ring Tests	52
4.1.2.1 General Observations	52
4.1.2.2 Test Results	54
4.1.3 Ring Tests with Reinforcing Steel Bars	60
4.2 CYLINDRICAL SAMPLES	66
4.3 WATER JETTING OF PVC ACCESS TUBES	70
4.4 SUMMARY OF WATER JETTING RESULTS	72
5. SUMMARY AND RECOMMENDATIONS	73
5.1 SUMMARY	73
5.2 PRINCIPAL FINDINGS	73
5.3 RECOMMENDATIONS FOR ADDITIONAL RESEARCH	75
REFERENCES	77
APPENDIX A - DATA SHEET FOR SELF-ROTARY SWIVEL WATER JET	79

LIST OF TABLES

TABLE	PAGE
Table 2.1 - Coring Results for Shaft 1 Repaired at the Muddy River Site (after Branagan et al. 2000)	7
Table 2.2 - Coring Results for Shaft 2 Repaired at the Muddy River Site (after Branagan et al. 2000)	7
Table 2.3 - Compressive Strength of Deleterious Materials at the Muddy River Site (after Branagan et al. 2000)	8
Table 2.4 - Compressive Strength of Deleterious Materials at Thomes Creek Bridge (Wahleithner 2009)	8
Table 2.5 - Splitting Tension Test Results for Jacklin Road Undercrossing	14
Table 2.6 - Cube Compression Test Results for Jacklin Road Undercrossing)	15
Table 3.1 - Ring Sample Test Approaches for Controlling Movement of the Water Jet in the Vertical Direction	35
Table 3.2 - General Description of Materials Tested during Water Jetting	41
Table 3.3 - Target Test Matrix for Water Jetting Investigation	42
Table 3.4 - Water Jetting Test Matrix and Summary	46
Table 3.5 - Summary of Ring and Cylindrical Samples Not Water Jetted	47
Table 4.1 - Final Erosion Distances for the Ring Samples	58
Table 4.2 - Final Effective Eroded Diameters for the Ring Samples	58
Table 4.3 - Average Shadow Heights for Test SCM-04	64
Table 4.4 - Average Shadow Heights for Test SCM-05	65
Table 4.5 -Example Results for Test Series CON-06, Standoff Distance Equal to 1.5 inches	67

LIST OF FIGURES

FIGURE	PAGE
Figure 2.1 - Spacing Requirements for Longitudinal Reinforcement and Inspection Access Tubing in Drilled Shafts (Caltrans, 2008)	4
Figure 2.2 - Quantifying Anomalies in Drilled Shafts using: (a) GGL Results; (b) GGL and CSL Results	5
Figure 2.3 - Photograph of a Concrete Core Sections Retrieved from the Thomes Creek Bridge Site	9
Figure 2.4 - Photograph of a Concrete Core Retrieved from Drilled Shaft #3 at the Jacklin Road Undercrossing	12
Figure 2.5 - Typical Water Jetting Process to Repair Defects in Drilled Shafts: (a) Introduce Water Jet; (b) Jet Anomaly; (c) Flush Cuttings and Inspect Void Space Left by Jetting; and (d) Grout Void Space	16
Figure 3.1 - Ring Samples used during Water Jetting: (a) Illustration of the Concept; (b) Construction Photo for 6- and 12-inch Diameter Samples	22
Figure 3.2 - Typical Ring Sample Mold: (a) Plan; (b) Elevation	23
Figure 3.3 - Illustration of a Typical Cylindrical Sample and Testing Concept	24
Figure 3.4 - Photograph of the Frame Apparatus used to Secure Cylindrical Test Cylinders	25
Figure 3.5 - Sketch of Test Frame and a Typical Cylindrical Specimen: (a) Plan; (b) Cross-Section A-A'	26
Figure 3.6 - Plan View of a 6-inch Inner Diameter Ring Sample with Discrete Longitudinal (Vertical) Bars	27
Figure 3.7 - Plan View of a 2-inch Inner Diameter Ring Sample Designed to Simulate a Section of a 3-foot Diameter Drilled Shaft (including #8 Longitudinal Reinforcement and #4 Transverse Reinforcement)	28
Figure 3.8 - Plan View of a 2-inch Inner Diameter Ring Sample Designed to Simulate a Section of a 6-foot Diameter Drilled Shaft (including #14 Longitudinal Reinforcement and #8 Transverse Reinforcement)	29
Figure 3.9 - Photograph of Ring Samples with Reinforcing Steel: (a) Discrete Longitudinal Bars; (b) Section of a 6-foot Diameter Drilled Shaft	30
Figure 3.10 - Sketch of Test Frame and Holes used to Mount PVC Specimens	31
Figure 3.11 - Photograph Showing the Water Jetting Test Equipment and Layout	32

LIST OF FIGURES (CONTINUED)

FIGURE	PAGE
Figure 3.12 -Photograph Showing the Self Rotary Water Jet and Nozzles	33
Figure 3.13 -Photograph Showing the Jet Collar Assembly and Cover Plate Attached to a Ring Sample during Testing	34
Figure 3.14 - Post-Test Photographs of 6-inch Diameter Ring Samples: (a) Jet Held Stationary; (b) Jet Cycled Up and Down	36
Figure 3.15 - Illustration of Erosion Measurements taken during Water Jetting: (a) Plan View; (b) Section View	37
Figure 3.16 - Example of an Eroded Cylindrical Sample after Water Jetting	38
Figure 3.17 - Erosion Measurement Locations for Ring Samples Cast with Reinforcing Steel Bars	39
Figure 4.1 - Post-Test Photograph of the 6-inch Diameter Ring Sample, SCM-01 Test Series; Erosion Measurement Locations Noted	49
Figure 4.2 - Average Erosion Depth with Minimum and Maximum Error Bars Measured for the SCM-01 Test Series	50
Figure 4.3 - Effective Eroded Diameter with Minimum and Maximum Error Bars Measured for the SCM-01 Test Series	51
Figure 4.4 - Photograph Showing Protected Binder Material and Shadowing Observed during Test Series SCM-01	53
Figure 4.5 - Average Erosion Measured for 6-inch I.D. Concrete Ring Samples	55
Figure 4.6 - Average Erosion Measured for 6-inch I.D. Ring Samples with Similar Compressive Strengths	56
Figure 4.7 - Average Erosion Measured for 6-inch I.D. Low Strength Concrete Ring Samples Subject to Stationary and Cyclic Jetting	57
Figure 4.8 - Average Effective Eroded Diameter for 6- and 12-inch I.D. Ring Samples	59
Figure 4.9 - Post-Test Photographs of Test SCM-04	60
Figure 4.10 - Post-Test Photographs of Test SCM-05	61
Figure 4.11 - Plan View Illustration of Shadow Effects Observed during Water Jetting of the SCM-04 and -05 Samples	62
Figure 4.12 - Average Erosion Measured during Tests SCM-04 and SCM-05	63

LIST OF FIGURES (CONTINUED)

FIGURE	PAGE
Figure 4.13 - Explanation of Shadow Height Measurements for Tests SCM-04 and SCM-05	64
Figure 4.14 - Cylinder Erosion Depth as a Function of Jetting Pressure and Standoff Distance for SCM-06 (compressive strength = 160 psi)	68
Figure 4.15 - Cylinder Erosion Depth as a Function of Jetting Pressure and Standoff Distance for CON-06 (compressive strength = 3,600 psi)	68
Figure 4.16 - Maximum Jetting Distance as a Function of Jetting Pressure for the 160 psi (SCM-06) and 3,600 psi (CON-06) Cylinder Tests	69
Figure 4.17 - Front View Post-Test Photographs of PVC Tubing	71
Figure 4.18 - Average Effective Eroded Diameter All Material Samples	72

CHAPTER 1

OVERVIEW

1.1 INTRODUCTION

Bridge foundation performance depends significantly upon the quality of construction. This is especially true for drilled shaft foundations installed in high groundwater conditions using slurry. It is estimated that approximately 20 percent of drilled shaft foundations constructed under these conditions have detectable anomalies (O'Neill and Sarhan 2004), where anomalies are identified by evaluating the homogeneity of concrete density using non-destructive testing methods (Liebich 2004). If an anomaly is detected within a constructed drilled shaft, the design engineer will determine its effect, if any, on foundation performance. In some cases, an anomaly will represent a defect that must be repaired in the field.

The current practice of many foundation contractors is to use grouting to repair small drilled shaft defects that are deeper than about ten feet below the ground surface. Grouting requires that the anomalous or deleterious material first be removed from the defective area with high-pressure water jetting, or water blasting, which scours out the deleterious material and creates a cavity for the subsequent grout. The water jetting process depends on the jet pressure used during the repair. If the applied jet pressure is too low, the deleterious material may not be completely removed. On the other hand, if the water pressure is too high, the structural integrity of "sound" concrete may be lessened, and/or excessive concrete beyond the defect may be removed. In addition, both jetting equipment and jetting technique play a role in the repair process.

Foundation contractors have worked to refine their water jetting repair procedures over the past decade. However, refinements have often been developed based on past field experiences and case histories rather than formal study, thereby leading to questions regarding method efficiency and performance. Indeed, recent investigations by Caltrans suggest that some previously accepted repair techniques are much less effective at mitigating defects than was initially believed (Liebich 2008; Liebich and Bonala 2007). Since Caltrans permits contractors to repair drilled shafts using water jetting and grouting, it is important to evaluate the effectiveness of this approach.

1.2 RESEARCH OBJECTIVES

The primary objective of this research is to establish an empirical relationship between water jetting pressure and the removal of deleterious materials from drilled shaft defects (e.g. low strength concrete, slurry mix concrete, semi-cemented sand, loose soil, etc.). The principal research activities

conducted as part of this study included: (1) a search of the existing literature and interviews with foundation contractors to identify the current state of water jet technology; and (2) a parametric laboratory investigation to examine water jetting effectiveness in relation to jetting pressure, standoff distance, jetting time, and characteristics of deleterious materials. The following report summarizes the research approach, results, and conclusions.

1.3 REPORT ORGANIZATION

Chapter 1 of the report provides an introduction to the project and lists the principal research objectives. Chapter 2 provides background information on the use of water jetting to mitigate defects in drilled shafts. Current procedures and equipment are described. In addition, a discussion is presented regarding the formation and detection of defects in drilled shafts. The characteristics of deleterious materials typically encountered in drilled shafts are described in relation to several case histories. Chapter 3 summarizes the approach taken by the research team to complete the experimental component of this investigation. The ring and cylindrical test specimens are described along with the testing equipment and protocols. A section describes the concrete and deleterious materials that the research team selected for use in this study. Methods used for sample preparation and quality control testing are detailed. Chapter 4 outlines and summarizes the test series completed as part of this research investigation. Test results are presented and analyzed. Water jetting effectiveness is assessed in this section of the report. The report concludes with Chapter 5, which includes a brief summary of the work performed, a discussion of the principal findings of the project, and recommendations for additional research.

CHAPTER 2

BACKGROUND

2.1 ANOMALIES IN DRILLED SHAFTS

Anomalies in drilled shafts (a.k.a. Cast-in-Drilled Hole (CIDH) piles) represent changes in the density homogeneity, which typically indicate contaminated concrete or a reduction in cross-sectional area. Anomalies may result from design deficiencies (O'Neill 2005). For example, if insufficient spacing is provided between reinforcing steel bars, then concrete flow to the outside of the drilled shaft can be impeded during placement. More often, however, anomalies occur due to difficult site conditions and/or problems during construction. For drilled shafts constructed in wet conditions under slurry, problems during drilling, concrete placement, and casing removal commonly lead to anomalies (O'Neill 2005).

Anomalous materials are deleterious materials found within the drilled shaft that were not planned as part of the original design. Examples of commonly occurring deleterious materials include low strength concrete, slurry mix concrete, semi-cemented material, soil-concrete mixtures, and soil (Liebich and Bonala 2007). When present, these deleterious materials may exist as thin bands or discontinuous, irregular shaped pockets. On occasion, an entire cross-section of a completed drilled shaft may be composed of deleterious material.

Various procedures exist for verifying the integrity of constructed drilled shafts and detecting anomalies (O'Neill and Reese 1999; Brown et al. 2010). Current practice by Caltrans commonly requires non-destructive evaluation (NDE) using gamma-gamma logging (GGL) and/or cross-hole sonic logging (CSL), each of which are considered downhole inspection methods (Liebich 2004; Likins et al. 2007). If an anomaly is confirmed within a drilled shaft, the designer must evaluate the effect the anomaly will have on design performance. If it is determined that an anomaly will have an adverse effect on performance, the anomaly is termed a defect and a repair is initiated.

2.2 ANOMALY DETECTION AND DEFECT ANALYSIS

2.2.1 Anomaly Detection Methods and Access Tubes

Prior to evaluating whether or not an anomaly will adversely affect a drilled shaft's performance, the designer must first assess the anomaly's approximate location, size, and shape. Caltrans currently employs gamma-gamma logging (GGL) and cross-hole sonic logging (CSL) to detect anomalies. GGL helps to verify the integrity of the concrete around the drilled shaft perimeter, and CSL helps to

verify the integrity of the concrete within the core (Skeen and Liebich 2004). Details regarding Caltrans' standards and procedures for non-destructive evaluation of drilled shafts are available in the literature and are not discussed within this report. Caltrans established a standard protocol for ascertaining the homogeneity of concrete density for the evaluation of construction of CIDH piles (Caltrans 2005).

Caltrans checks all wet constructed drilled shafts with at least one form of NDE (Liebich, 2004). To allow GGL and CSL instrumentation to travel up and down along the length of the drilled shaft, the foundation contractor must cast 2-inch inside diameter Schedule 40 PVC access tubes within the concrete. Caltrans requires a minimum of two access tubes per drilled shaft. When access tubes are required, the diameter of the drilled shaft must be at least 24 inches (Caltrans 2008).

Access tubes are placed around the perimeter of the drilled shaft and inside the outermost spiral or hoop steel reinforcement. A minimum 3-inch clear spacing is provided between the access tubes and adjacent vertical steel reinforcement, as noted on Figure 2.1. The maximum center-to-center spacing between adjacent access tubes is 33 inches as measured along an effective diameter passing through the inspection tube centers (Caltrans 2008). For accurate results, Caltrans specifies that the tubes be kept parallel to the axis of the drilled shaft and as vertical as possible during construction.

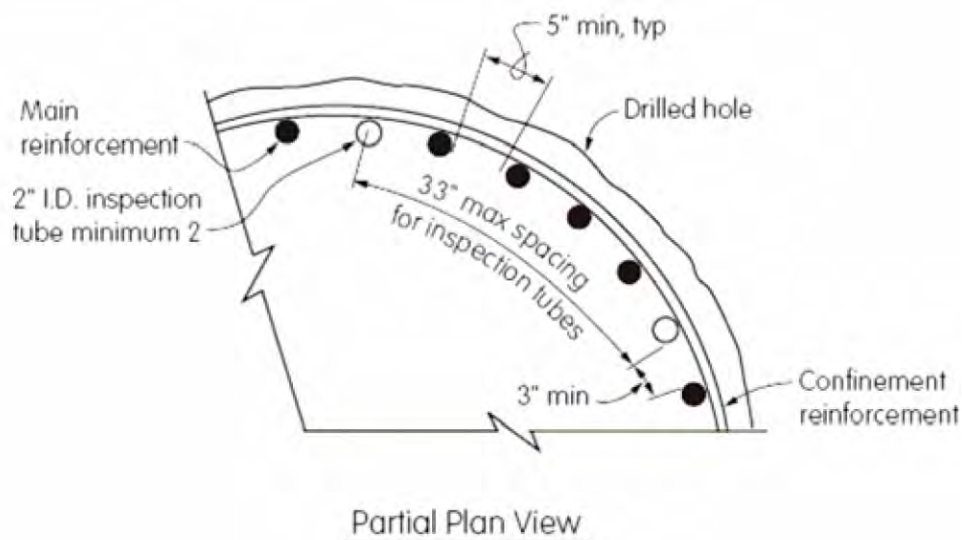


Figure 2.1 - Spacing Requirements for Longitudinal Reinforcement and Inspection Access Tubing in Drilled Shafts (Caltrans, 2008)

2.2.2 Anomaly and Defect Analysis

If an anomaly is detected during GGL, the designer will use the relative sample method to approximate a maximum affected cross section. For example, if an anomaly is positively detected in two of eight inspection tubes, the engineer assumes that 2/8 (or 25 percent) of the cross-section is compromised, as illustrated on Figure 2.2(a). When GGL and CSL testing are combined, the two methods can provide a comprehensive means for detecting and quantifying anomalies within drilled shafts. Figure 2.2(b) illustrates how the size of an anomaly can be more accurately estimated when combining positive test results from GGL and CSL. It is noted that the vertical extent of anomaly can be difficult to determine using these methods. Further, the transition between deleterious materials and uncontaminated (i.e. "good") concrete will not necessarily be distinct.

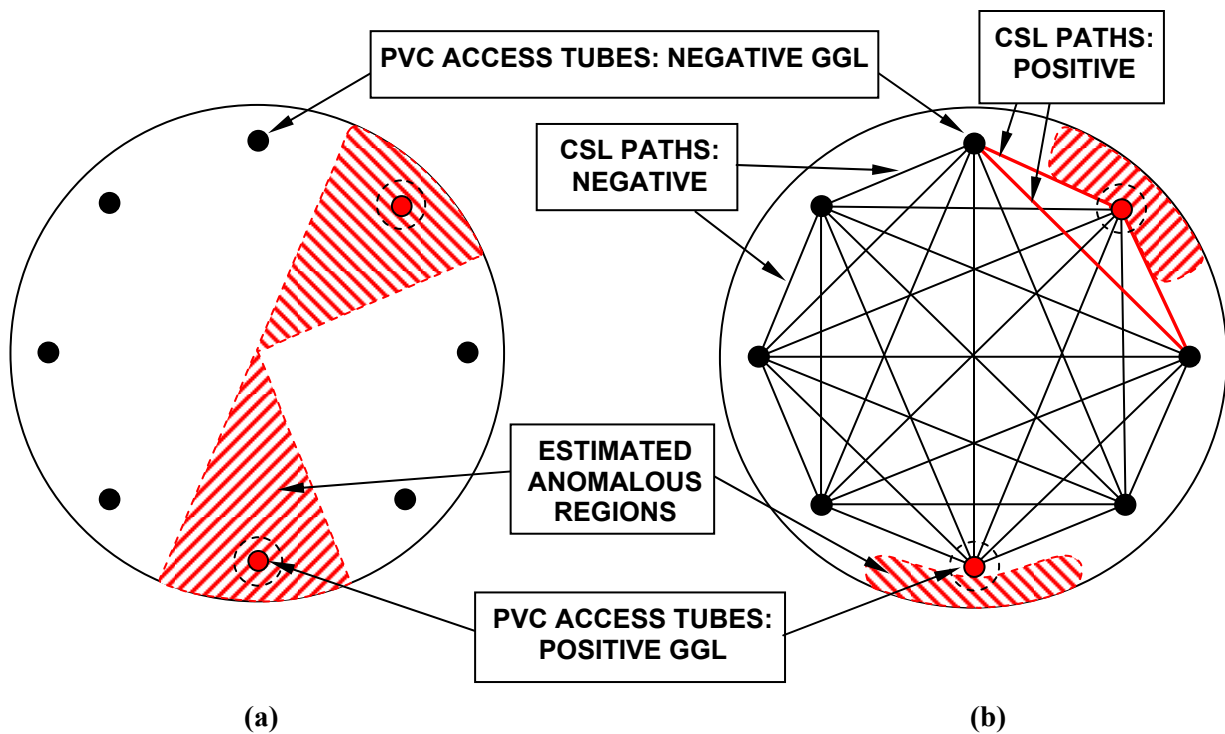


Figure 2.2 - Quantifying Anomalies in Drilled Shafts using: (a) GGL Results; (b) GGL and CSL Results

After the NDE establishes the size and location of the anomaly, the designer then determines whether or not the anomaly constitutes a defect requiring repair. Defects are defined as anomalies that compromise a drilled shaft's structural, geotechnical, or corrosive performance (Skeen and Liebich 2004). Typically, an anomaly presents a structural concern if it is located within a shaft's critical zone of moment, or if it affects a large portion of the cross-section. Geotechnical concerns arise if the detected anomaly is located on the shaft exterior at a depth originally designed to provide

frictional capacity. In addition, an anomaly at or near the tip of the drilled shaft can reduce bearing capacity and potentially affect geotechnical performance. The potential for corrosion is often a concern when the anomaly is located on the shaft exterior and above the water table. Since foundation contractors often use water jetting to repair geotechnical, corrosive, or small structural defects, accurate NDE identification and characterization of anomalies is imperative for utilizing water jetting in a repair. Skeen and Liebich (2004) provide a more detailed discussion of drilled shaft defect identification and mitigation.

2.3 CASE HISTORIES OF DEFECTS IN DRILLED SHAFTS

Case histories of defects in drilled shafts are described in the literature, providing general information on the size and shape of defects encountered in practice. The case histories also provide some insight into the types of deleterious materials found in drilled shaft anomalies. Several researchers have cored through detected anomalies and subsequently tested the core specimens for strength and other material properties. The following section summarizes the results of several case histories with focus on properties measured for deleterious materials.

2.3.1 Trabuco Creek Bridge

Skeen and Liebich (2004) describe a bridge widening project that required the installation of 13-foot diameter drilled shafts approximately 62 feet deep. For one of the drilled shafts, NDE revealed a defect located primarily on the shaft exterior. An attempt was made to repair the defect using grouting. When this method failed, Caltrans mandated an unearthing repair of the defect. Excavation performed to a depth of 21 feet determined the defect to be approximately 2 feet tall, 1 foot thick, and 3 feet wide. Investigation of the defect itself showed that the deleterious materials consisted primarily a sandy soil with a 3-inch lens of clay. The investigators did not measure any specific engineering properties for the deleterious materials.

2.3.2 Muddy River Bridge

Branagan et al. (2000) describe the construction, testing, and repair of drilled shafts designed to support a 188-foot, 2-span bridge over the Muddy River in Overton, Nevada. CSL detected anomalous material in a pair of 7-foot diameter, 68-foot deep drilled shafts located near the center of the bridge span. Contractors originally constructed the shafts, designated Shaft 1 and Shaft 2, using 8-foot diameter steel casings to a depth of 20 feet. The contractor attempted to stabilize the holes below 20 feet using a bentonite slurry; however, after some difficulty the contractor elected to place a

Portland cement slurry and re-drill the shafts a day later. The paper states that "construction observations made during concrete placement raised questions regarding shaft integrity."

CSL testing of Shafts 1 and 2 revealed multiple zones of anomalous material, and subsequent cores largely confirmed these findings. Branagan et al. (2000) state that the cores of the anomalous zones were consistent with defects caused by soil and water intrusion into the shaft. Coring results for both shafts are provided in Tables 2.1 and 2.2.

Table 2.1 - Coring Results for Shaft 1 Repaired at the Muddy River Site (after Branagan et al. 2000)

Depth (ft)	Material Description
0 - 6	Good Concrete
6 - 6.5	Poor Concrete
6.5 - 8.5	Loose Aggregate (poor recovery)
8.5 - 9.5	Poor Concrete
9.5 - 10	Loose Aggregate
10 - 66	Good Concrete
66 - 79*	Extremely Soft Sandy Clay to Clayey Sand with concrete fragments
79 - 80	Native Lean Clay: trace sand, very stiff, reddish-brown, moist

* - The planned tip elevation equaled 68 feet

Table 2.2 - Coring Results for Shaft 2 Repaired at the Muddy River Site (after Branagan et al. 2000)

Depth (ft)	Material Description
0 - 3	Good Concrete
3 - 5	Void
5 - 9.5	Good Concrete
9.5 - 10	Sand with Cement
10 - 13.5	Poor concrete
13.5 - 16	Poor, but better concrete; possibly slurry mixed
16 - 50	Good Concrete
50 - 52	Poor Concrete
52 - 66	Sandy Gravel: native soils, cement, and coarse and fine aggregate; medium dense to dense, light brown
66 - 69*	Gravelly Sand with Cement: some native soil, medium dense
69 - 77	Good Concrete, below tip elevation
77 - 80	Native Lean Clay: trace sand, very stiff, reddish-brown, moist

* - The planned tip elevation equaled 68 feet

Branagan et al. (2000) also performed unconfined compression tests on "poor concrete" core specimens extracted from Shaft 2. The results of these tests are summarized in Table 2.3. The design strength of the concrete was 4,000 pounds per square inch (psi). As shown in Table 2.3, measured compressive strengths for the deleterious materials were less than half of the design value for the concrete shaft.

Table 2.3 - Compressive Strength of Deleterious Materials at the Muddy River Site (after Branagan et al. 2000)

Depth (ft)	Height (in)	Area (in ²)	Compressive Strength (psi)	CSL Wave Velocity (ft/sec)
10.5 - 11.0	6	4.23	350	Lost signal
12.0 - 12.5	6	4.49	1,150	5,800
13.5 - 14.0	6	4.49	1,710	6,800

2.3.3 Thomes Creek Bridge

Caltrans recently replaced the Thomes Creek Bridge on Interstate 5 near Corning, California. After the construction of the bridge foundation, Caltrans detected several anomalies within an 8-foot diameter drilled shaft (Wahleithner 2009). GGL of the drilled shaft showed the potential presence of deleterious material at depths of approximately 6.5, 69, and 130 feet. GGL conducted in all of the inspection tubes detected an anomaly between the depths of 69 and 82 feet. In addition, all of the tested CSL tube-pair combinations in the same depth region detected an anomaly. To supplement the non-destructive evaluation, Caltrans retrieved and tested 3.33 inch diameter cores from various depths. Compressive strengths for several cores are summarized in Table 2.4. The design strength of the concrete was 4,000 pounds per square inch (psi).

Table 2.4 - Compressive Strength of Deleterious Materials at Thomes Creek Bridge (Wahleithner 2009)

Core Number	Depth (ft)	Compressive Strength (psi)
34 A	69.2	4,750
34 B	70.5	4,340
37	73.5	1,380
41	75.5	1,250
42	76.1	680

Shown on Figure 2.3 is a photograph of several core sections taken from the Thomes Creek drilled shaft. Core numbers corresponding to those summarized in Table 2.4 are noted on the photograph. The photograph shows that the core was significantly fractured in the area of the detected anomaly. Inspection of these core sections showed that the anomalous materials contained significantly less coarse aggregate than the sound concrete.

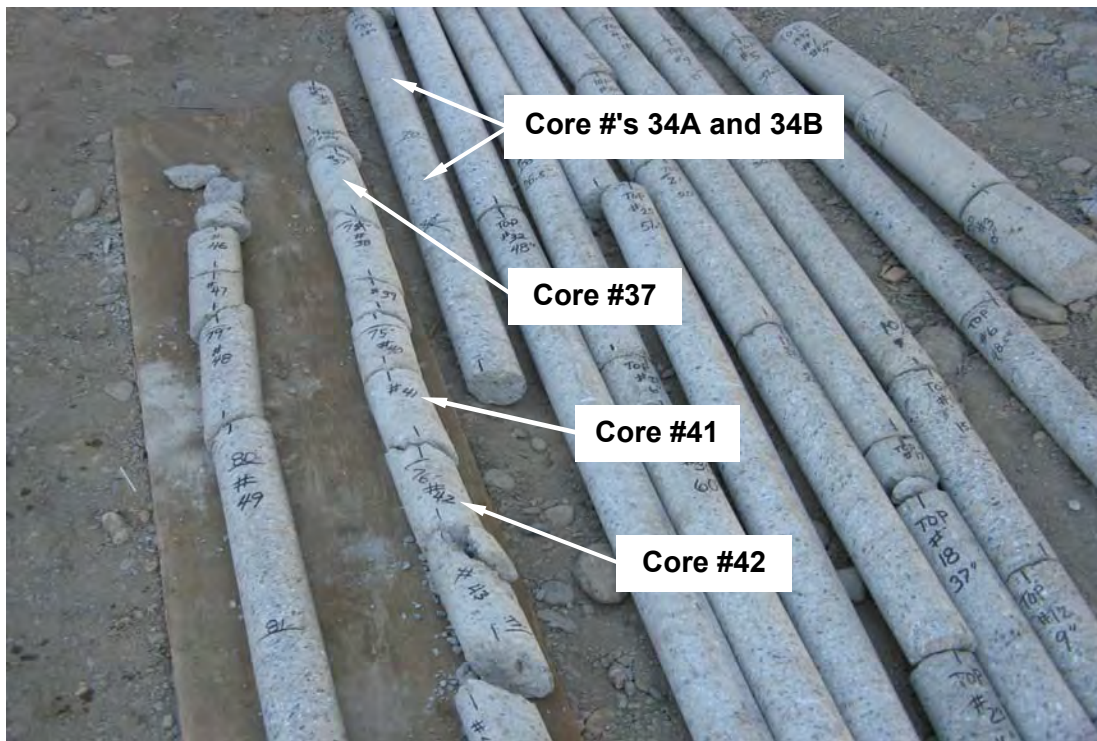


Figure 2.3 - Photograph of a Concrete Core Sections Retrieved from the Thomes Creek Bridge Site (photo provided by Jason Wahleithner)

2.3.4 West Sylmar Overhead

Construction on the HOV Connector Project from Interstate 5 to California State Route 14 near Santa Clarita began in July of 2008. As a part of this project, contractors installed drilled shafts at the West Sylmar Overhead. After construction, Caltrans detected foundation anomalies in one of the drilled shafts, and the drilled shaft required repair before being put into service. The contractor constructed the drilled shaft with 8.5-foot diameter permanent steel casing and an 8-foot drilled rock socket. The total length of the drilled shaft was approximately 80 feet. The completed shaft included eight PVC inspection tubes.

GGL detected two separate anomalies requiring repair (Caltrans 2009). These defects were located at depths of approximately 1 and 20 feet below the ground surface. Following these findings, a contractor performed CSL on all 28 tube-pair combinations. By combining results from both tests, Caltrans developed a three dimensional profile of the anomalies for analysis. Anomaly A-A, the shallowest of the four detected anomalies, extended from a depth of about 1.3 to 4 feet. GGL in this region detected the anomaly through five of eight inspection holes. Due to debonding of the access tubes to a depth of 10 feet, CSL could not determine concrete integrity over this interval. Therefore, Caltrans concluded from the GGL results that the anomaly affected a maximum of 63 percent of the shaft cross-section.

Anomaly B-B occupied a region of the shaft from a depth of 19.4 to 21 feet. GGL detected this anomaly in five of eight inspection tubes, and CSL detected anomalous material between three separate tube pairs. Based on these results, Caltrans concluded that a maximum 22 percent of the cross-section contained anomalies, with the affected area primarily outside of the steel reinforcing cage extending around approximately 60 percent of the drilled shaft perimeter.

Cores were not retrieved as part of this case history, so material properties for the deleterious materials are not available. However, the case history does highlight the potential extent of anomalies encountered in the field. Caltrans eventually required the repair of anomalies A-A and B-B. The foundation contractor used water jetting followed by grouting to repair the defect at B-B. Additional access holes were drilled through the shaft between two of the access tube pairs to decrease water jetting distances and provide better coverage of the shaft cross-section requiring repair. For the defect at A-A, the foundation contractor unearthed the drilled shaft to a depth of 4 feet and removed the deleterious material (slurry mix concrete) using hand held chipping guns and a backhoe mounted 1,200-foot-pound breaker.

2.3.5 Jacklin Road Undercrossing

For this project, the foundation contractor installed multiple drilled shaft foundations during the HOV/SMART Lane widening of the Jacklin Road Undercrossing on Interstate 680 near Milpitas, California (Sykes 2009). After construction, Caltrans detected foundation defects in two of the seven installed drilled shafts and required that repairs be made before putting the foundations into service. This case history summary focuses on drilled shaft #3, a 2-foot diameter shaft that included two PVC access tubes. These tubes were affixed to the interior of the reinforcing steel cage approximately 15 inches apart.

GGL of the drilled shaft's two inspection tubes detected the presence of two separate anomalies. Anomaly A-A was detected between the depths of 8.5 and 9.5 feet, and anomaly B-B was detected between approximately 12 and 14.5 feet. The GGL tests indicated a decrease in bulk density of approximately 10 and 12.5 pounds per cubic foot at anomalies A-A and B-B, respectively. Since both inspection tubes detected the anomalies at both locations, Caltrans concluded that the anomalies could potentially affect the entire shaft cross-section at both locations A-A and B-B (Sykes 2009).

Caltrans requested the completion of CSL to confirm the results of the GGL. The results of CSL indicated a less compromised shaft than originally concluded from the GGL results alone. CSL test results showed that the wave velocity dropped 18 percent at a depth of about 9 feet (anomaly A-A), thereby indicating questionable material but not a serious flaw. At about 12 feet below the ground surface (anomaly B-B), the wave velocity only dropped 9 percent, which generally indicates acceptable material. Based on the GGL and CSL results, Caltrans eventually concluded that the two anomalies only affected concrete in the perimeter of the drilled shaft outside the inspection tubes, or about 64 percent of the shaft cross section.

To repair the drilled shaft, the foundation contractor cored a 13-inch diameter section from the center of the shaft to a depth of about 18.5 feet. After removal of the concrete section, the contractor installed an 11-inch O.D., 3-inch thick seamless steel tube from a depth of about 5 to 18 feet. Caltrans specified the steel tubing based on its ability to sustain both the axial and moment demands on the drilled shaft. The tube extended through both anomalous regions. The contractor used 4,000-psi grout to fill the cored section of drilled shaft.

The research team obtained a portion of the concrete core removed from the drilled shaft during its repair. Representatives from Cal Poly were not present at the project site when the core was taken. The core, approximately 7.5 inches in diameter, broke into sections between 4 and 36 inches long during the coring process. The foundation contractor marked depths (in feet) on the core sections to identify their original position within the drilled shaft. Multiple sections of the core were missing. Figure 2.4 presents a photograph of the core sections laid out in the laboratory. As noted on the figure, the core included sections between approximately 6.5 and 18 feet; the section between approximately 14 and 16.5 feet was missing. There were some concerns regarding the accuracy of the depth markings on the core sections. In particular, markings on adjacent core sections from a depth of approximately 9 feet suggested that these sections overlapped by about 3 inches. However, this was the only significant discrepancy noted.

As part of this investigation, the research team dissected the concrete core into 2-inch thick slices and 2- to 3-inch square cubes. The slices and cubes were inspected, logged, and eventually tested for

strength following the splitting tension (ASTM C496) and compression (ASTM C109) test standards, respectively. The time between the original retrieval of the core and its dissection was approximately 15 months. The core consisted of normal strength concrete originally designed for 4,000 psi compressive strength.

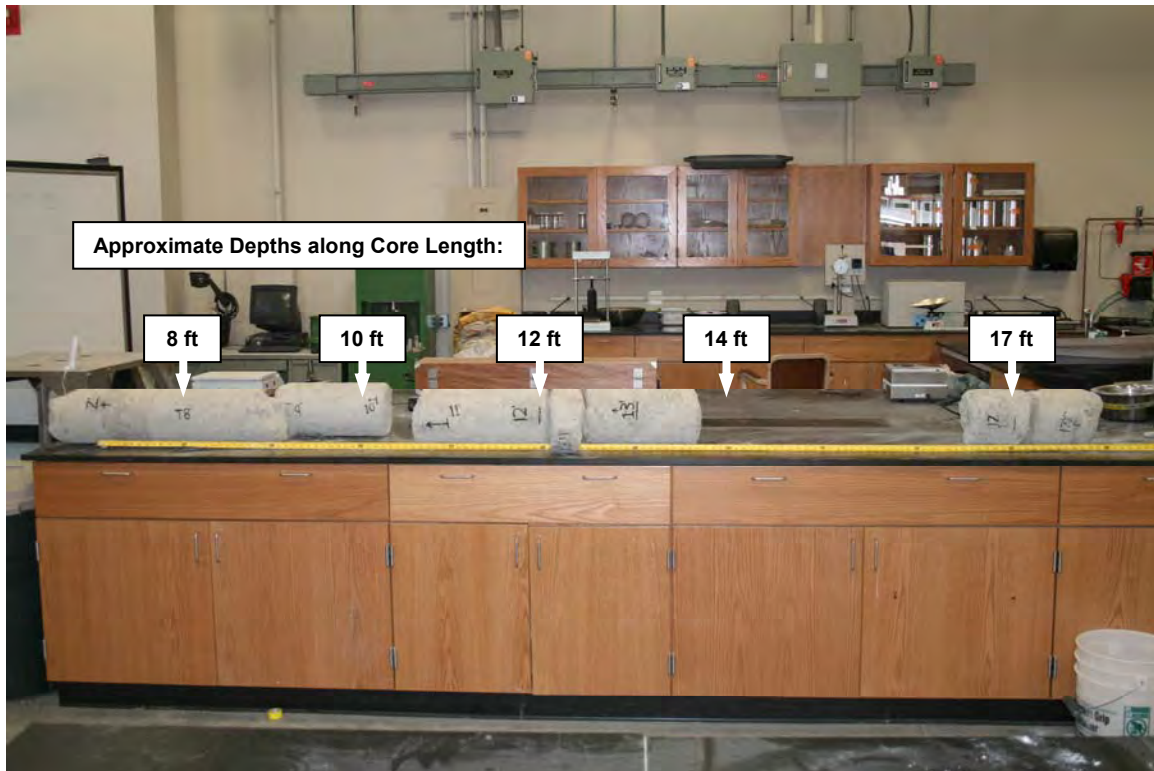


Figure 2.4 - Photograph of a Concrete Core Retrieved from Drilled Shaft #3 at the Jacklin Road Undercrossing

2.3.5.1 Observations of Core Sections

Cross-sections cut from the drilled shaft core revealed various types of anomalies. The most prevalent type of anomaly was an apparent mixture of concrete and bentonite slurry (i.e. slurry mix concrete). The resulting deleterious material was less dense, appeared visibly lighter in color, included cementitious material that loosely adhered to the aggregates, and had a higher porosity when compared to sound concrete. Differences in porosity were observed after the core samples were saturated: the anomalous materials remained moist much longer than the sound concrete materials.

The nature of the slurry mix concrete anomalies varied throughout the core length. In some locations, the anomaly existed as a thin layer with the boundary between sound concrete and deleterious

material difficult to distinguish. In other locations, the boundary between sound-concrete and deleterious material appeared well defined. However, even within these well-defined anomalous zones, the anomaly shape varied further. A cut made at the end of a core section (depth = 8.75 feet) revealed a well defined anomaly occupying a majority of the core cross section. The anomaly formed an irregularly shaped pocket within the core, extending in both the longitudinal and transverse directions. For another location in the core (depth = 12.5 feet), cut slices revealed transverse bands of deleterious material approximately 1-inch thick.

A second anomaly type observed in the core was a small zone of soil floating within concrete, which was visible within a core section taken from a depth of about 9 feet. The soil had a volume of approximately 2 to 3 cubic inches and was surrounded by slurry mix concrete. Visual and manual classification of the soil indicated it to be a fat clay. This finding suggests the clay was from the bentonite slurry, as opposed to a collapsed piece of the drill hole wall. This finding is consistent with O'Neill's (2005) assertion that small, un-hydrated balls of slurry can become entrapped in a drilled shaft due to insufficient mixing. O'Neill states that this type of anomaly is virtually impossible to detect, except by excavation and visual inspection. The investigation did not reveal additional anomalies of this type in the core.

A third anomaly observed in the core included regions of concrete containing large air voids. Aggregates held together with thin coats of cement binder characterized the concrete in these regions. Where observed, the voids occupied a region covering approximately 15 percent of the core cross-section. The voids extended through multiple slices over a longitudinal distance of approximately 6 inches.

It is noted that the ends of the intact cores nearest the missing core sections had a higher prevalence of the deleterious material, thus suggesting that some of the missing core sections consisted of relatively weak deleterious material. Intact weak material such as this would likely be difficult to retrieve during the coring process.

2.3.5.2 Strength Test Results of Core Samples

The research team completed splitting tension tests for 24 core slices, each approximately 2 inches thick. A loading rate of about 60 pounds per second was selected based on the effective area of the specimens and the ASTM recommended loading rate of 100-200 psi per minute. Overall, the splitting tension tests showed a high amount of variance, even within non-anomalous zones of the concrete core. Results of these tests are summarized in Table 2.5. As noted, measured strengths varied between approximately 300 and 650 psi with no definitive correlation observed between strength and

the location of deleterious materials observed within the core. Based on these findings, the results were deemed inconclusive.

Table 2.5 - Splitting Tension Test Results for Jacklin Road Undercrossing

Approximate Depth Range (feet)	No. of Tests	Visual Inspection	Range of Splitting Tensile Strength (psi)
8-9	6	Deleterious Material Observed	288 to 598
9-10	4	Deleterious Material Observed	346 to 661
11-12	6	Sound Concrete	305 to 553
13-14	5	Sound Concrete	334 to 455
17-18	3	Sound Concrete	287 to 461

In addition to the splitting tensile tests, the team performed unconfined compression tests on 14 cube specimens cut from the core. These tests were performed at a loading rate of approximately 35 psi per second. The cubes were tested to allow for testing of zones too small for a full splitting tension sample. Compression test results for the cube samples are summarized in Table 2.6.

The zones of concrete that appeared visually sound tested at an average compressive strength equal to 9,091 psi. This unusually high strength is likely due to the extended curing time for the samples (over one year) and the relatively small cube samples. As summarized in Table 2.6, lower compressive strengths were measured for those cube samples containing deleterious material. Though the sample size is small, the compressive strengths appear to correlate well with the amount of deleterious materials observed as well as observations made with CSL. Recall that CSL tests were conducted across the center of the drilled shaft, which is coincident with the original location of the extracted concrete core. Overall, strengths measured for samples containing deleterious material were found to be approximately 10 to 30 percent of strengths measured for nearby samples presumed to be free of deleterious material (i.e. sound concrete). The lower strengths varied between approximately 1,000 and 3,000 psi.

Table 2.6 - Cube Compression Test Results for Jacklin Road Undercrossing)

Depth (feet)	Drop in CSL Reading	Visual Inspection (& Number of Cube Samples)	Average Cube Compressive Strength (psi)	Relative Strengths*
7.3	-	Sound Concrete (4)	9,339	1.03
7.7	-	Sound Concrete (4)	9,239	1.02
8.8	18%	Significant Deleterious Material (1)	1,141	0.13
10.0	-	Sound Concrete (3)	8,504	0.94
12.3	9%	Deleterious Material Observed (1)	3,058	0.34
12.5	9%	Deleterious Material Observed (1)	2,367	0.26

* - Relative strength = average cube strength / reference strength for sound concrete (9,091 psi)

2.4 MITIGATION OF DRILLED SHAFT DEFECTS USING WATER JETTING

Different methods exist for the repair of defects in drilled shaft foundations (Brown et al. 2010). A patch or hand repair is often appropriate for defects found within approximately ten feet of the ground surface. For defects at deeper depths, structural supplements, foundation supplements, pressure grouting, or perimeter jet grouting of the drilled shaft may be warranted as mitigation techniques, depending on the location of the defect and its potential affect on drilled shaft performance. Water jetting or blasting also represents an option for repairing defects at deeper depths, particularly when PVC inspection tubes are utilized (Goodwin 2007). As part of this procedure, high pressure water jetting within an inspection tube is used to remove the PVC tube and deleterious materials from a defective region of a drilled shaft. The resulting cavity is then filled with grout. This method for removing deleterious materials from drilled shafts is the focus of this research study. Water jetting procedures and equipment are summarized in subsequent sections of this report.

2.4.1 Procedures and Equipment

In 2007, the West Coast Chapter of the International Association of Foundation Drilling (ADSC), in cooperation with Holdrege & Kull Consulting Engineers and Caltrans, proposed a Standard Mitigation Plan for the repair of defects in drilled shaft foundations (ADSC West Coast Chapter 2007). Included in this plan is a general description of the procedure for water jetting a defect. This procedure is illustrated on Figure 2.5. The Standard Mitigation Plan is described in some detail in the following section of this report.

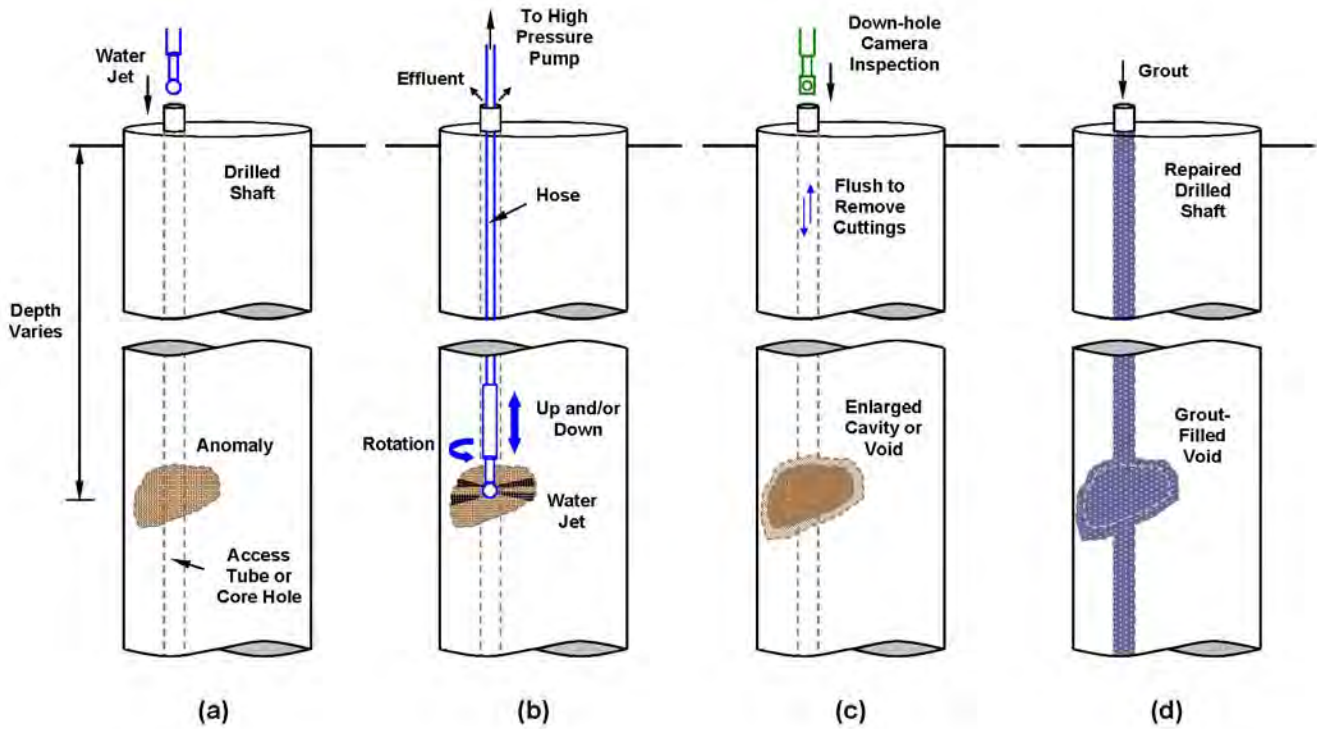


**Figure 2.5 - Typical Water Jetting Process to Repair Defects in Drilled Shafts:
 (a) Introduce Water Jet; (b) Jet Anomaly; (c) Flush Cuttings and Inspect Void
 Space Left by Jetting; and (d) Grout Void Space**

A water jet consists of a head, either fixed or self-rotating, which is fitted with one or more high-pressure nozzles. As shown on Figure 2.5, repair work begins with the water jet being lowered into the drilled shaft through existing PVC access tubes and/or cored holes extending from the top of the shaft. For the former case, a section of the access tube must be removed prior to jetting the anomaly and deleterious materials. Foundation contractors typically use the water jet to cut and remove the tube in the area of the anomaly. After removal of the tube, the jet is free to cut the surrounding deleterious material and flush it to the surface. Periodic straining of solids from the flushed effluent allows for monitoring of water jetting progress. In addition, inspection using a downhole camera can aid in the evaluation of water jetting effectiveness. Once the deleterious materials are satisfactorily removed, the cavity created during water jetting is filled with a relatively low-slump, mortar-type grout mix (or a high slump grout with microfine cement if permeation grouting is used).

Researchers have investigated the application of water jetting for concrete demolition and removal (e.g. Momber 2005; Wright et al. 1997), soil cutting and trenching (e.g. Rockwell 1981; Atmatzidis and Ferrin 1983), and pipe cleaning (Wolgammott and Zink 1999). As summarized in these references,

the effective removal and/or cutting of concrete and soil with a water jet will depend on several factors, including nozzle type, nozzle angle, pressure, rotation speed, standoff distance, and material strength. For the water jetting of anomalies in drilled shaft foundations, contractors commonly use water blasting equipment designed for cleaning and material removal operations.

Between 2008 and 2010, the research team informally surveyed a number of personnel employed by ADSC member firms in California who perform their own water jetting or subcontract this work out to specialty contractors (e.g. American Water Jetting; Cal Marine Cleaning; Grout Repair Specialists). Survey results show that repair procedures are generally similar among those contractors using water jetting to repair drilled shaft defects on Caltrans projects.

When repairing a defect, the contractor will initially remove the PVC access tube within the area of the drilled shaft to be repaired. Contractors generally consider this part of the process to be difficult and time consuming. Water jetting is used to cut the PVC tube. To accomplish this task, contractors report using self- or manually-rotated water jet heads with single or multiple nozzles. Jetting pressures range from about 9,000 to 15,000 pounds per square inch (psi). The procedure involves carefully cutting the PVC tube into small pieces, which can then be flushed out of the access hole. For example, under one method, a single-point nozzle angled at 90 degrees from vertical is used to cut the PVC tube into 1-inch high rings (or less) in the area of the defect. The nozzle is spun inside the tube to make these cuts. After the rings are cut, a vertical cut is made along the length of the tube to help loosen the rings and remove them from the hole. Contractors reported removing the PVC access tube from about 18 to 36 inches above and below the location of the defect, as per Caltrans requirements. Prior to water jetting, a contractor will often grout the PVC access tube from the bottom of the shaft to a short distance below the defect to prevent the loss of cuttings downhole. A downhole camera is now regularly used by contractors to confirm the removal of the PVC access tube in the vicinity of the defect.

Water jetting for removal of deleterious materials commences after the PVC access tube has been removed. For this operation, contractors reported using jetting pressures ranging from about 10,000 to 15,000 psi and flow rates between 10 and 20 gallons per minute. All contractors surveyed reported that the water jet is turned inside the drilled shaft during this operation. Some contractors will hand-turn a single-point water jet nozzle inside the shaft by rotating the hose at the ground surface. One contractor uses a pneumatic device and a rotary swivel (also located at the ground surface) to rotate a single-point water jet nozzle at variable speeds within the drilled shaft. Several contractors use water jets designed as self-rotating swivels, which are similar to those used in pipe cleaning operations. These water jets are equipped with multiple nozzles oriented at different angles. Water flowing

through the jet causes the head to rotate downhole and independent of the hose. Rotation speeds approach approximately 1,000 revolutions per minute (rpm) for typical water jetting pressures and flow rates.

All of the contractors surveyed use a bottom-up strategy when water jetting deleterious materials from a drilled shaft. Initially, the spinning water jet is positioned at a set elevation within the drilled shaft as material is cut and flushed to the surface. Some contractors will hold the water jet at a given elevation for a set period of time (1 to 2 minutes). Other contractors will keep the water jet at a given elevation until the return water runs clear at the surface. All contractors reported visually inspecting the return water at the ground surface as a means of monitoring the water jetting operation. After jetting is complete for a particular elevation, the water jet is repositioned by raising it a short distance within the drilled shaft. Water jetting is then repeated and cuttings are flushed to the surface. Contractors surveyed as part of this study reported raising the water jet between 0.25 and 1 inches during the repositioning process. One contractor reported that it typically takes about an hour to cover one foot of vertical elevation when water jetting within a drilled shaft. The total vertical distance covered during water jetting is controlled by the size and shape of the defect. Water jetting is performed within the area of the access tube where the PVC had been removed.

Nozzle and head designs for water jets are considered proprietary information by specialty contractors working in this area, so detailed descriptions of water jetting equipment are not readily available. One foundation contractor surveyed as part of this study operates water jetting equipment for the repair of drilled shafts and agreed to provide specific water jet design details in support of this research. This contractor water jets drilled shafts using a Stoneage™ "Gopher" self-rotating swivel designed for tube and pipe cleaning. The jet is equipped with six nozzles, three each oriented at 80 and 90 degrees. The contractor uses nozzle tips with orifice diameters that range between 0.035 and 0.038 inches.

After water jetting is complete, the resulting cavity is flushed of cuttings. Contractors reported using high flow volume (under low pressure) to flush cuttings from the drilled shaft. One contractor reported that high pressure air can also be used to remove cuttings. One contractor reported that their firm has used a single-point water jet for cutting and a rotary water jet for flushing. Flushing is sometimes followed by inspection using a downhole camera. The downhole camera can be useful for evaluating the effectiveness of the flushing operation and for determining the size of the cavity. The quality of the drilled shaft concrete cannot be assessed from downhole camera footage. Contractors have found that the downhole camera is most effective for confirming the removal of the PVC access tube prior to water jetting the deleterious materials.

2.4.2 Standard Mitigation Plan

In 2007, the West Coast Chapter of the International Association of Foundation Drilling (ADSC), in cooperation with Holdrege & Kull Consulting Engineers and Caltrans, proposed a Standard Mitigation Plan for the repair of anomalies in drilled shaft foundations (ADSC West Coast Chapter 2007). The group developed two repair methodologies based on their knowledge of the drilled shaft industry and standard construction practices. The first repair method, "Plan A", requires soil excavation and manual removal of the defect, followed by the placement of sound concrete. The second repair method, "Plan B", utilizes high pressure water jetting to remove the defect. Grout fills the resulting cavity. These plans are meant to serve as guidelines for engineers and foundation contractors. Because every repair situation is unique, Caltrans allows engineers and foundation contractors to modify the standard mitigation plans, if reasonable justification can be presented. A site-specific mitigation plan must be submitted by the contractor, and approved by Caltrans, prior to the commencement of any drilled shaft repair work. The following sections describe repair methods A and B in some detail.

2.4.2.1 Plan A - Basic Repair

Plan A, also known as a "basic repair", suffices for defects at or near the top of the drilled shaft. This method requires the excavation of soil surrounding the drilled shaft to a depth one foot below the defect. Once the defect is exposed, the contractor mechanically removes all of the deleterious material from the shaft. Care is taken not to remove too much competent concrete surrounding the defect. At least one inch of uncontaminated concrete must be chipped away to confirm that the underlying material is competent.

If a foundation contractor is unsure if the anomalous concrete requires removal, he or she can core a 3-inch diameter sample to determine the integrity of the anomalous concrete. This can help the contractor and Caltrans determine if mitigation of the anomaly is necessary. The foundation contractor must perform visual inspection and compressive strength tests in accordance with Caltrans standard practices. The plan states, "If visual inspection or the results of compressive strength testing indicate that the concrete is not acceptable, the unacceptable concrete shall be mechanically removed." (ADSC West Coast Chapter 2007).

After a foundation contractor repairs a drilled shaft defect, an engineer must inspect and approve the extent of the excavation. If the engineer finds additional deleterious material, the foundation contractor must remove the identified material and resubmit the drilled shaft for inspection. Once approved, the contractor can build forms surrounding the drilled shaft and fill the cavity with

concrete. Only after the concrete has sufficiently cured may the contractor remove the forms and replace the earthen material. Plan A specifies that all replaced soil must be compacted to the proper relative compaction. In select cases, Caltrans also accepts two-sack sand slurry as replacement for the earthen materials.

2.4.2.2 Plan B - Grout Repair

Plan B, also known as "grout repair", is suitable for defects at depths too deep to practically perform the basic repair. This plan specifies the use of water jetting to remove the deleterious materials from the drilled shaft. Subsequent grouting seals the cavity that results from the water jetting.

Water jetting is typically performed through PVC access tubes cast into the drilled shaft, although it can also be performed through pre-cored holes. To begin the procedure, the contractor uses the water jet to cut through and remove the PVC access tubes for distances 2 feet above and below the detected anomaly. The Standard Mitigation Plan recommends a water jetting pressure of 9,000 to 15,000 psi (with flow rates equal to 10 to 15 gallons per minute) to remove the deleterious material. This pressure is typically low enough to preserve the competent concrete while removing the deleterious material. Jetting continues until no further solids return in the washing water.

After anomaly removal, a high volume, low pressure flush serves to clean the cavity and the inspection tubes. Flushing should continue until the effluent returning from the drilled shaft becomes clear (ADSC West Coast Chapter 2007). The Standard Mitigation Plan recommends that operators monitor the effluent exiting the drilled shaft for suspended solids. This will help notify the operator if any earthen material from outside of the drilled shaft is present in the return effluent. If earthen material is detected, the operator must immediately discontinue water jetting.

Prior to grouting, Caltrans may require inspection of the water jetted cavity with a downhole camera. Downhole cameras can show the size and surface characteristics of the excavated cavity. Dry conditions are preferred for this inspection, but a submerged camera may be used, as long as visibility remains clear. After inspection, grouting can commence. The Standard Mitigation Plan suggests and outlines two methods for grouting repair, namely permeation grouting and replacement grouting (ADSC West Coast Chapter 2007).

After completing the repair, the contractor is required to prepare a mitigation report for Caltrans. This report outlines the procedure and observations made during the repair, and must note any deviations made from the original mitigation plan.

CHAPTER 3

PROJECT APPROACH

3.1 INTRODUCTION

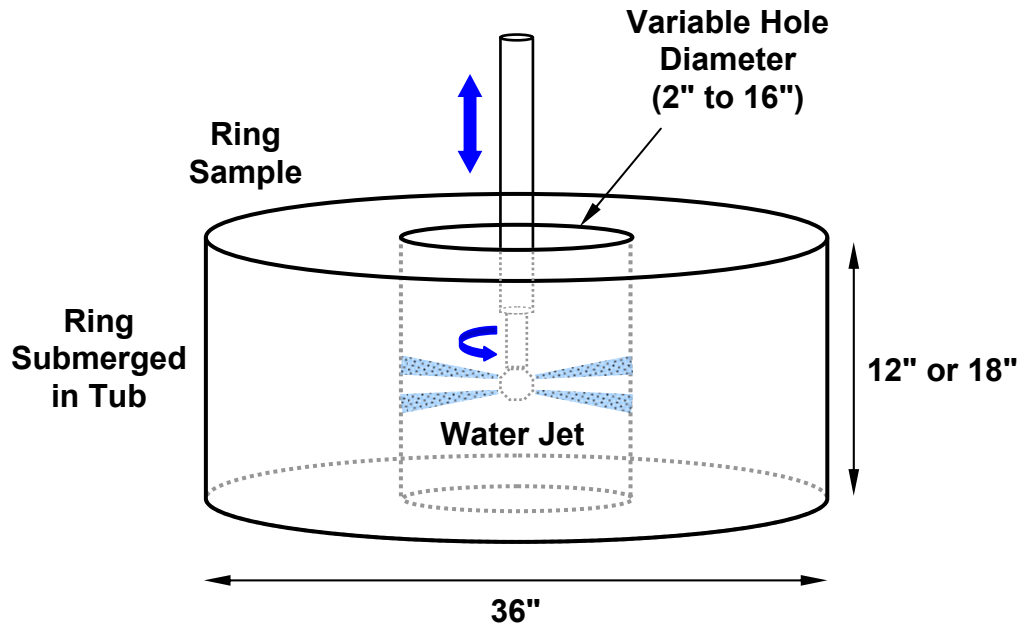
A principal objective of this research is to examine the effectiveness of water jetting as a method for the removal of deleterious materials from drilled shaft foundations. In support of this objective, the research team completed a parametric laboratory investigation to measure water jetting effectiveness in relation to jetting pressure, standoff distance, jetting time, and characteristics of deleterious materials. The research team considered testing representative drilled shaft sections constructed with built-in defects containing different types of deleterious materials. However, based on the results of a preliminary experiment, this approach proved impractical. As an alternative, the research team designed a series of experiments where material removal rates could be easily and accurately measured during water jetting. Both ring-shaped and solid cylindrical material specimens were tested during these experiments. The approach used in this laboratory investigation is described in the following sections of this report.

3.2 LABORATORY TEST SPECIMENS

3.2.1 Ring Specimens

Figure 3.1(a) illustrates a typical ring sample fitted with a water jet, which rotates inside the ring and can be moved up and down during testing. The research team constructed the ring samples using circular-shaped concrete forms fitted with plywood bases. Figure 3.1(b) shows two concrete samples during construction. Smaller cardboard tubes formed the inside diameter of each ring. These cardboard tubes were removed (by hand) from the inside of each ring prior to water jetting. A sketch of a typical ring sample mold is shown on Figure 3.2.

The outside diameter of each ring specimen was approximately 36 inches, and the height was typically 18 inches. The large diameter provided a measure of safety during jetting since blowout of the sample was a concern. A sample height of 18 inches provided room for the water jet to be safely moved up and down during testing while still providing adequate cover. During initial testing the research team constructed ring samples with 12 inch heights; however, this configuration ended up providing inadequate cover at the top and bottom of the specimen.

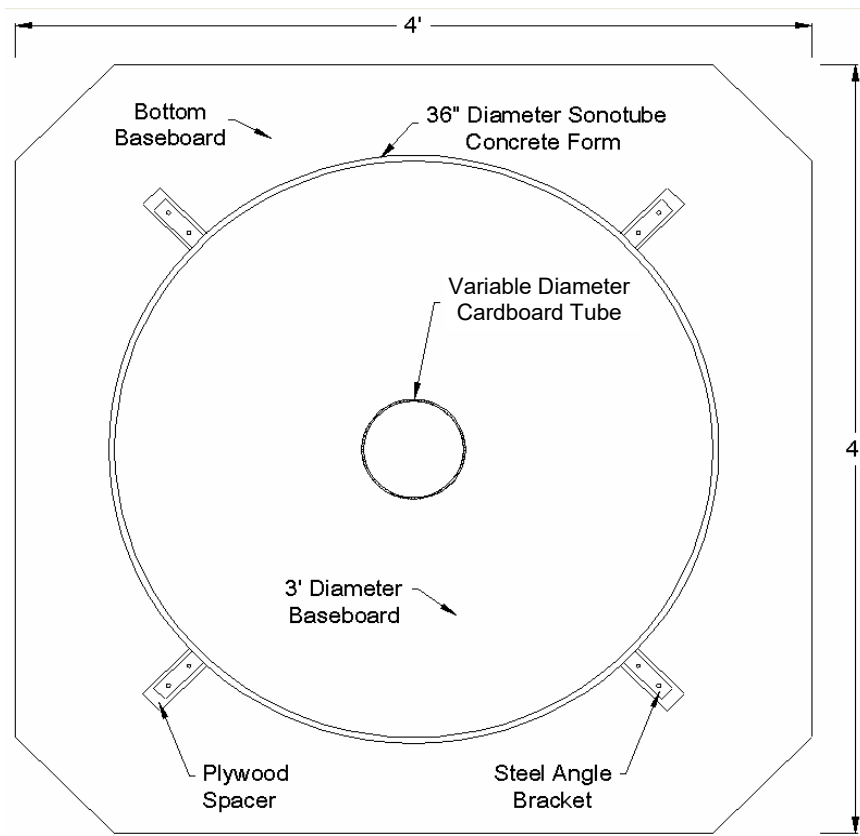


(a)

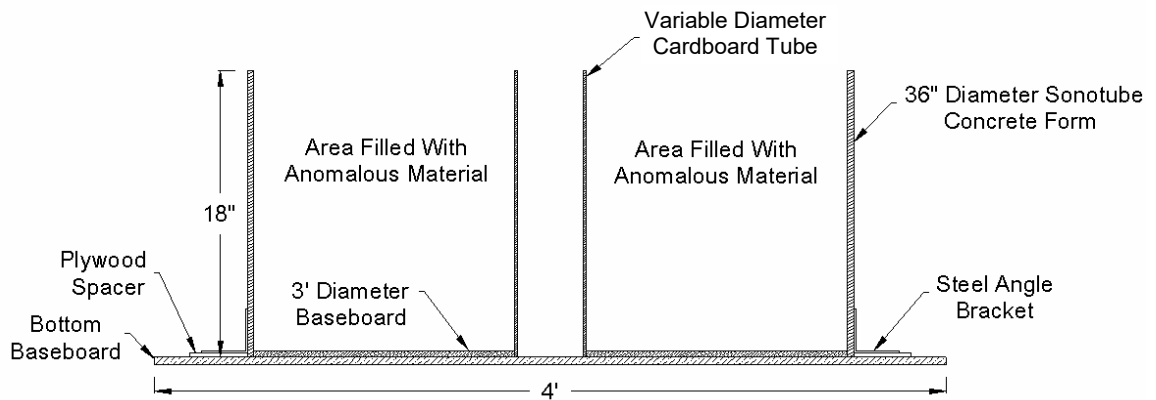


(b)

Figure 3.1 - Ring Samples used during Water Jetting: (a) Illustration of the Concept; (b) Construction Photo for 6- and 12-inch Diameter Samples



(a)



(b)

Figure 3.2 - Typical Ring Sample Mold: (a) Plan; (b) Elevation

Ring samples with various inside diameters were used during testing; however, most of the samples had inside diameters of 6 or 12 inches. During initial testing the research team constructed rings with inside diameters of 2, 4, 6, 12, and 16 inches. In addition, one test ring was fitted with a section of a Schedule 40 PVC access tube. Initial testing revealed high erosion levels during jetting of the 2- and 4-inch inside diameter rings and smaller erosion levels during jetting of the larger diameter rings. Based on these results, the research team decided to test 6- and 12-inch inside diameter rings for the majority of the subsequent water jetting experiments. It was felt that these sample rings would provide valuable experimental results while still being relatively easy to construct and test. Testing of the ring fitted with a PVC access tube proved difficult and time consuming because the process of removing the tube is so difficult. During this experiment, several iterations were required to cut and remove only a small section of the tube. Since removing the PVC tube from within a drilled shaft was not considered within the scope of this research, the research team chose not to include PVC tubes in samples tested during subsequent experiments.

3.2.2 Cylindrical Specimens

Figure 3.3 shows a typical cylindrical sample with the surrounding test apparatus. In these tests, 6-inch by 12-inch cylindrical samples were positioned at standoff distances (from the water jet) ranging between 1.5 and 16 inches. The samples were constructed in general accordance with ASTM procedures for the preparation of compression test cylinders.

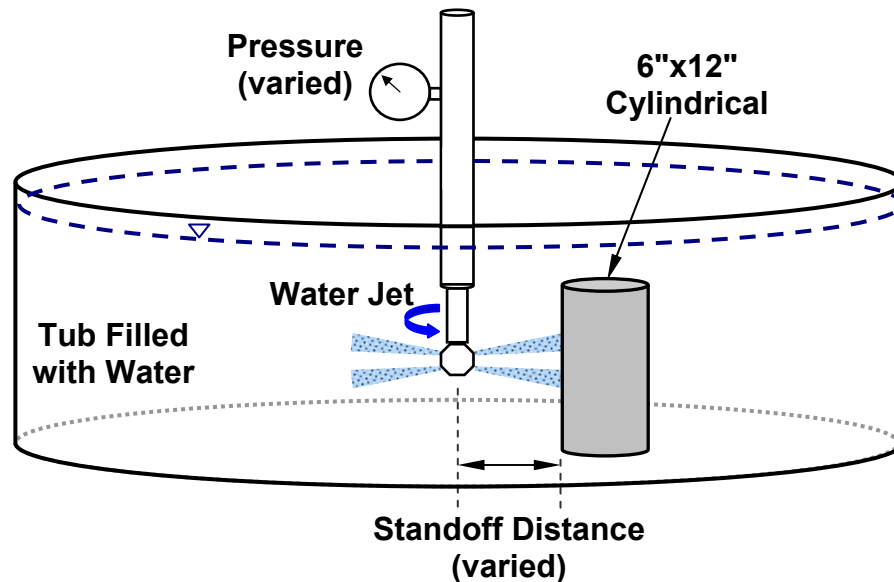
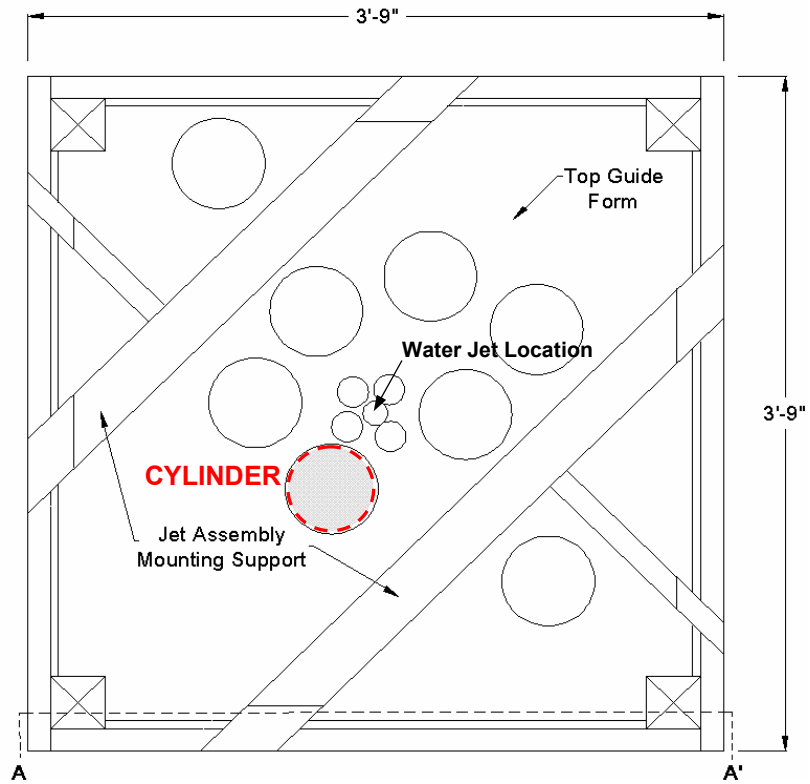


Figure 3.3 - Illustration of a Typical Cylindrical Sample and Testing Concept

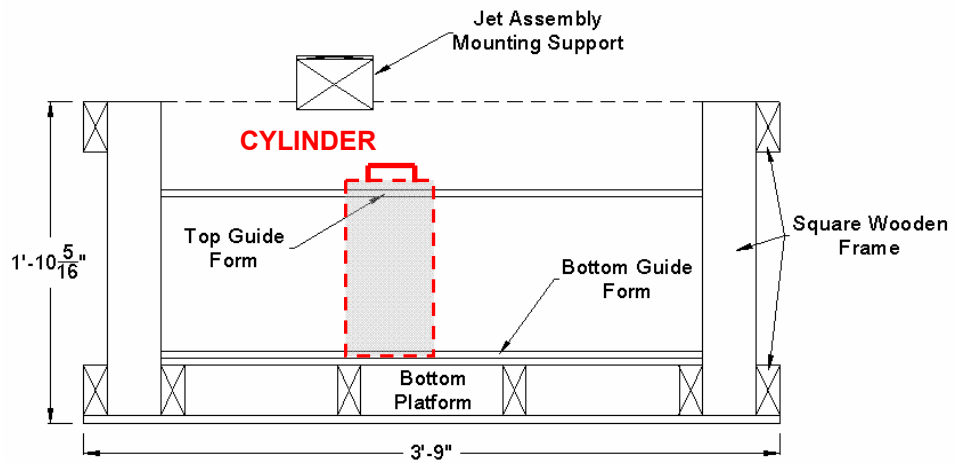
As shown on Figures 3.4 and 3.5, a wood frame secured the cylinders and water jet during testing. Circular cutouts in the top and bottom of the frame held the cylinders in their prescribed locations for the duration of the test, which allowed for simultaneous testing of multiple specimens at different standoff distances. The research team fitted each cylindrical specimen with a rebar "handle" at the top, as shown. The handle allowed for easier placement of the cylindrical specimens in the frame apparatus.



Figure 3.4 - Photograph of the Frame Apparatus used to Secure Cylindrical Test Cylinders



(a)



(b)

Figure 3.5 - Sketch of Test Frame and a Typical Cylindrical Specimen:
(a) Plan; (b) Cross-Section A-A'

3.2.3 Ring Specimens with Reinforcing Steel Bars

The research team cast four ring specimens with reinforcing steel to evaluate the influence the steel has on water jetting effectiveness in drilled shafts. Four ring samples were cast with longitudinal and transverse reinforcing steel bars. These ring samples had the same overall dimensions as those described earlier. Figure 3.6 shows, in plan view, a reinforcing steel layout that included four longitudinal (vertical) steel bars. The bars were evenly spaced around the inside diameter of a 6-inch sample ring. Plywood forms at the top and bottom of the sample fixed the bars in place during material placement and curing. The research team selected #4, #8, #11, and #14 bars because of their typical use as steel reinforcement in drilled shafts. Two identical ring samples were prepared using this sample arrangement.

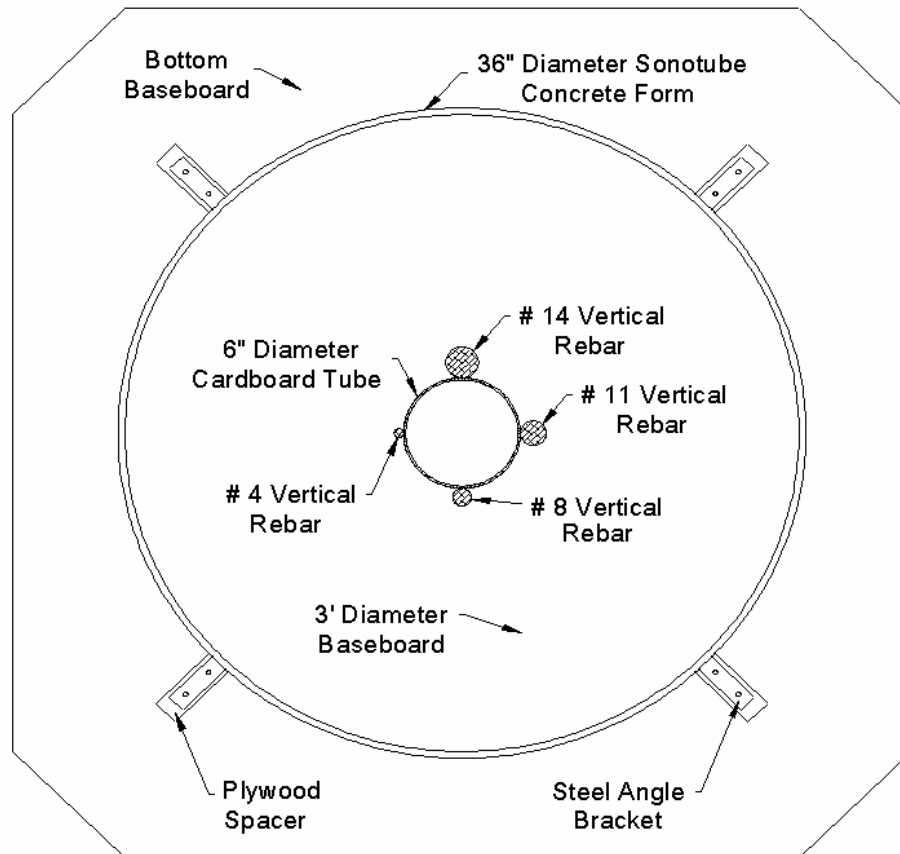


Figure 3.6 - Plan View of a 6-inch Inner Diameter Ring Sample with Discrete Longitudinal (Vertical) Bars

Figure 3.7 illustrates the second reinforcing steel layout used in this study. With this layout, the research team recreated (approximately) a portion of a typical reinforcing steel cage designed for a 3-foot diameter drilled shaft. Access for water jetting was provided through a 2.25-inch diameter hole at the center of the ring. This hole was designed to represent the hole created by a typical PVC access tube. Three-inch clear spacings were provided between the access hole and adjacent steel bars, as per the minimum spacing requirements stipulated by Caltrans. Other clear spacings between bars were based on typical drilled shaft designs. One curved transverse (horizontal) reinforcing bar was tied to the longitudinal steel at approximately the mid-height of the ring. In addition, the research team bundled some of the bars and added additional longitudinal steel at two locations (6 inches from the access hole) to further study the influence of reinforcing steel on water jetting effectiveness.

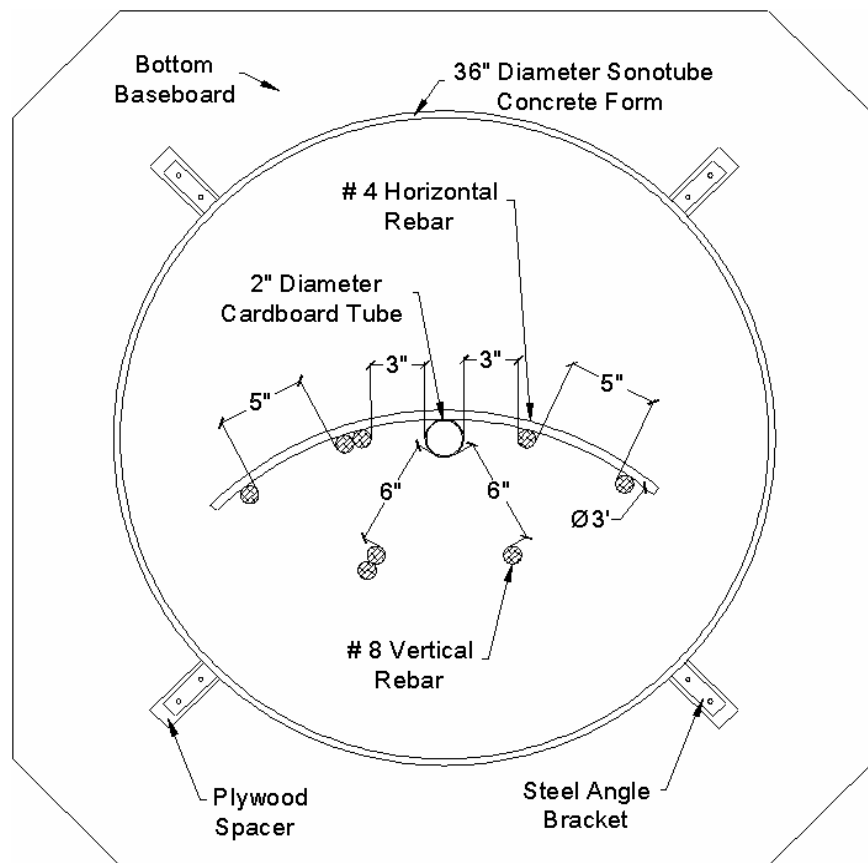


Figure 3.7 - Plan View of a 2-inch Inner Diameter Ring Sample Designed to Simulate a Section of a 3-foot Diameter Drilled Shaft (including #8 Longitudinal Reinforcement and #4 Transverse Reinforcement)

Figure 3.8 illustrates the third reinforcing steel layout examined as part of this study. This layout was similar to the layout illustrated on Figure 3.7. However, in this new case, the research team recreated (approximately) a portion of a typical reinforcing steel cage designed for a 6-foot diameter drilled shaft. As before, the research team bundled some of the bars and added additional longitudinal steel at two locations (6 inches from the access hole) to further study the influence of reinforcing steel on water jetting effectiveness

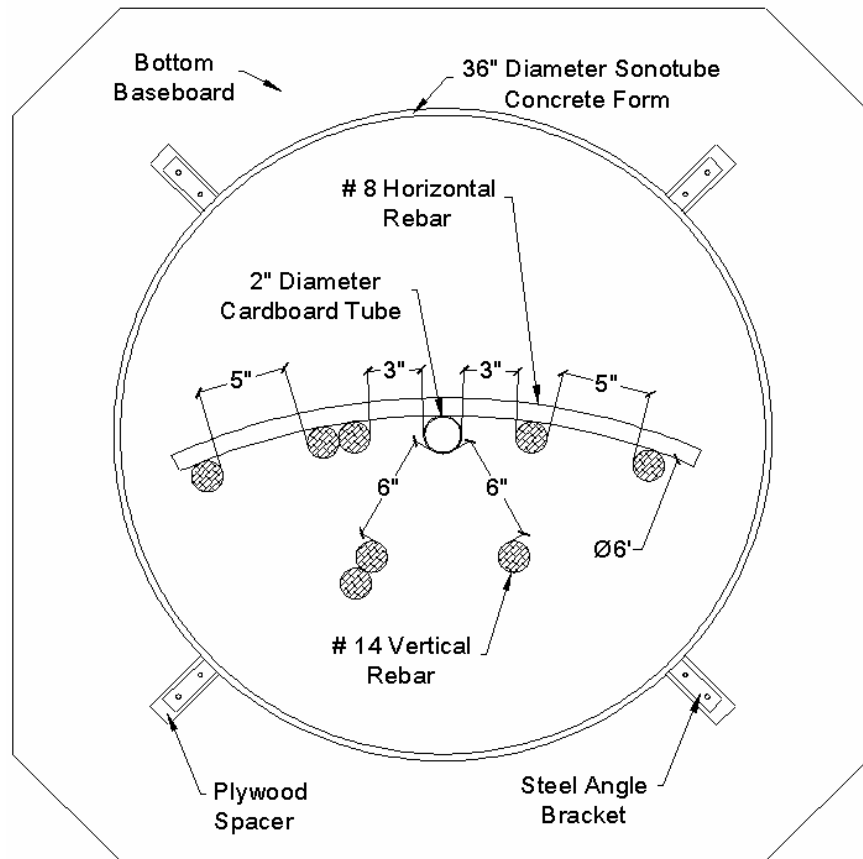


Figure 3.8 - Plan View of a 2-inch Inner Diameter Ring Sample Designed to Simulate a Section of a 6-foot Diameter Drilled Shaft (including #14 Longitudinal Reinforcement and #8 Transverse Reinforcement)

Shown on Figure 3.9 are photographs of the two ring samples that incorporated reinforcing steel. Note the presence of the plywood forms at the top of each ring. The forms held the longitudinal steel bars in place during material placement and curing.



(a)



(b)

Figure 3.9 - Photograph of Ring Samples with Reinforcing Steel: (a) Discrete Longitudinal Bars; (b) Section of a 6-foot Diameter Drilled Shaft

3.2.4 PVC Access Tube Specimens

The research team performed additional tests to assess the erosion characteristics of PVC tubing. Sections of Schedule 40, 2-inch inside diameter PVC tubes similar to those used as access tubes in typical drilled shaft construction were fixed next to the water jet at standoff distances of approximately 0.20 and 0.44 inches. One would expect a standoff distance in this range for a water jet lowered within a 2-inch inside diameter inspection tube. The research team mounted PVC specimens (vertically) in the test frame used during the cylindrical sample tests, as illustrated on Figure 3.10. The ends of the PVC tubes were affixed to the test frame and held in place during water jetting.

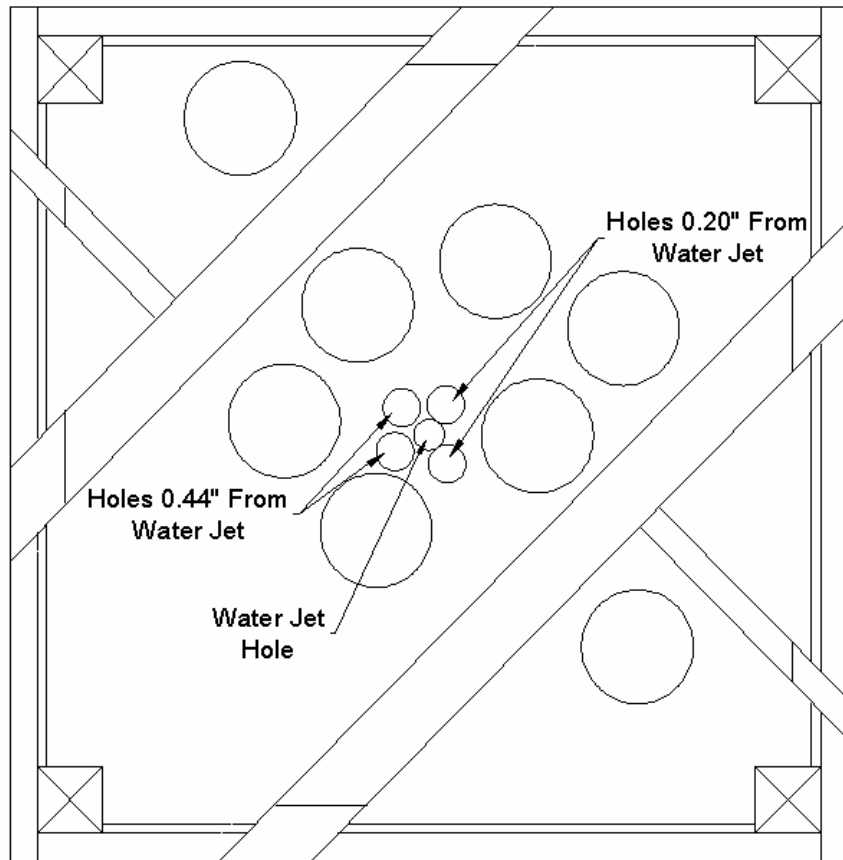


Figure 3.10 - Sketch of Test Frame and Holes used to Mount PVC Specimens

3.3 LABORATORY WATER JETTING PROCEDURES

3.3.1 Equipment

The photograph on Figure 3.11 illustrates the equipment and test arrangement used during this research program. The essential components included a high-pressure pump, a water jet, high-pressure hoses, a water storage tank, recycling tanks, and water tubs. The water tubs consisted of wood frames and plastic sheeting, which were built around the test samples and filled with water prior to water jetting. When the cylindrical specimens were tested, the previously described test frame was submerged within a water tub.

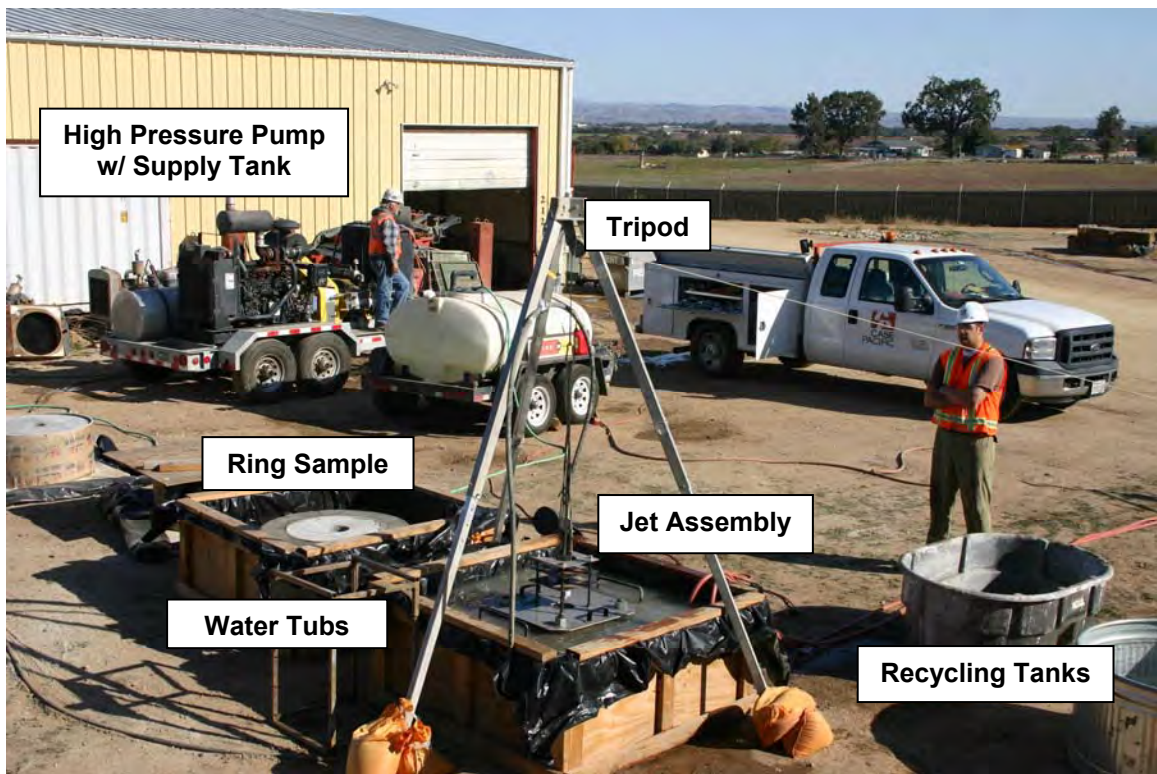


Figure 3.11 - Photograph Showing the Water Jetting Test Equipment and Layout

All of the water jetting experiments conducted as part of this study simulated submerged conditions, as typically encountered in practice during field repair operations. Material samples were submerged under approximately 4 inches or more of water during testing. Submersible pumps collected water from the tubs during water jetting to prevent overflowing and to allow for recycling.

The research team designed and machined a simple collar assembly to secure the water jet during testing and to position it within the test apparatus. The water jet and collar assembly are shown on

Figures 3.12 and 3.13. The water jet used in this study was a Stoneage™ "Gopher" self-rotating swivel designed for tube and pipe cleaning. This equipment is typical of that used in drilled shaft repairs. The jet was equipped with six nozzles, three each oriented 80 and 100 degrees from the longitudinal axis. The upper and lower nozzles had openings of 0.038 and 0.035 inches, respectively. With these nozzles, the jet rotated at approximately 1,000 rpm for operating pressures ranging between about 10,000 and 12,000 psi. The flow rate during operation was equal to approximately 24 gallons per minute. Product details for the water jet are included in Appendix A.

Shown on Figure 3.13 is a detail of the water jet collar. Prior to water jetting, a 0.25-inch thick steel plate with a 14-inch diameter access hole was fastened to a ring sample (or to the frame used during testing of the cylindrical specimens and PVC access tubes). The collar assembly attached to this plate and centered the water jet nozzle horizontally. The collar could be fixed in the vertical direction, or it could be left free to move up and down along four guide rods. A rope, pulley, and tripod system centered over the test sample allowed the research team to raise and lower (i.e. cycle) the collar and water jet over a vertical distance of 6 inches. The tripod and collar are illustrated on Figure 3.11. As noted on Figure 3.13, the research team included a pressure gauge in the water line directly behind the water jet and a 12-inch extension. The gauge allowed for direct measurement of water jetting pressure during testing.

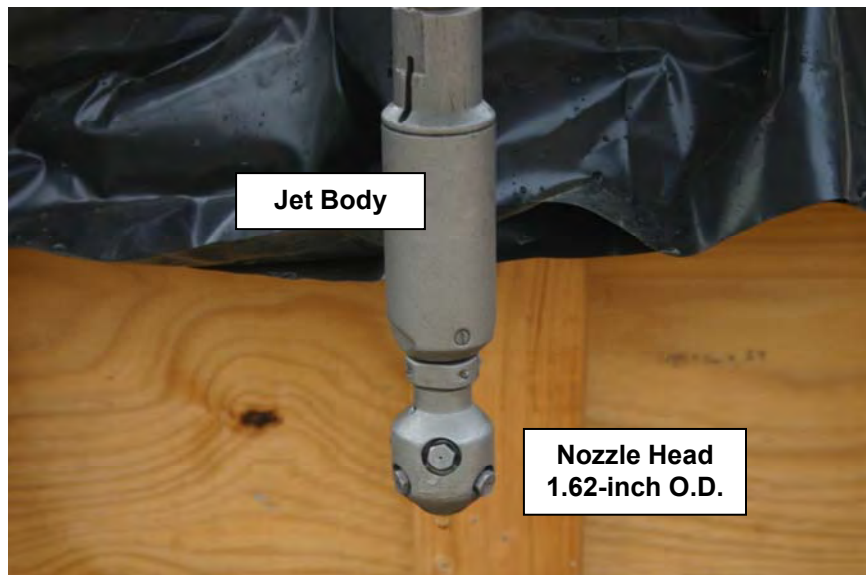


Figure 3.12 -Photograph Showing the Self Rotary Water Jet and Nozzles

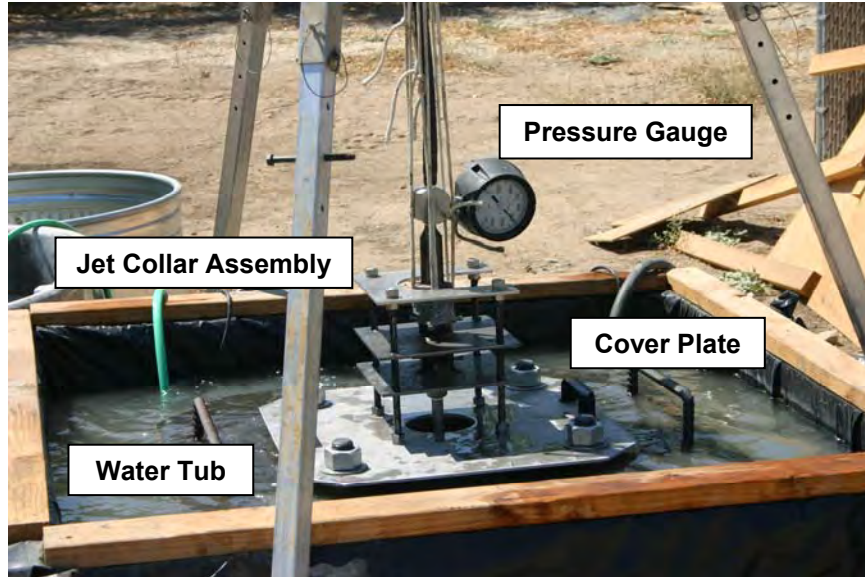


Figure 3.13 -Photograph Showing the Jet Collar Assembly and Cover Plate Attached to a Ring Sample during Testing

3.3.2 Ring Sample Testing Procedure

For testing the ring samples, the research team adopted the following water jetting procedure. The ring sample was first submerged and fitted with the cover plate, collar assembly, and water jet. This process would typically take 30 to 60 minutes. The pump was then started and the water jet was pressurized. Jetting commenced for a specified time interval. During jetting, a team member periodically recorded the jetting pressure from a gauge located near the nozzle. Water jetting pressures between 10,000 and 11,000 psi were used for all of the ring sample tests.

Using the cover plate and collar assembly, the research team centered and fixed the water jet horizontally within each ring prior to testing. Vertical movement of the water jet was permitted, depending on the purpose of the experiment. Table 3.1 describes the three different approaches that the team used to control the movement of the water jet in the vertical direction. The three different approaches are termed "stationary", "cycled", and "steady upward" in this study. The purpose behind each approach is briefly stated in Table 3.1. As noted in the table, erosion measurements were recorded at different water jetting time intervals during the stationary and cycled experiments. The research team commonly adhered to the following schedule when taking and recording erosion measurements during a ring sample experiment: 0.5, 1, 2, 4, 8, 16, and 32 minutes of water jetting.

Table 3.1 - Ring Sample Test Approaches for Controlling Movement of the Water Jet in the Vertical Direction

Approach	Description	Purpose
Stationary	Water jet fixed vertically and centered within the ring; jetting time varied in between erosion measurements.	Used during initial experiments to refine testing procedures.
Cycled	Water jet cycled up and down within the center of the ring over a vertical distance of 6 inches; cyclic rates ranged between 6 and 8 cycles per minute; jetting time varied in between erosion measurements.	Used to help continually flush cuttings from the ring during jetting.
Steady Upward	Water jet initially positioned at the bottom of the guide rods on the collar assembly; water jetting conducted for approximately 2.5 minutes; water jet raised approximately 1/2-inch and jetting process repeated; water jetting conducted over a total vertical distance of 6 inches in approximately 30 minutes; erosion measurements taken at the end of experiment.	Used to simulate practice used by contractors in the field.

At the end of a water jetting time interval, jetting was stopped and the collar assembly was removed. The water inside the ring sample was then removed so the jetted surface could be examined and erosion measurements could be made. Figure 3.14 includes post-test photographs showing the general pattern of erosion observed during the "stationary" and "cycled" experiments. The x-shaped erosion pattern shown on Figure 3.14(a) occurred due to the angled orientation of the water jets on the rotating nozzle. The cavity-shaped pattern on Figure 3.14(b) occurred due to the cycling of the water jet up and down over the 6-inch vertical distance. The research team observed a similar cavity-shaped erosion pattern during the post-test examination of ring samples water jetted according to the "steady upward" approach.

The team measured erosion distance at eighteen different points within a ring sample for three cross-sections and three elevations (each spaced 3 inches apart). Figure 3.15 illustrates the measurement schedule. For cases where the water jet was stationary, the team measured erosion distances within the well-defined incisions apparent on Figure 3.14(a), and not according to the guide illustrated on Figure 3.15. In all tests, erosion measurements were manually recorded to the nearest 1/16-inch. The un-jetted inside portion of a ring served as the "zero" reference for these measurements.



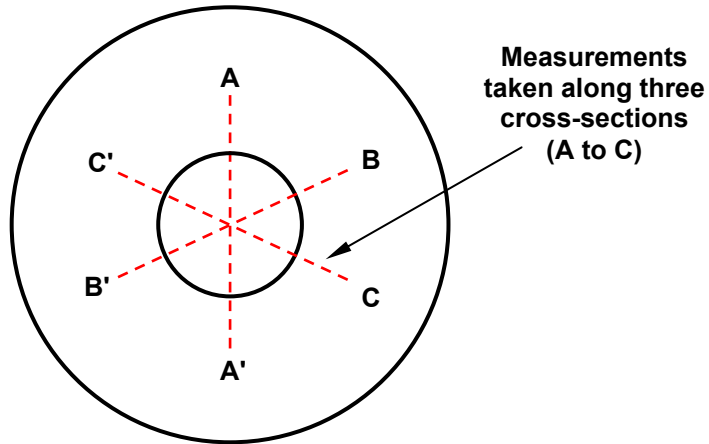
(a)



(b)

**Figure 3.14 - Post-Test Photographs of 6-inch Diameter Ring Samples:
(a) Jet Held Stationary; (b) Jet Cycled Up and Down**

(a) Plan View:



(b) Section View:

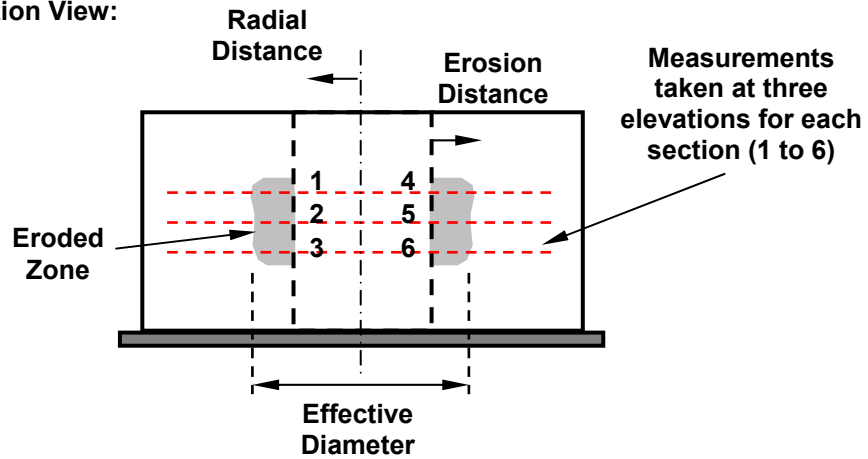


Figure 3.15 - Illustration of Erosion Measurements taken during Water Jetting:
(a) Plan View; (b) Section View

In general, water jetting during the ring experiments continued until the research team observed negligible erosion for successive time intervals. When a test was deemed complete, the ring samples were cut apart and photographed.

3.3.3 Cylindrical Sample Testing Procedure

The research team used the following procedure when testing the cylindrical test specimens. Test cylinders were labeled and secured at different standoff distances within the test frame shown on Figure 3.5. The frame, cylinders, and water jet were then submerged within a water tub. Note that the research team used the previously described jet collar assembly to hold the water jet in place

during testing. Samples were water jetted at constant pressure for approximately 1 to 2 minutes while keeping the jet stationary in the vertical direction. After jetting was complete, the research team removed the cylinders from the tub and noted any erosion. Erosion depths were measured using the original cylinder face as the "zero" reference. Figure 3.16 shows a side view of an eroded cylinder and the typical erosion pattern observed after water jetting was complete. The figure also illustrates how erosion depths were measured.

Once data were recorded, the research team prepared another set of concrete cylinders for water jetting. These cylinders were tested at the same standoff distances and a different jetting pressure. Extensively eroded cylinders were replaced with new ones for each new test. However, if erosion was slight, a cylinder was reused by rotating it such that the subsequent water jetting impacted an unaffected face. Several sets of cylinders were tested to examine erosion effects for standoff distances between 1.5 and 16 inches and water jetting pressures between 2,400 and 10,700 pounds per square inch. For example, the cylinder shown on Figure 3.16 had an unconfined compressive strength of 160 psi and was tested at a standoff distance of 4 inches for a jetting pressure of 6,000 psi.

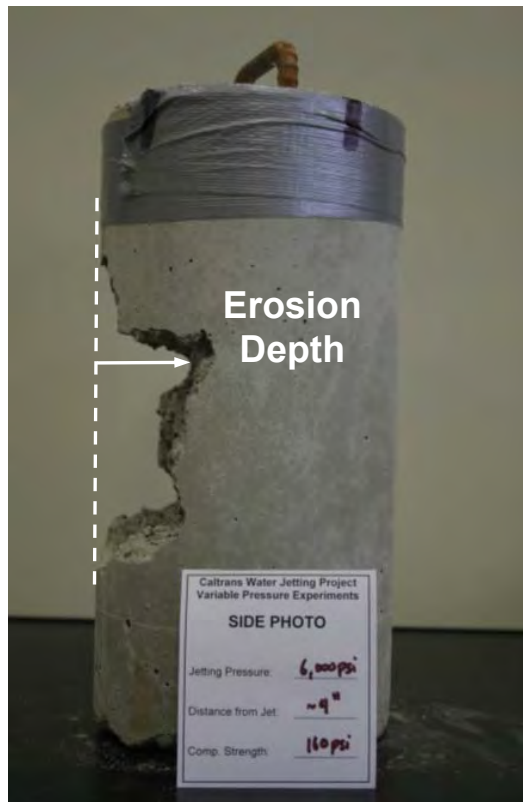


Figure 3.16 - Example of an Eroded Cylindrical Sample after Water Jetting

3.3.4 Ring Sample with Reinforcing Steel Bars Testing Procedure

The research team followed the water jetting procedure described previously when testing the ring samples cast with reinforcing steel bars. Both "cycled" and "steady upward" approaches were employed. The research team modified its procedure for taking erosion measurements to accommodate the reinforcing steel present in the ring samples. Erosion distances for the 6-inch inner diameter ring samples were measured at twelve different points for two cross-sections and three elevations (each spaced 3 inches apart). Figure 3.17 illustrates the measurement schedule in plan view only.

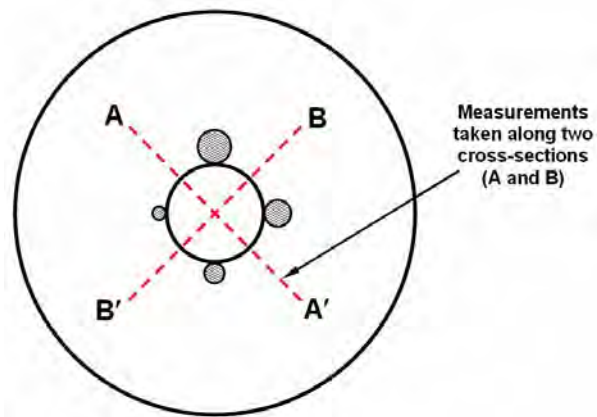


Figure 3.17 - Erosion Measurement Locations for Ring Samples Cast with Reinforcing Steel Bars

For those 2-inch inner diameter ring samples cast with a portion of a reinforcing steel cage, the "steady upward" water jetting approach was used. No intermediate erosion depths were measured during these tests. Only the final erosion depths were recorded. These depths were obtained after the samples were cut apart, inspected, and photographed.

3.3.5 PVC Access Tube Specimen Testing Procedure

The research team tested the PVC tube specimens following a procedure similar to that used during the concrete cylinder tests. Test specimens were labeled and secured at different standoff distances within the test frame, as illustrated on Figure 3.10. The frame, PVC tube specimens, and water jet were then submerged within a water tub. The tube specimens were then water jetted at constant pressure for approximately 1 minute while keeping the jet stationary in the vertical direction. After jetting was complete, the research team removed the tube specimens from the tub and noted any

erosion. Each tube specimen was photographed. Several sets of tube specimens were tested to examine erosion effects for water jetting pressures ranging between approximately 2,000 and 10,000 psi. New tube specimens were used for each new water jetting pressure.

3.4 CONCRETE AND DELETERIOUS MATERIALS

3.4.1 Caltrans Practice

Caltrans outlines several requirements for drilled shaft concrete and for pouring concrete under "wet" conditions (e.g. Caltrans Standard Specifications 2010; Caltrans Foundation Manual 2008).

According to the Standard Specifications (Caltrans 2010), a contractor may use graded aggregates with nominal maximum aggregate sizes of 1-inch, 1/2-inch, or 3/8-inch as they see fit. The minimum 28-day compressive strength shall be 3,600 pounds per square inch (psi). In addition, the concrete slump should be 6 to 8 inches and cannot exceed 9 inches. The concrete must be "dense and homogeneous" (Caltrans 2010). To ensure this uniformity, the maximum permissible variation between slumps from the same batch of concrete shall not exceed 2 inches. The pouring method shall also not cause segregation in the concrete.

When constructing drilled shafts under "wet" conditions, it is typical for contractors to use drilling slurries. Caltrans outlines specific requirements for concrete placed in drilled shafts constructed using drilling slurries. It states that concrete poured under drilling slurry shall have a minimum of 675 pounds of cement per cubic yard of concrete. In addition, the aggregates shall have a nominal maximum aggregate size of either 1/2-inch or 3/8-inch.

The Foundation Manual (Caltrans 2008) outlines pouring procedures for "wet" construction of drilled shafts. When drilling slurries are used, it is important to use a tremie or rigid tube to deliver the structural concrete. This tube must be kept, at a minimum, "10 feet below the rising head of the concrete" (Caltrans 2008). Keeping this concrete head prevents water and debris from infiltrating the concrete tube. As the structural concrete is pumped into the drilled shaft, the drilling slurry is pumped from the top of the shaft. Concrete pouring starts at the bottom of the drilled shaft and is gradually raised while maintaining the appropriate concrete head. Concrete is typically pumped into the drilled shaft until uncontaminated concrete is observed at the surface. More requirements for drilled shaft construction can be found within the above listed standards and manuals.

3.4.2 Deleterious Materials in Drilled Shafts

Earlier sections of this report include descriptions of anomalies, defects, and deleterious materials observed in drilled shafts. Examples of commonly occurring deleterious materials include low

strength concrete, slurry mix concrete, semi-cemented material, soil-concrete mixtures, and soil (Liebich and Bonala 2007). When present, these deleterious materials may exist as thin bands or discontinuous, irregular shaped pockets. On occasion, an entire cross-section of a completed drilled shaft may be composed of deleterious material. Case histories show that compressive strengths of deleterious materials can vary widely. As detailed in Chapter 2.3, compressive strengths ranging from about 350 to 3,000 psi have been measured for deleterious materials found in drilled shaft defects. These observations, the deleterious material descriptions by Liebich and Bonala (2007), and Caltrans' concrete requirements for drilled shafts were all used as input when selecting the materials and mix designs to be tested as part of this water jetting study.

3.4.3 Material Mix Designs

3.4.3.1 Objectives

The research team selected five different mix designs for testing, as noted in Table 3.2. These mixes included low strength concrete containing 3/8-inch aggregate (SCM); concretes with a range of strengths containing 1-inch crushed (angular) or river-run (rounded) aggregate (CON); a 1-inch aggregate concrete mixed with bentonite slurry (SMX); a 5-sack per yard sand-cement grout with relatively low strength (GRT); and a low strength bentonite-cement grout (CLY). In selecting these materials, the team planned to systematically test the affect of material type, aggregate size, and compressive strength on water jetting effectiveness. A target testing matrix is shown in Table 3.3, which illustrates the plan for varying unconfined compressive strength and material type during water jetting. General descriptions of the different materials follow in this report. Heavin (2010) and Schaffer (2011) provide additional details on the different material mix designs.

Table 3.2 - General Description of Materials Tested during Water Jetting

Material Designation	Material Description	Max. Size Aggregate (in)	Aggregate Shape	Tested Comp. Strength (psi)
SCM	Low strength concrete with high sand content	0.375	Angular	160 to 2,350
CON	Typical concrete mix used in civil engineering design	1	Angular & Rounded	650 to 4,600
SMX	Typical concrete mixed with bentonite slurry	1	Angular	1,850
GRT	Low strength 5-sack per yard sand cement grout	0.125	-----	1,900
CLY	Low strength bentonite-cement grout	<0.0001	-----	5 to 10

Table 3.3 - Target Test Matrix for Water Jetting Investigation

Material Designation	Target Unconfined Compressive Strengths (psi)				
	0 to 500	500-1,000	1,000-2,000	2,000-3,000	3,000+
SCM	◆	◆	◆		
CON (angular)		◆	◆	◆	◆
CON (rounded)				◆	
SMX			◆		
GRT			◆		
CLY	◆				

3.4.3.2 Low Strength Concrete (SCM)

The research team designed a low strength concrete (semi-cemented) material to investigate the influence of compressive strength on water jetting effectiveness. This material consisted of 3/8-inch by #8 coarse aggregate (crushed angular granite), sand (ASTM C33), cement (Type II/V), and water. A higher sand content was used to limit compressive strengths and simulate deleterious materials commonly encountered in constructed drilled shafts. Saturated surface dry (SSD) weights (in pounds per cubic yard) for a typical mix design were about 700, 2250, and 250 for the coarse aggregate, sand, and cement, respectively. The team varied the sand content, cement content, and curing time to achieve the desired target compressive strengths. Air entrainers and superplasticizers were added to the various mixes to achieve the desired slump range of 7 to 9 inches. The low strength concrete mixes were delivered to the site by ready-mix truck.

3.4.3.3 Concrete (CON)

The research team designed a normal strength concrete to investigate the influence of compressive strength, aggregate size, and aggregate shape on water jetting effectiveness. This material consisted of 1-inch by #4 coarse aggregate (granite - angular and rounded), sand (ASTM C33), cement (Type II/V), and water. Saturated surface dry (SSD) weights (in pounds per cubic yard) for a typical mix design were about 1400, 1600, and 450 for the coarse aggregate, sand, and cement, respectively. The research team used two different methods to vary the compressive strengths of the different mixes (Heavin 2010). For the first method, Class F fly ash was used in different proportions as weight replacement for the cement, keeping the water-to-cementitious materials ratio constant. The

percent of fly ash of the total cementitious material ranged from 25 to 72 percent. For the second method, the water-to-cement ratio was varied. Air entrainers and superplasticizers were added to the various mixes to achieve the desired slump range of 7 to 9 inches. The concrete mixes were delivered to the site by ready-mix truck.

3.4.3.4 Slurry Mix Concrete (SMX)

The slurry mix concrete consisted of a normal strength concrete (CON) mixed with a bentonite slurry. Bentonite slurry, also known as mineral slurry, is a mixture of powdered bentonite (standard 200 mesh) and water. This material is commonly used during drilled shaft construction in "wet" conditions to help support the borehole. The slurry mix concrete material was designed to simulate a deleterious material that could potentially form within a drilled shaft under wet construction conditions. The research team selected this material to study the influence of material type on water jetting effectiveness.

The bentonite slurry used in this study consisted of 80 pounds of bentonite per 100 gallons of water, which represents typical construction practice. The concrete included 1-inch crushed granite aggregates. The team agreed on a target compressive strength between 1,000 and 2,000 psi for the slurry mix concrete. To achieve this goal, the research team prepared and tested concrete batches with 10, 15, 25, 37.5, and 50 percent slurry replacement by volume. Results showed a replacement rate of 15 percent bentonite slurry achieved the desired compressive strength after 14 to 28 days of curing. To create the bentonite slurry, the team slowly mixed the bentonite with water in a 32 gallon drum. The slurry hydrated for a minimum of 24 hours before the team mixed it with the concrete. The final slurry mix concrete was prepared at the test site using a 2.5-cubic foot electric drum mixer. The target slump for the mix was 7 to 9 inches.

3.4.3.5 Sand-Cement Grout (GRT)

The research team designed a typical "5-sack" sand-cement grout to investigate the influence of material type on water jetting effectiveness. The grout simulated a deleterious material free of coarse aggregates. This material consisted of medium sand (ASTM C33), cement (Type II/V), and water. Saturated surface dry (SSD) weights (in pounds per cubic yard) for a typical mix design were about 2,800 and 500 for the sand and cement, respectively. The team varied the water content and curing time to achieve the desired target compressive strength. The grout mix was delivered to the site by ready-mix truck.

3.4.3.6 Bentonite-Cement Grout (CLY)

The research team designed a bentonite-cement grout to represent the clayey soils sometimes encountered as deleterious materials in and around constructed drilled shafts. The team tested this material to study the influence of soil on water jetting effectiveness. A bentonite-cement grout was selected over an actual soil because the grout material could be prepared relatively easily and cured quickly. The research team agreed on a target compressive strength between about 5 and 15 psi for the grout mixture. To achieve this goal, the research team prepared and tested various batches following procedures recommended by Mikkelsen (2002). The final mix included water, cement (Type II/V), and bentonite at a weight ratio of approximately 5-to-1-to-0.7, respectively.

The research team mixed the bentonite-cement grout on-site within a 150 gallon tub. To help ensure a mix with a smooth consistency and an accurate water-to-cement ratio, the team first mixed the water and cement in the mixing tub using electric drills fitted with stirrer attachments. While continuing to mix the sample, the team then slowly added powdered bentonite. Bentonite was continuously added until the watery mix transitioned to an oily/slimy consistency (Mikkelsen 2002). The grout was then left to thicken for approximately 5-10 minutes before placement. The final grout mixture had a consistency comparable to that of pancake batter with a marsh funnel viscosity equal to approximately 50 seconds.

3.4.4 Sample Preparation and Quality Control Testing

The research team constructed and cured the ring and cylindrical test specimens in the field at the water jetting test site. This site was the equipment yard for the Case Pacific Company in Paso Robles, California. The ring samples were poured from a ready-mix truck (SCM, CON, GRT), a portable electric drum mixer (SMX), or a tub (CLY). Slump tests were performed, as appropriate. The team vibrated the concrete (CON) and slurry mix concrete (SMX) ring samples during material placement. The team also vibrated the ring samples that included reinforcing steel bars. A cylindrical test specimen was prepared by rodding three equal lifts in general accordance with current ASTM procedures (ASTM C31).

During curing, the ring samples were covered with plastic sheeting and plywood to provide protection and limit moisture loss. The team placed plastic freezer bags over the cylindrical samples to help limit moisture loss during curing. In addition, plywood tents were constructed over the ring and cylindrical samples to shade them from direct sunlight. In general, curing lasted two to five weeks, depending on the target compressive strengths for the samples and the availability of the water jetting equipment.

During each sample pour, test cylinders (for evaluating compressive strength) were prepared in general accordance with ASTM procedures. Curing of these test cylinders occurred on site next to the ring samples. The compressive strengths of the ring and cylindrical test specimens were monitored during curing by periodically load testing the test cylinders. At least two test cylinders were tested on the same day the water jetting was completed. After water jetting, the research team typically retrieved a number of intact cores and cube samples from the ring samples to test for compressive strength and confirm results.

3.5 WATER JETTING TEST MATRIX

Table 3.4 provides a complete listing of the ring and cylindrical samples tested as part of this research investigation. The table identifies each test series based on sample material (i.e. SCM, CON, SMX, GRT, or CLY). Note that a test series typically included multiple water jetting experiments. Material characteristics are identified in Table 3.4 for each sample (i.e. aggregate size, aggregate shape, and average unconfined compressive strength). The table also provides ring dimensions (i.e. inside diameter) and the approach used during water jetting. The three different jetting approaches were described in Table 3.1. Water jetting durations are also reported in Table 3.4, as applicable. The results from the water jetting experiments described in Table 3.4 are summarized in the following chapter of this report.

3.6 SAMPLES NOT WATER JETTED

In the spring of 2010 Caltrans instructed the project team to carry-out a supplemental testing program on a new set of ring and cylindrical samples. The objective of these new experiments was to investigate water jetting effectiveness for elevated jetting pressures between approximately 15,000 and 20,000 pounds per square inch (psi). Eight ring samples and two sets of cylindrical samples were prepared using low strength concrete (SCM) with target compressive strengths of 500, 1500, 2500 and 4000 psi. The water jetting experiments were designed to be similar to those described previously in this report, except that the jetting pressures would be higher. The new ring and cylindrical samples were never tested, however, as water jetting personnel and equipment were not made available to the research team. The research team was unable to schedule water jetting through the fall of 2010. The team requested a no-cost extension to the project in October, but Caltrans did not approve this request. A stop work order was subsequently given for the project in December 2010. Table 3.5 summarizes the samples that were prepared but not tested.

Table 3.4 - Water Jetting Test Matrix and Summary

Test Series	Test Type	Max. Aggregate (inches)	Aggregate Shape	Avg. Comp. Strength (psi)	Ring Inside Diameter (inches)	Jetting Approach (see Table 3.1)	Total Jetting Time (minutes)
SCM-01	Ring	0.375	Angular	560	2, 4, 6, 12, 16	Stationary	11, 11, 7, 4, 9
SCM-02	Ring	0.375	Angular	630	6, 12	Cycled	18, 20
SCM-03	Ring	0.375	Angular	2,350	6, 12	Cycled	24, 24
SCM-04	Ring w/Steel	0.375	Angular	160	6	Cycled	31
SCM-05	Ring w/Steel	0.375	Angular	160	6, 2, 2	Steady Upward	28, 30, 30
SCM-06	Cylindrical	0.375	Angular	160	-----	Stationary	-----
CON-01	Ring	1	Angular	4,590	6, 12	Cycled	24, 18
CON-02	Ring	1	Angular	4,820	6, 12	Cycled	24, 18
CON-03	Ring	1	Angular	6,560	6, 12	Cycled	32, 16
CON-04	Ring	1	Angular	655	6	Cycled	32
CON-05	Ring	1	Rounded	2,120	6	Cycled	32
CON-06	Cylindrical	1	Angular	3,600	-----	Stationary	-----
SMX-01	Ring	1	Angular	1,850	6, 12	Cycled	32, 20
GRT-01	Ring	0.125	-----	1,900	6, 12	Cycled	32, 22
CLY-01	Ring	-----	-----	5	6	Cycled	2
CLY-02	Ring	-----	-----	9	12	Cycled	8
CLY-03	Ring	-----	-----	7	12	Cycled	13

Table 3.5 - Summary of Ring and Cylindrical Samples Not Water Jetted

Test Series	Test Type	Max. Aggregate (inches)	Aggregate Shape	Target Comp. Strength (psi)	Ring Inside Diameter (inches)	Jetting Approach (see Table 3.1)	Total Jetting Time (minutes)
SCM-07	Ring	0.375	Angular	500	6, 6	Cycled	NOT TESTED
SCM-08	Ring	0.375	Angular	1,500	6, 6	Cycled	NOT TESTED
SCM-09	Ring	0.375	Angular	1,500	2, 2	Steady Upward	NOT TESTED
SCM-10	Ring	0.375	Angular	2,500	6, 6	Cycled	NOT TESTED
SCM-11	Cylindrical	0.375	Angular	500	-----	Stationary	NOT TESTED
SCM-12	Cylindrical	0.375	Angular	4,000	-----	Stationary	NOT TESTED

CHAPTER 4

TEST RESULTS

4.1 RING SAMPLES

Data collected during the ring sample experiments included water jetting pressure, ring dimensions, erosion due to jetting at different time intervals, total jetting time, material characteristics, and material compressive strength at the time of water jetting. These data are summarized in the following sections of this report. Data are presented for the initial ring tests on low strength concrete (i.e. Test Series SCM-01), the subsequent ring tests on various materials, and the ring tests on samples cast with longitudinal and transverse reinforcing steel.

4.1.1 Initial Ring Tests

The research team conducted an initial set of experiments using 12-inch tall ring samples consisting of SCM (low strength concrete) material. The team water jetted rings with inside diameters of approximately 2, 4, 6, 12, and 16 inches. The average compressive strength of the SCM material was approximately 560 psi at the time of water jetting, as evaluated from compression tests performed on two test cylinders.

During testing, the water jet was held stationary in the vertical direction and allowed to rotate as designed. Therefore, an "x" shaped erosion pattern was observed within the ring during testing, as noted on Figure 4.1. The research team measured the depth of erosion (from the inside face of the ring) within the "x" shaped patterns at different time intervals. Depth measurements were taken within the top and bottom erosion cavities along three cross-sections offset from one another by approximately 60 degrees. Erosion measurement locations for a single cross-section are illustrated on Figure 4.1. Recording erosion in this fashion meant that the team recorded twelve erosion depths for each time interval. From these measurements, the research team reported a minimum erosion depth, average erosion depth, and maximum erosion depth for each time interval (Heavin 2010).

The research team implemented the following test procedure for each water jetting time interval. The water pump was started, and the jetting pressure was quickly raised to the target value. For these tests, the target pressure (10,000 to 11,000 psi) was typically reached in under 5 seconds. Interval timing began once the target pressure was achieved. Water jetting then commenced for a specified period of time, which was measured using a stopwatch. When water jetting ended for a particular time interval, the team removed the water jet, drained water from the ring, removed cuttings from the

ring, and recorded depth measurements. Depth measurements were made by using a simple hand-held probe and were recorded to the nearest 1/16-inch.

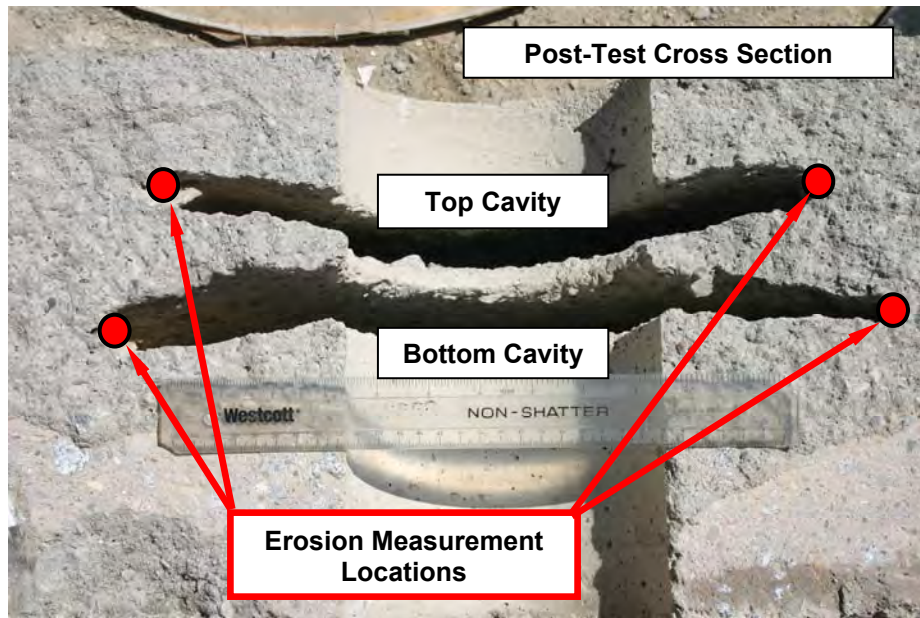


Figure 4.1 - Post-Test Photograph of the 6-inch Diameter Ring Sample, SCM-01 Test Series; Erosion Measurement Locations Noted

Figure 4.2 illustrates the variation of erosion depth as a function of total jetting time for the five ring samples examined during test series SCM-01. The graph shows average erosion depth with minimum and maximum depth measurements included as simple "error bars." Measurement of erosion depth within the 2-inch I.D. ring was made difficult due to space constraints, so only two data points are shown. The team measured the second data point after water jetting was complete and the ring sample had been cut in half.

Test results for the 2-, 4-, and 6-inch I.D. rings show that erosion rates decreased with jetting time as the radial distance between the nozzle and the cutting surface increased. Also, the majority of the total erosion occurred within the first 1 to 2 minutes of jetting. The team observed different behavior for the 12- and 16-inch I.D. rings. Figure 4.2 shows that erosion rates for these samples initially decreased with time and then increased significantly with time during a later stage of the test. An objective of these experiments was to continue water jetting until negligible erosion was measured with increasing time. The team achieved this objective for the 2-, 4-, and 6-inch I.D. ring tests but not for the 12- and 16-inch I.D. ring tests. Time constraints on the availability of the water jetting

equipment prevented the team from continuing these two ring tests beyond 4 and 8.5 minutes, respectively.

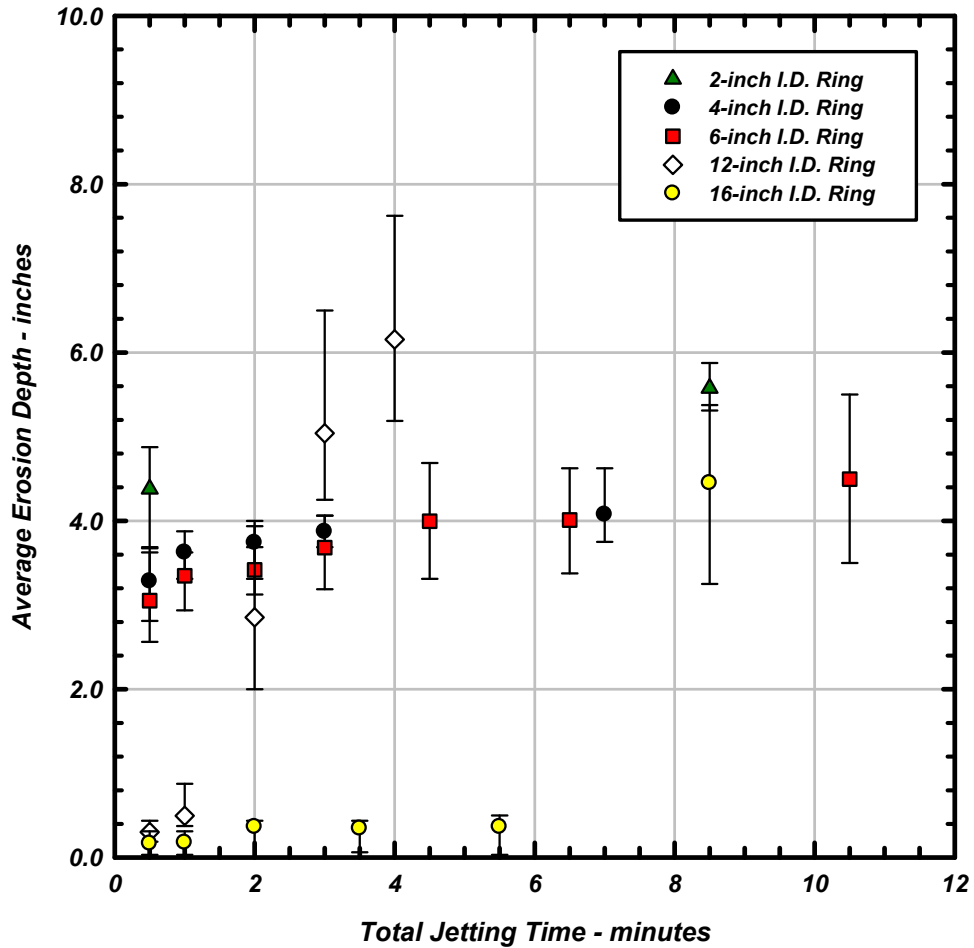


Figure 4.2 - Average Erosion Depth with Minimum and Maximum Error Bars Measured for the SCM-01 Test Series

Figure 4.3 illustrates the variation of effective eroded diameter as a function of total jetting time for the five ring samples examined during test series SCM-01. Effective eroded diameter is defined on Figure 3.15 and represents the sum of the initial ring diameter and twice the average erosion depth. This dimension approximates the size of the eroded cavity that forms around the water jet during jetting. The graph on Figure 4.3 shows average eroded diameter with minimum and maximum diameters included as simple error bars. Also shown is a hand-drawn trendline (based approximately on the reported data), which illustrates how average effective eroded diameter increases with jetting time. This trendline has a peak effective eroded diameter of 18 inches.

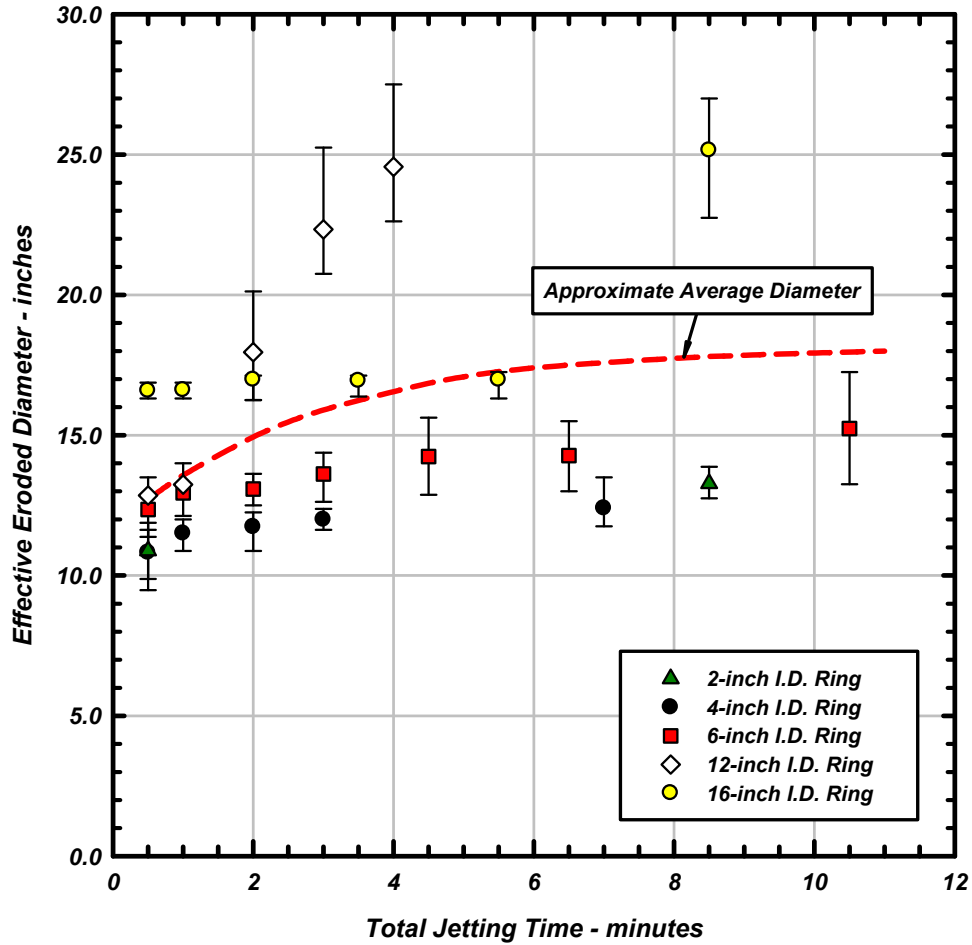


Figure 4.3 - Effective Eroded Diameter with Minimum and Maximum Error Bars Measured for the SCM-01 Test Series

Figure 4.3 shows that final effective eroded diameter generally ranged between 12 and 25 inches for the SCM-01 test series. Total jetting times for these tests exceeded 7 minutes. The 2-, 4-, and 6-inch I.D. ring samples showed similar levels of erosion after water jetting. However, the 12- and 16-inch I.D. ring samples showed higher levels of erosion. This result suggests that the size of the void space surrounding the water jet may influence jetting effectiveness. A larger initial space around the water jet generates fewer cuttings and allows for easier flow of water and cuttings during jetting, which presumably leads to less interference between the nozzles and the cutting surface. Indeed, during this project the research team observed that the jet nozzles clogged and required cleaning more often when fitted in the smaller diameter ring samples.

However, the above hypothesis does not explain the behavior observed for the 16-inch I.D. ring sample where erosion spiked after 5.5 minutes of water jetting. The level of erosion observed for this

test is not consistent with other test results discussed later in this report. One could speculate that some of the SCM-01 ring samples were weaker than expected or contained defects. When evaluating the strengths of these samples, the research team collected one set of test cylinders for the entire pour, which included five ring samples. During future tests, the team collected test cylinders for each individual ring in an attempt to better quantify material strengths. One could also speculate that boundary effects played a role during the 12- and 16-inch I.D. ring tests. The "x" shaped erosion cavities within these samples came within approximately 3 to 4 inches of the top and side faces of the ring. Under the elevated jetting pressures, the ring samples could have weakened and cracked along these erosion lines thus attributing to higher erosion levels. During future tests, the research team increased the thickness of the ring samples (from 12 to 18 inches) to reduce the potential for boundary effects during jetting.

Regardless of the explanation, the erosion data measured for the 12- and 16-inch I.D. ring samples represent the largest observed during our entire testing program. As emphasized later in this report, these data should be used with caution since the research team did not observe similar erosion levels for similar materials with similar strengths.

4.1.2 Subsequent Ring Tests

During subsequent ring tests, the research team water jetted 6- and 12-inch I.D. samples cast with various materials at different compressive strengths. The results of test series SCM-02, SCM-03, CON-01 to -05, SMX-01, GRT-01, and CLY-01 to -03 are described in this section of the report. These test series are summarized in Table 3.4. All of the ring samples were 18 inches thick. The water jet was cycled up and down during these tests according to the procedure described in Table 3.1. The team decided to cycle the water jet up and down to better flush the cuttings from inside the ring and reduce the potential for clogging of the water jet nozzles. In addition, a new jet collar plate design allowed for cuttings to be readily flushed from the inside of the ring. During the initial ring experiments the plate was fixed to the top of the sample effectively trapping the cuttings within the ring during water jetting. The modified jet collar plate allowed for easier flushing of cuttings from the ring and better represented the water jetting conditions encountered in practice.

4.1.2.1 General Observations

Cuttings observed during water jetting consisted of individual aggregates from the material mixes. During jetting, the aggregates dislodged from the sample as the more easily eroded cement binder was removed. For weaker materials, the jetted surfaces appeared relatively smooth. For stronger materials, the jetted surfaces were rougher with aggregates exposed at the surface and held in place by

very little binder. When examining jetted surfaces in the concrete samples, the research team observed that larger, protruding aggregates often created small zones of protected or "shadowed" concrete where jetting effectiveness was reduced and binder materials were less easily eroded. Such zones occurred on opposite sides of the aggregates from the water jet. In the field, downhole camera inspection of water jetted drilled shafts has revealed these shadow zones adjacent to longitudinal and transverse reinforcing steel bars (Liebich 2008). Figure 4.4 shows an incident of shadowing observed during the SCM-01 test series.

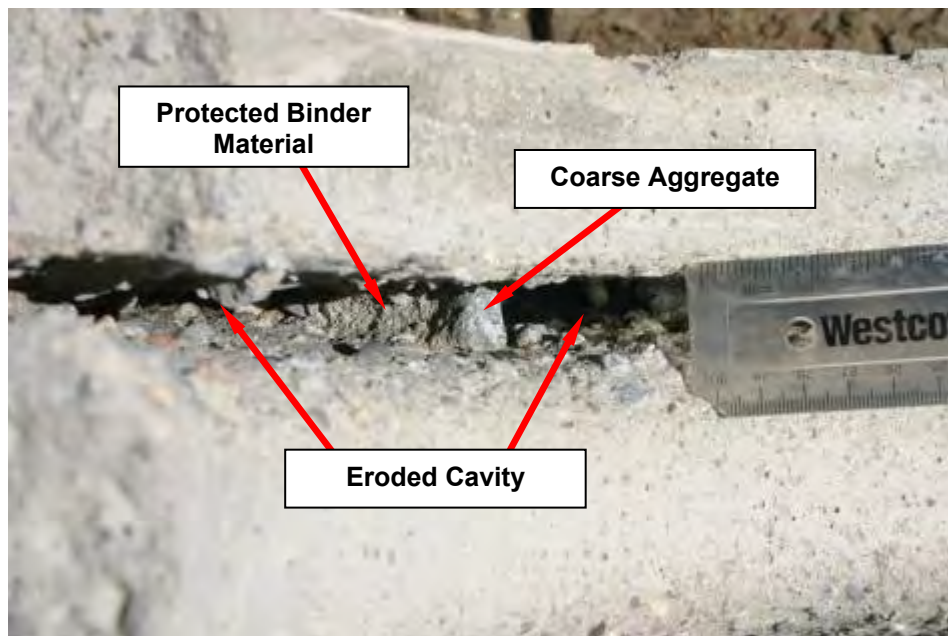


Figure 4.4 - Photograph Showing Protected Binder Material and Shadowing Observed during Test Series SCM-01

For the concrete ring samples (SCM, CON, and SMX series), the research team did not observe large pieces of concrete in the cuttings. Further, the cut surfaces did not show signs of spalling. However, this was not the case for the bentonite-cement samples (CLY series). For these materials, the jetted surfaces appeared more irregular with evidence that some material had been removed in small chunks. Rockwell (1981) observed similar behavior when water jetting clays for trench excavation. As expected, the team observed significant erosion when jetting the bentonite-cement samples. As erosion extended further into the ring sample, large chunks of clay occasionally fell from the roof of the jetting cavity into the path of the water jet. Interestingly, only small chunks of clay were found in the bottom of the cavity after jetting, which suggests that the larger chunks were broken down as they

circulated and washed around the water jet. It is possible that these chunks interfered with the water jetting occurring at the outer surfaces of the cavity.

4.1.2.2 Test Results

The research team implemented a testing procedure similar to that described for the SCM-01 test series. This procedure was described in Section 4.1.1 of this report. All tests were performed using jetting pressures that ranged between approximately 10,000 and 11,000 psi. As noted, the water jet was cycled up and down during these tests. Therefore, a cylindrical cavity developed within the ring samples during jetting, as described on Figure 3.14(b). The research team took erosion measurements within this cavity according to the schedule described on Figure 3.15. Recording erosion in this fashion meant that the team recorded eighteen erosion depths for each time interval. From these measurements, the team reported a minimum erosion distance, average erosion distance, and maximum erosion distance for each time interval (Heavin 2010).

Figure 4.5 presents test results for 6-inch concrete ring samples with four different compressive strengths. During each of these tests, the team cycled the water jet up and down over a distance of 6 inches at a rate of approximately 7 cycles per minute. The plot shows average erosion distance as a function of jetting time, with erosion distance defined on Figure 3.15. The results on Figure 4.5 show that the effectiveness of the water jet depends on the compressive strength of the material: the weakest material eroded most easily. Erosion rates for the samples decrease with time as the radial distance between the nozzle and the cutting surface increases. The results also show that approximately 80 percent of the final erosion occurs after about 8 minutes of water jetting. Data trends similar to those apparent on Figure 4.5 were observed for all of the 6- and 12-inch ring tests summarized in this section.

Figure 4.6 shows average erosion distance as a function of jetting time for tests SCM-03, CON-05, SMX-01, and GRT-01. Results are shown for tests conducted using 6-inch ring samples. The materials used in these tests had similar compressive strengths but different aggregate characteristics. The results on the figure suggest that aggregate characteristics, including particle size and angularity, do not strongly influence jetting effectiveness. This includes the shadowing of concrete behind large aggregates which, while noticeable, did not affect the overall erosion results. Average erosion distances on Figure 4.6 are similar for all four materials at similar time intervals. Further, the removal rates are consistent and show diminishing water jetting effectiveness after about 15 to 20 minutes of jetting.

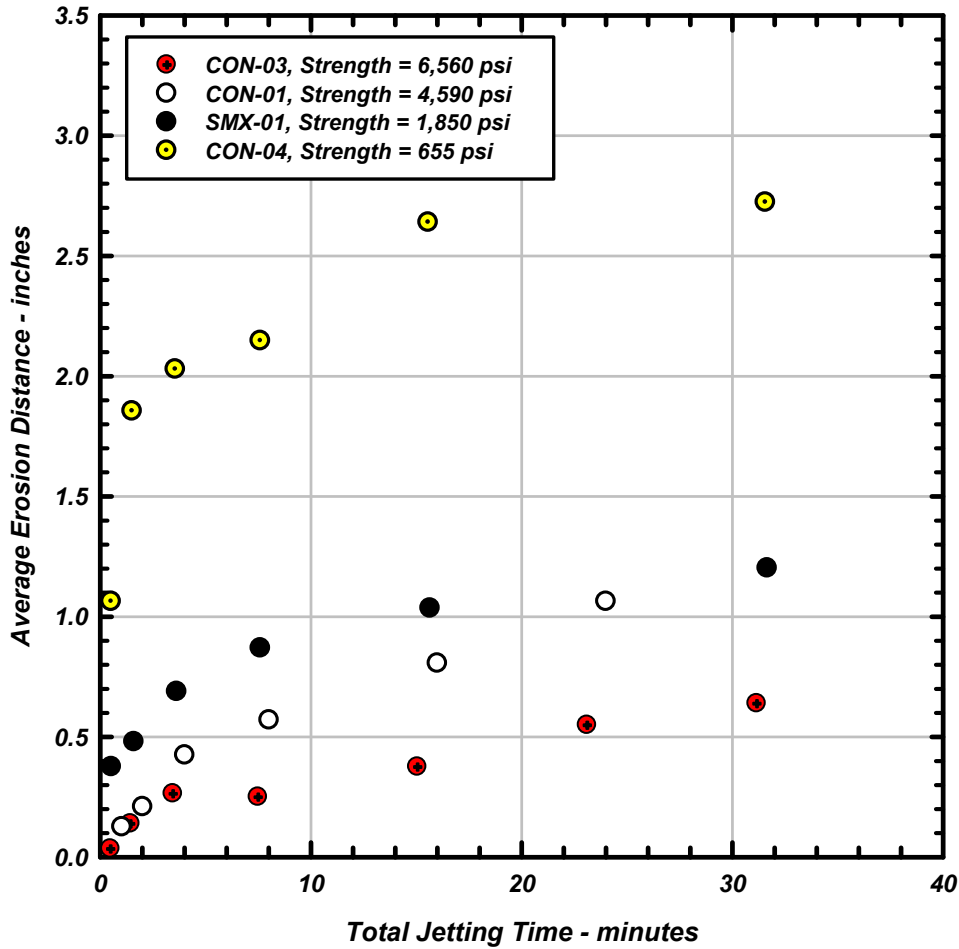


Figure 4.5 - Average Erosion Measured for 6-inch I.D. Concrete Ring Samples

Compared on Figure 4.7 are the results of three water jetting tests: SCM-01, SCM-02, and CON-04. Each test was performed using a 6-inch ring. For SCM-01, the water jet remained in a fixed vertical position during jetting. For SCM-02 and CON-04, the research team cycled the water jet up and down following the procedure described previously. As evident on Figure 4.7, ring sample SCM-01 experienced approximately 15 to 80 percent more erosion than sample SCM-02, when considering the range of erosion measured for SCM-01 after about 10.5 minutes of water jetting. Even though the rings both included low strength concrete materials, a larger amount of erosion would be expected for ring sample SCM-01 since this sample was about 13 percent weaker than sample SCM-02. Also, one would expect potentially more erosion over the same time interval since the stationary jet used during test SCM-01 was in direct contact with a relatively small area of the sample for the entire testing period. During the cyclic test (SCM-02), the jet was in direct contact with this same area of the sample for only a fraction of the time; therefore, less erosion would be expected over the same time

increment. Based on the design of the test apparatus and the testing procedure, the research team estimated that a sample subject to cyclic jetting is in direct contact with the jet for approximately one-fifth of the time observed for the stationary jet.

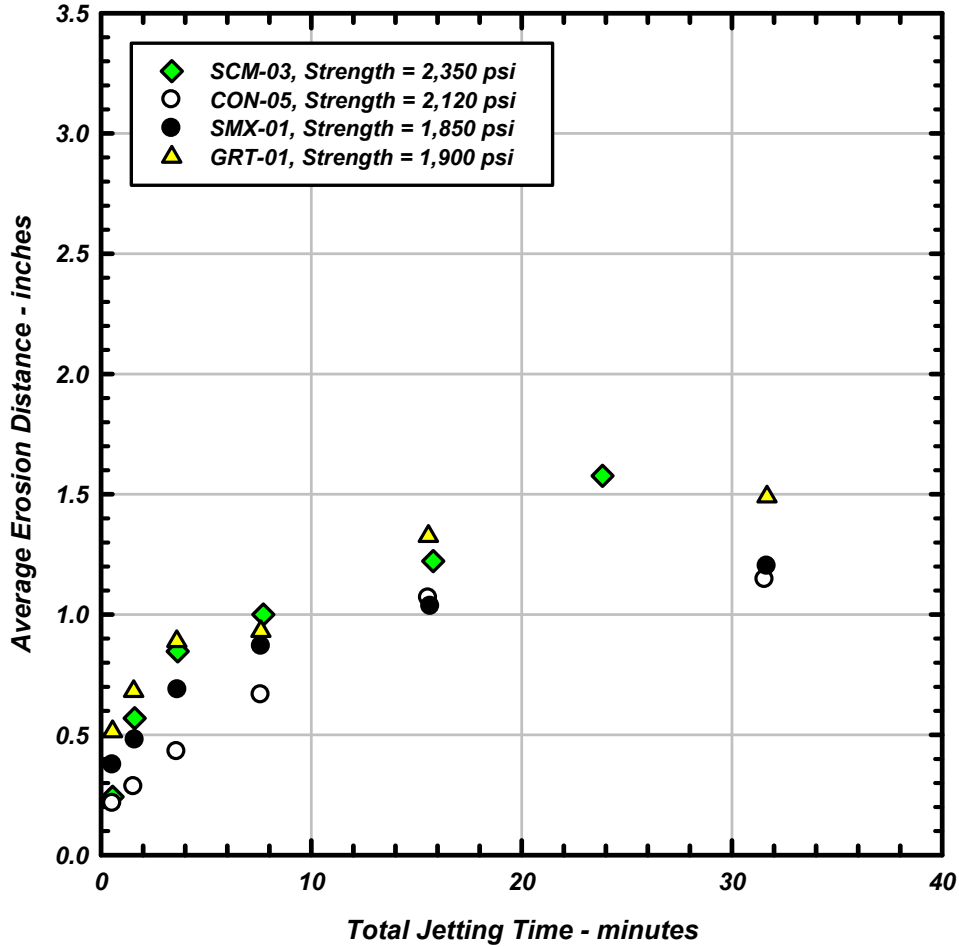


Figure 4.6 - Average Erosion Measured for 6-inch I.D. Ring Samples with Similar Compressive Strengths

Curves 1 and 2 on Figure 4.7 represent trendlines for the erosion distances measured during tests SCM-01 and SCM-02, respectively. Also included on Figure 4.7 is a modified version of Curve 2: the time values of this curve were divided by five (to account for jetting time differences between SCM-01 and SCM-02) and the erosion values were increased by 13 percent (to account for differences in compressive strength between SCM-01 and SCM-02). As apparent, the modified curve falls within the range of data measured during SCM-01. This result further illustrates the influence of compressive strength on water jetting effectiveness. In addition, the result suggests that contact time during water jetting has some influence on jetting effectiveness and erosion rate.

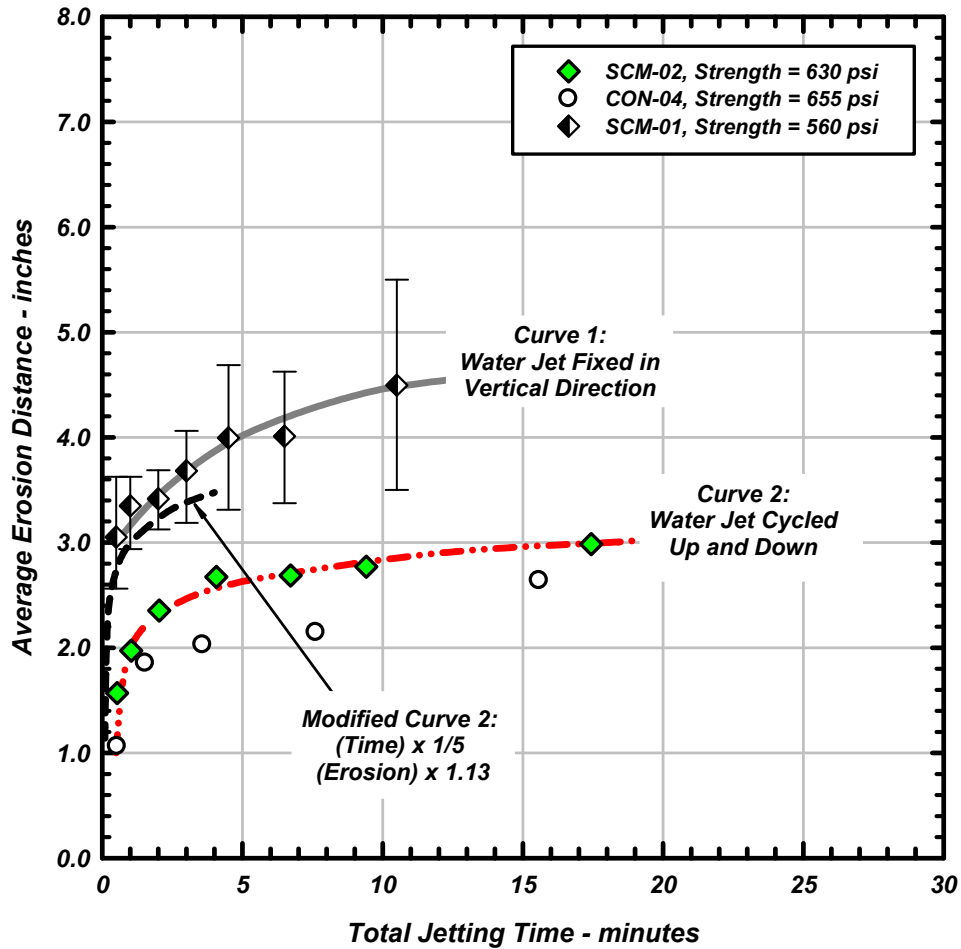


Figure 4.7 - Average Erosion Measured for 6-inch I.D. Low Strength Concrete Ring Samples Subject to Stationary and Cyclic Jetting

The research team further investigated jetting approach and contact time by performing supplemental experiments on the 12-inch rings tested under series CON-02 and SMX-01. After cyclic jetting was completed for a sample, the water jet was fixed inside the ring. The ring was then water jetted for several more minutes. Erosion levels measured after this supplemental jetting were negligible for both samples, indicating that the stationary jetting approach did not cause continued erosion. Standoff distance controlled the level of erosion measured for these samples - not jetting approach.

Table 4.1 summarizes final erosion distances for the ring tests described in this section. Final erosion distances represent the level of erosion measured at the conclusion of water jetting. Total water jetting times typically ranged between about 20 and 30 minutes, with some exceptions. Table 3.4 lists total jetting times for each test. Table 4.1 includes minimum, maximum, and average final erosion distances for both the 6-inch and 12-inch I.D. ring samples. Compressive strengths are also listed for

each test series. The absence of erosion data in Table 4.1 means that a ring test was not performed. As reported in Table 3.4, both 6- and 12-inch ring samples were not prepared for all of the test series.

Table 4.1 - Final Erosion Distances for the Ring Samples

Test Series	Strength (psi)	Inches of Erosion: 6" Rings			Inches of Erosion: 12" Rings		
		Min.	Avg.	Max.	Min.	Avg.	Max.
SCM-02	630	2.375	2.986	3.875	0.625	1.590	2.750
SCM-03	2,350	0.875	1.576	2.625	0.250	0.465	0.875
CON-01	4,590	0.625	1.063	1.625	0.188	0.271	0.438
CON-02	4,820	0.500	0.806	1.125	0.000	0.111	0.125
CON-03	6,560	0.375	0.639	1.000	0.000	0.139	0.188
CON-04	655	1.875	2.722	3.750	-----	-----	-----
CON-05	2,120	0.375	1.146	2.250	-----	-----	-----
SMX-01	1,850	0.625	1.201	1.875	0.250	0.351	0.438
GRT-01	1,900	0.375	1.490	2.250	0.188	0.433	0.750
CLY-01	5	5.312	5.826	6.312	-----	-----	-----
CLY-02	9	-----	-----	-----	1.000	2.510	4.125
CLY-03	7	-----	-----	-----	4.625	5.313	6.000

Table 4.2 shows how the final effective eroded diameter varied for each of the ring samples listed in Table 4.1. Effective eroded diameter is defined on Figure 3.15 and represents the sum of the initial ring diameter and twice the erosion distance along a particular cross-section.

Table 4.2 - Final Effective Eroded Diameters for the Ring Samples

Test Series	Strength (psi)	Eff. Diameter (in): 6" Rings			Eff. Diameter (in): 12" Rings		
		Min.	Avg.	Max.	Min.	Avg.	Max.
SCM-02	630	12.00	12.35	12.88	14.63	15.55	16.50
SCM-03	2,350	9.00	9.53	10.00	12.88	13.31	13.75
CON-01	4,590	8.25	8.50	8.75	12.75	12.92	13.25
CON-02	4,820	7.50	7.99	8.25	12.38	12.60	12.75
CON-03	6,560	7.13	7.57	8.13	12.38	12.53	12.75
CON-04	655	11.38	11.82	12.50	-----	-----	-----
CON-05	2,120	7.88	8.67	9.25	-----	-----	-----
SMX-01	1,850	8.25	8.78	9.00	12.90	13.08	13.31
GRT-01	1,900	8.13	9.35	10.13	12.94	13.24	13.81
CLY-01	5	17.00	18.03	19.00	-----	-----	-----
CLY-02	9	-----	-----	-----	16.25	17.40	18.50
CLY-03	7	-----	-----	-----	21.625	23.000	24.375

Effective eroded diameter approximates the size of the eroded cavity that forms around the water jet during jetting. Table 4.2 includes minimum, maximum, and average final diameters for both the 6-inch and 12-inch I.D. ring samples.

Average final effective eroded diameters in Table 4.2 are plotted as a function of compressive strength (on a logarithmic scale) on Figure 4.8. The results further demonstrate the influence of compressive strength on water jetting effectiveness. An effective eroded diameter of approximately 23 inches was observed for one of the bentonite-cement samples, representing the largest effective eroded diameter reported. Figure 4.8 shows that effective eroded diameters are larger for the 12-inch ring samples, in comparison with the 6-inch samples. This result provides further evidence that the size of the void space surrounding the water jet influences jetting effectiveness.

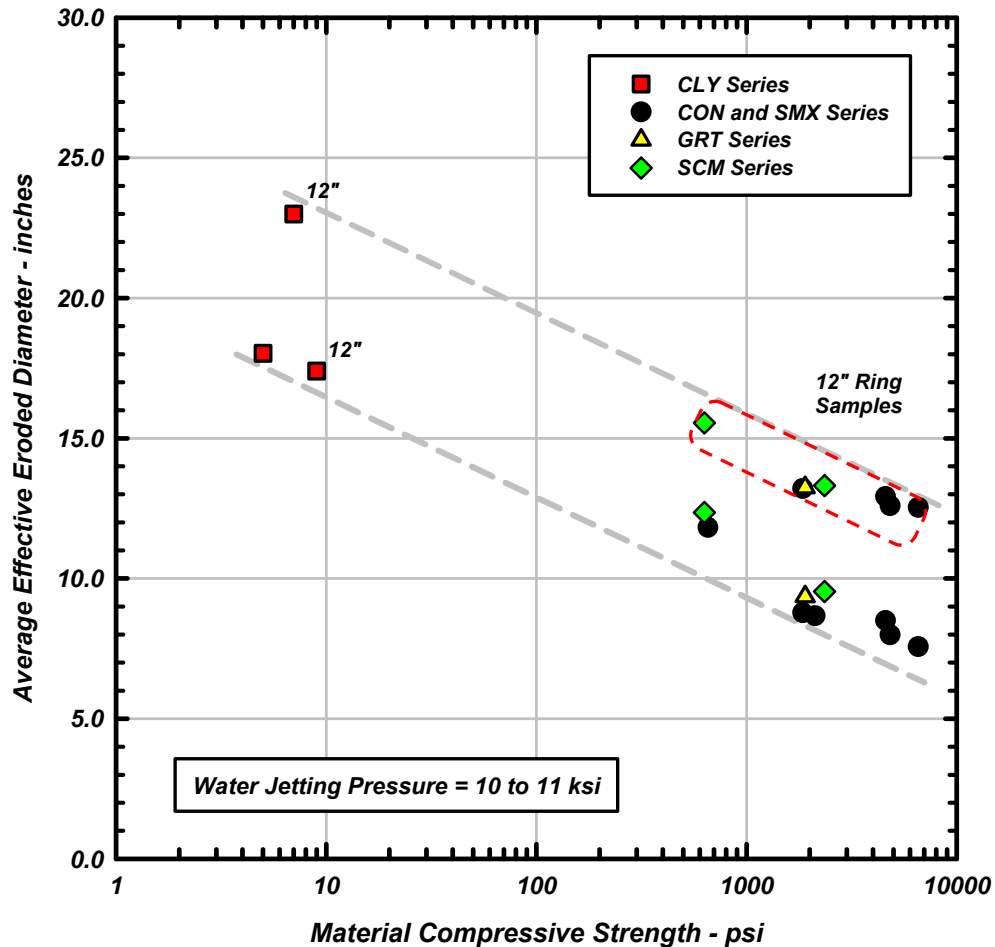


Figure 4.8 - Average Effective Eroded Diameter for 6- and 12-inch I.D. Ring Samples

4.1.3 Ring Tests with Reinforcing Steel Bars

Test series SCM-04 and SCM-05 included four ring samples cast with longitudinal and transverse reinforcing steel bars. The primary objective of these tests was to evaluate the influence of reinforcing steel on water jetting effectiveness. The four sample configurations were described in Chapter 3 of this report on Figures 3.6, 3.7, and 3.8. Table 3.4 lists sample dimensions and material properties for the four ring samples. The rings had inside diameters of 2 and 6 inches and included low strength concrete (SCM) material. All of the rings were 18 inches thick (Schaffer 2011).

Figure 4.9 includes a post-test photograph of the 6-inch I.D. ring sample tested under series SCM-04. The photo shows a cross-section through the center of the ring sample, including the water jetted cavity and two of the longitudinal reinforcing steel bars. The water jet was cycled up and down during this test following the procedure described previously. As noted on Figure 4.9, the team observed shadow zones of un-eroded material behind the reinforcing steel bars.

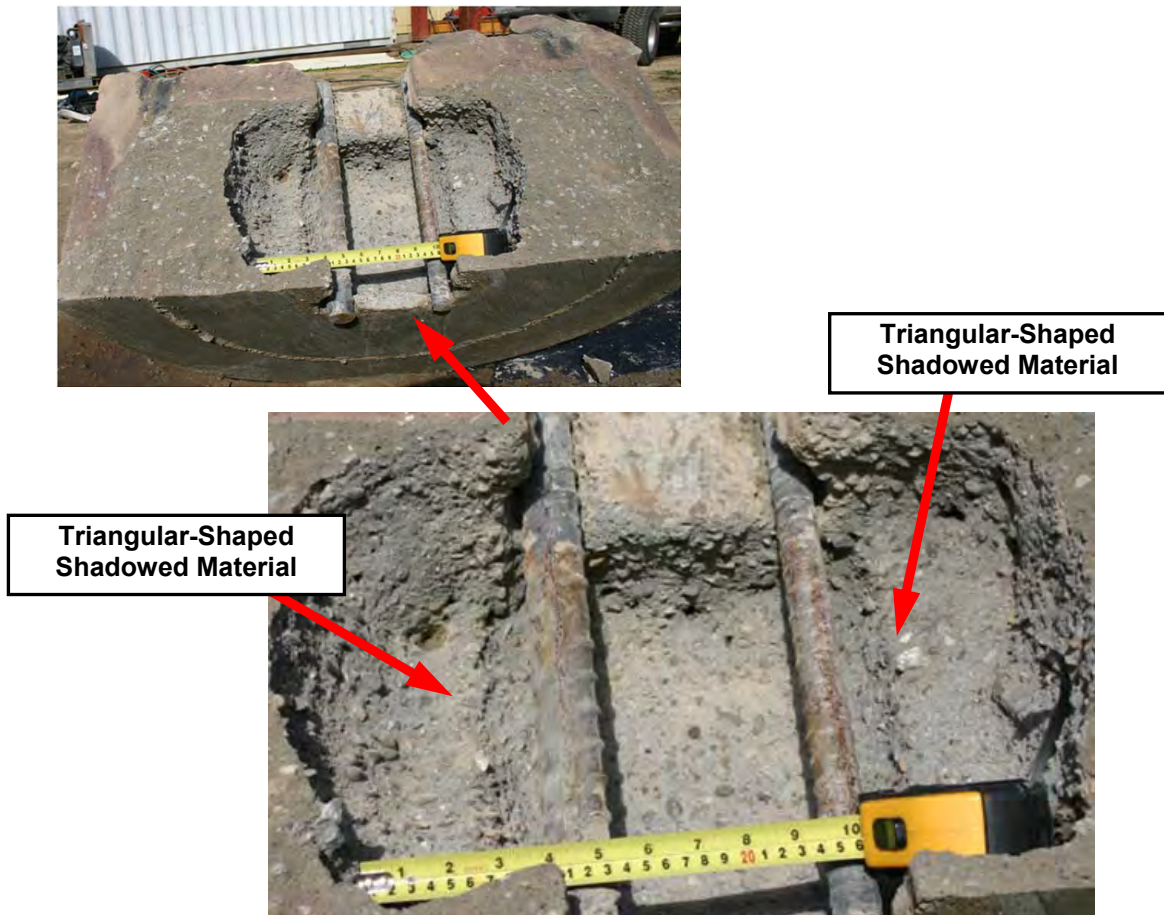


Figure 4.9 - Post-Test Photographs of Test SCM-04

Figure 4.10 shows post-test photographs of the 6-inch I.D. ring sample tested under series SCM-05. This ring sample was configured the same as SCM-04. However, during this experiment, the research team raised the water jet steadily upward during water jetting. The "steady upward" approach to water jetting is described in Table 3.1. The results summarized on Figure 4.10 are similar to those included on Figure 4.9. However, the surface of the jetting cavity is rougher for test SCM-05. The "steady upward" jetting approach leads to this rougher, less polished cavity surface.

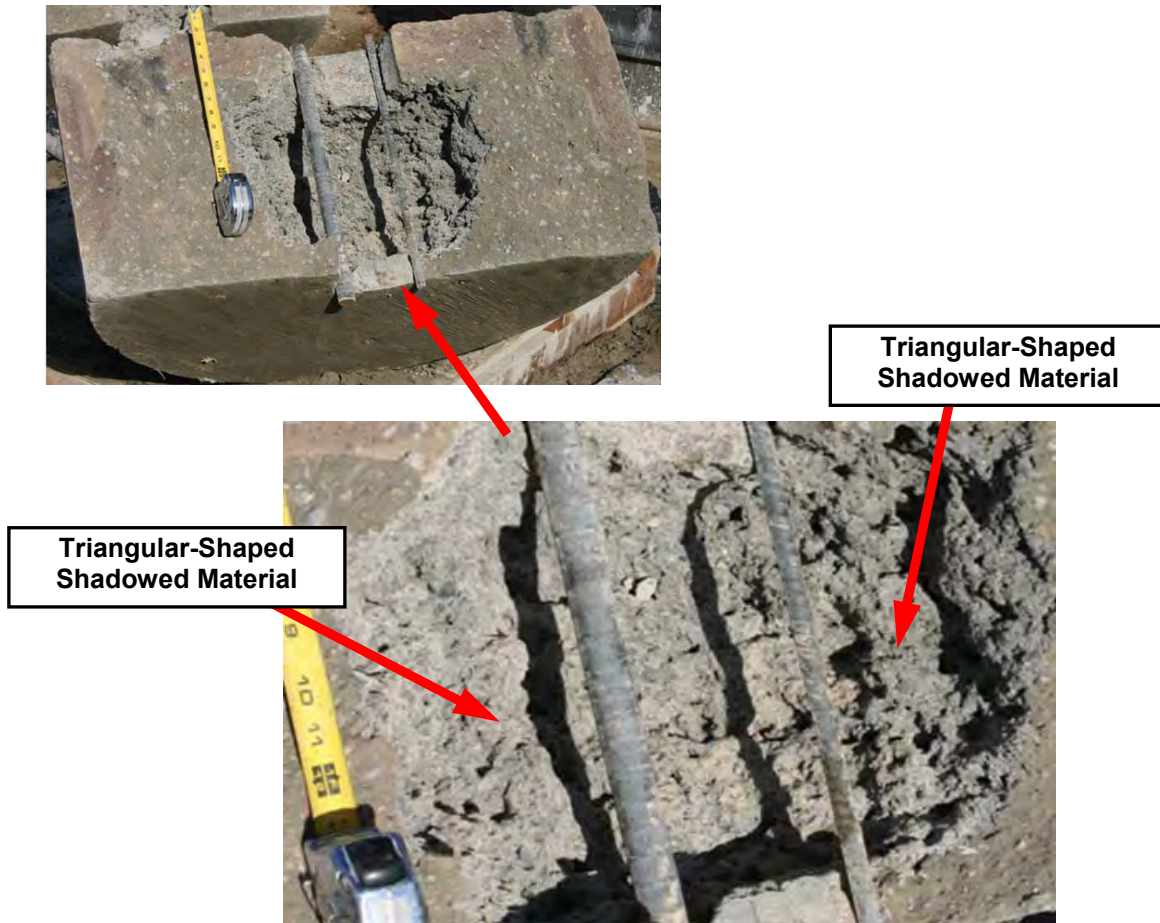


Figure 4.10 - Post-Test Photographs of Test SCM-05

Figure 4.11 illustrates, in general, the team's observations for the 6-inch inside diameter rings cast with the #4, #8, #11, and #14 longitudinal reinforcing steel bars. Recognizable shadow zones developed directly behind each of the bars cast within the sample. The size of a shadow zone tended to increase with increasing bar diameter. The shadows were more clearly distinguishable for the test where the water jet was cycled up and down during testing (SCM-04). Similar size shadows were observed for the test where the water jet was raised steadily upward (SCM-05); however, the jetting

surfaces in this test were rougher, more pitted, and less clearly defined. It is noted that the effective diameter of the eroded cavity was similar in size for tests SCM-04 and SCM-05, which indicates that the method of jetting (i.e. cyclic up and down versus steady upward) did not significantly influence water jetting effectiveness. During water jetting, concrete materials were completely removed from around all of the reinforcing bars in the sample. The bars were essentially blasted clean of aggregates and cement binder. Similar results were observed for the ring samples that were cast with a typical rebar cage section.

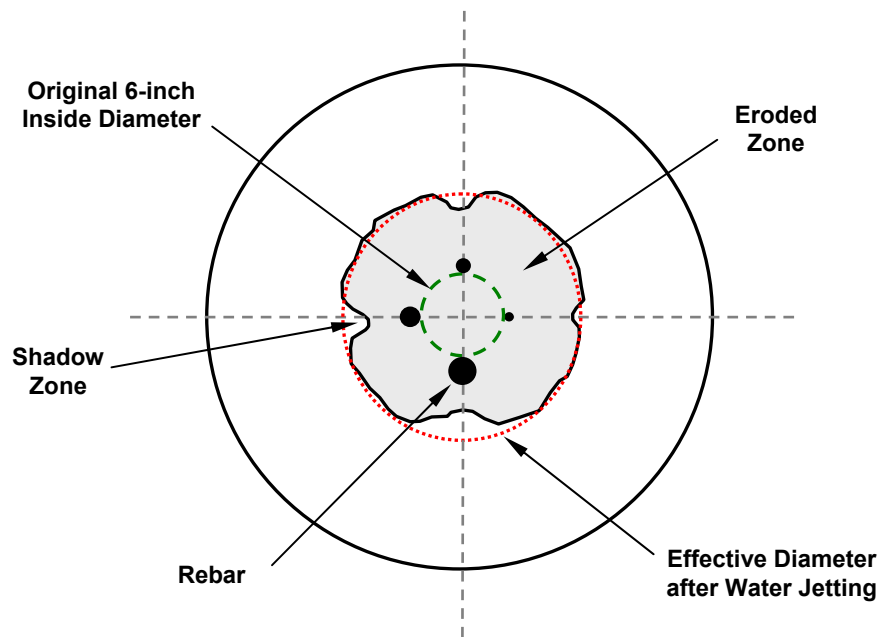


Figure 4.11 - Plan View Illustration of Shadow Effects Observed during Water Jetting of the SCM-04 and -05 Samples

The final erosion distances measured for tests SCM-04 and SCM-05 were comparable with erosion distances observed for similar ring samples where reinforcing steel bars were not included. Figure 4.12 shows the erosion distances measured during these tests. Erosion measurements during these tests were found using the schedule illustrated on Figure 3.17. A single data point is shown for test SCM-05 since erosion measurements were taken only at the conclusion of water jetting. From the data on Figure 4.12, average effective eroded diameters for the SCM-04 and SCM-5 6-inch I.D. ring samples were found to be 16.2 and 15.5 inches, respectively. These results compare favorably with the data presented on Figure 4.8.

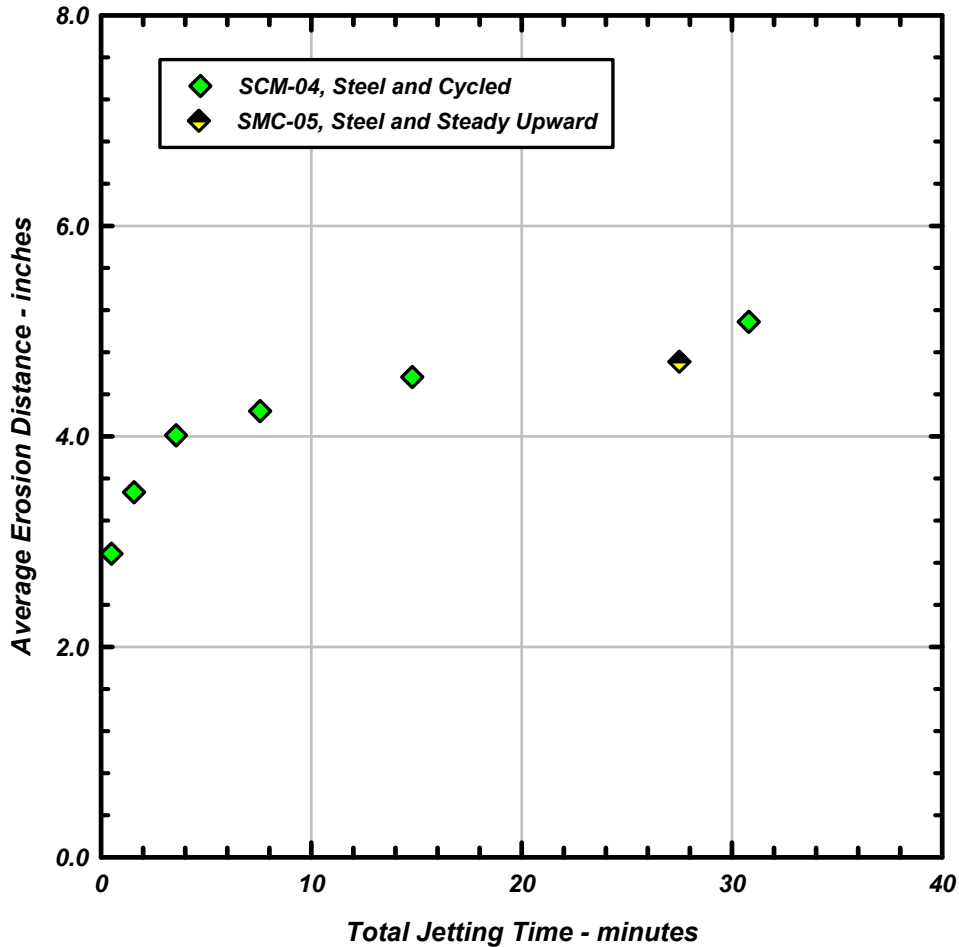


Figure 4.12 - Average Erosion Measured during Tests SCM-04 and SCM-05

The erosion results for tests SCM-04 and SCM-05 suggest that the reinforcing steel within the eroded zone does not interfere with jetting effectiveness (except immediately behind the reinforcing steel bars). Certainly, the overall effectiveness of a water jetting operation could be influenced by the spacing between the reinforcing steel bars. Additional ring samples tested in this study included reinforcing steel layouts that are typical in design practice. Closely spaced reinforcing steel bars could create overlapping shadow zones of anomalous material, which could be difficult to remove without coring additional access holes from the top of the drilled shaft. The results on Figure 4.11 also show that the "cyclic" and "steady upward" jetting approaches led to similar erosion levels after extended periods of jetting. As noted previously, the method of jetting did not significantly influence water jetting effectiveness during these experiments.

The research team quantified the shadow effect observed behind the reinforcing steel bars by measuring the distance from the rear edge of the bar to the eroded surface (i.e. shadow apex).

Figure 4.13 illustrates the shadow height (s) as defined in this study. Shadow height is computed by subtracting the amount of erosion directly behind the reinforcing steel bar (x) from the average effective eroded diameter (Schaffer 2011).

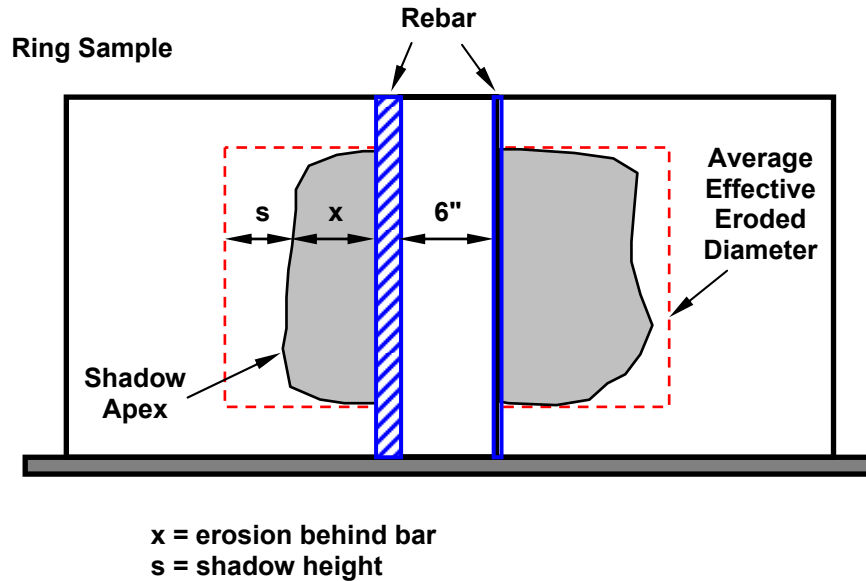


Figure 4.13 - Explanation of Shadow Height Measurements for Tests SCM-04 and SCM-05

Tables 4.3 and 4.4 summarize average shadow heights for tests SCM-04 and SCM-05, respectively. Average shadow heights are computed for each of the four reinforcing steel bars used in these tests. The research team computed average erosion behind each bar by recording gap measurements at approximately 2-inch vertical intervals within the eroded cavity. Four to seven gap measurements were recorded for each bar.

Table 4.3 - Average Shadow Heights for Test SCM-04

Long. Bar #	Bar Diameter (in)	Distance from Rebar to Shadow Apex at Various Heights within the Cavity "x" (in)	Average "x" (in)	Average Shadow Height "s" (in)
#4	0.5	2.5, 3.5, 3.0, 3.75	3.19	1.40
#8	1.0	2.125, 1.875, 3.0, 2.625, 3.125	2.55	1.54
#11	1.41	1.25, 1.25, 2.5, 2.75, 2.5	2.05	1.63
#14	1.69	1.75, 0.75, 2.625, 1.625, 2.25	1.80	1.60

Table 4.4 - Average Shadow Heights for Test SCM-05

Long. Bar #	Bar Diameter (in)	Distance from Rebar to Shadow Apex at Various Heights within the Cavity "x" (in)	Average "x" (in)	Average Shadow Height "s" (in)
#4	0.5	2.125, 1.875, 2.75, 2.5, 3.25, 2.75, 3.25	2.64	1.57
#8	1.0	2.0, 1.75, 3.0, 1.875, 2.75	2.28	1.43
#11	1.41	3.25, 0.5, 2.5, 1.5, 2.25, 2.0, 2.25	2.04	1.26
#14	1.69	0.5, 0.125, 1.75, 1.375, 1.625, 1.25, 1.375	1.14	1.87

The research team encountered some difficulties when testing the ring samples cast with rebar cage sections (i.e. longitudinal and transverse reinforcing steel arrangements). Figures 3.7 and 3.8 show the configurations used during these two tests. The team constructed each ring sample with a 2-inch diameter access hole designed to represent the hole created by a typical PVC access tube in practice. These samples were tested using the "steady upward" approach: the water jet was raised slowly upward a distance of 6 inches over a period of 30 minutes (Schaffer 2011).

After dissecting these samples, the research team found that several of the longitudinal reinforcing bars moved during water jetting, which made it difficult to draw conclusions regarding shadow effects. In addition, the team found evidence that the water jet ceased rotating at different times during the tests (i.e. tube-like jetting cavities were observed inside the ring instead of surfaces like the ones shown on Figures 4.9 and 4.10). Clogging of the 2-inch diameter access hole and the water jet assembly likely caused the jet to stop rotating during testing. This clogging occurred despite the fact that water jetting effluent was allowed to escape through the bottom and top of the ring sample (The team cut a hole through the plywood base and tested the sample on a small platform, which permitted the cuttings to flush up and down from inside the ring). Overall, the seizing of the water jet swivel reduced the efficiency and effectiveness of the jetting operation for these samples, which has implications for practice.

The research team observed some evidence of shadowing after testing the ring sample cast with rebar cage sections. In general, shadow effects were more pronounced for rebar located farther from the water jet. In addition, the team observed larger shadows behind areas where longitudinal and transverse reinforcing steel segments were tied together.






4.2 CYLINDRICAL SAMPLES

Data collected during the cylindrical sample experiments included water jetting pressure, standoff distance, erosion depth, material characteristics, and material compressive strength at the time of water jetting. These data are summarized in the following section of this report. The research team conducted water jetting tests on two sets of 6- by 12-inch concrete cylinders with 160 and 3,600 psi compressive strengths (i.e. test series SCM-06 and CON-06, respectively). Standoff distances for these tests ranged from 1.5 to 16 inches, and water jetting pressures varied between 2,400 and 10,700 psi. Figure 3.16 shows the typical erosion pattern observed for a concrete cylinder subject to water jetting and depicts how erosion depths were measured. Chapter 3 summarizes the procedure the research team followed when testing the cylindrical samples. Recall that the cylindrical samples were jetted for a period of 1 to 2 minutes for each jetting pressure. Previous ring tests incorporating a stationary water jet showed that the majority of observed erosion occurs during this 1 to 2 minute time period (see Figure 4.2).

Table 4.5 illustrates the results of a cylinder test performed under test series CON-06. These results were typical of those observed during testing of the cylindrical samples. Shown in Table 4.5 are photographs of five 3,600 psi cylindrical samples each subject to different water jetting pressures. Each sample was placed at a standoff distance from the water jet equal to 1.5 inches. Erosion patterns are visible on four of the five samples included in Table 4.5. The only exception is sample (a). For sample (a), the jetting pressure was not high enough to cause erosion during the 1 to 2 minute jetting interval. Therefore, erosion was not visible on the cylindrical specimen. As summarized in the table, maximum erosion depth increased as the jetting pressure increased, which was expected. The research team used this data to prepare graphs showing erosion depth as a function of standoff distance.

Figure 4.14 shows measured erosion depth as a function of standoff distance and jetting pressure for sample SCM-06 (160 psi). In all instances for which erosion occurred, an increase in jet pressure resulted in a corresponding increase in erosion depth. The team did not observe any erosion on cylinders located at standoff distances of 12 inches or greater. It is noted that sample SCM-06 was not tested at close range under high jetting pressures because the test cylinder would have been eroded completely through. Figure 4.15 shows measured erosion depth as a function of standoff distance and jetting pressure for sample CON-06 (3,600 psi). The results are similar to those presented on Figure 4.14, but the erosion depths are smaller. The research team did not observe any erosion on cylinders located at standoff distances of 7.75 inches or greater. In addition, the team did not observe erosion for any of the cylinders tested under a jetting pressure of 2,400 psi.

Table 4.5 -Example Results for Test Series CON-06, Standoff Distance Equal to 1.5 inches

				
<p>(a) Jetting Pressure: 2,400 psi</p>	<p>(b) Jetting Pressure: 4,000 psi</p>	<p>(c) Jetting Pressure: 6,000 psi</p>	<p>(d) Jetting Pressure: 8,200 psi</p>	<p>(e) Jetting Pressure: 10,700 psi</p>
<p>Jetting Interval: 1-2 minutes</p>	<p>Jetting Interval: 1-2 minutes</p>	<p>Jetting Interval: 1-2 minutes</p>	<p>Jetting Interval: 1-2 minutes</p>	<p>Jetting Interval: 1-2 minutes</p>
<p>Maximum Erosion Depth: 0 in.</p>	<p>Maximum Erosion Depth: 0.28 in.</p>	<p>Maximum Erosion Depth: 0.63 in.</p>	<p>Maximum Erosion Depth: 0.91 in.</p>	<p>Maximum Erosion Depth: 1.16 in.</p>

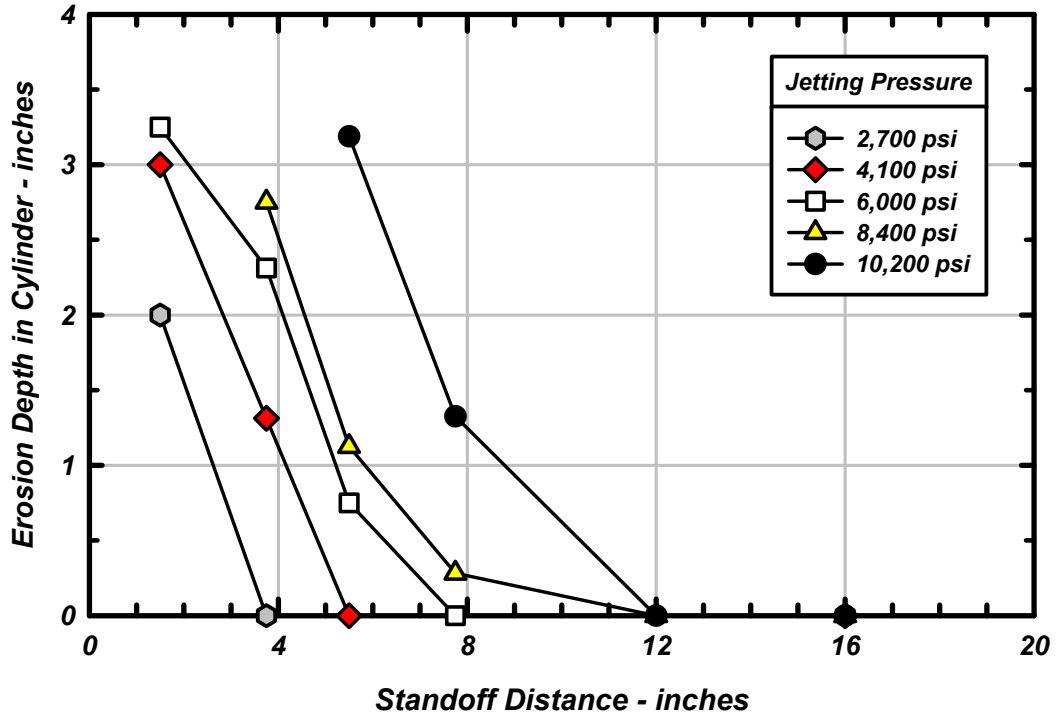


Figure 4.14 - Cylinder Erosion Depth as a Function of Jetting Pressure and Standoff Distance for SCM-06 (compressive strength = 160 psi)

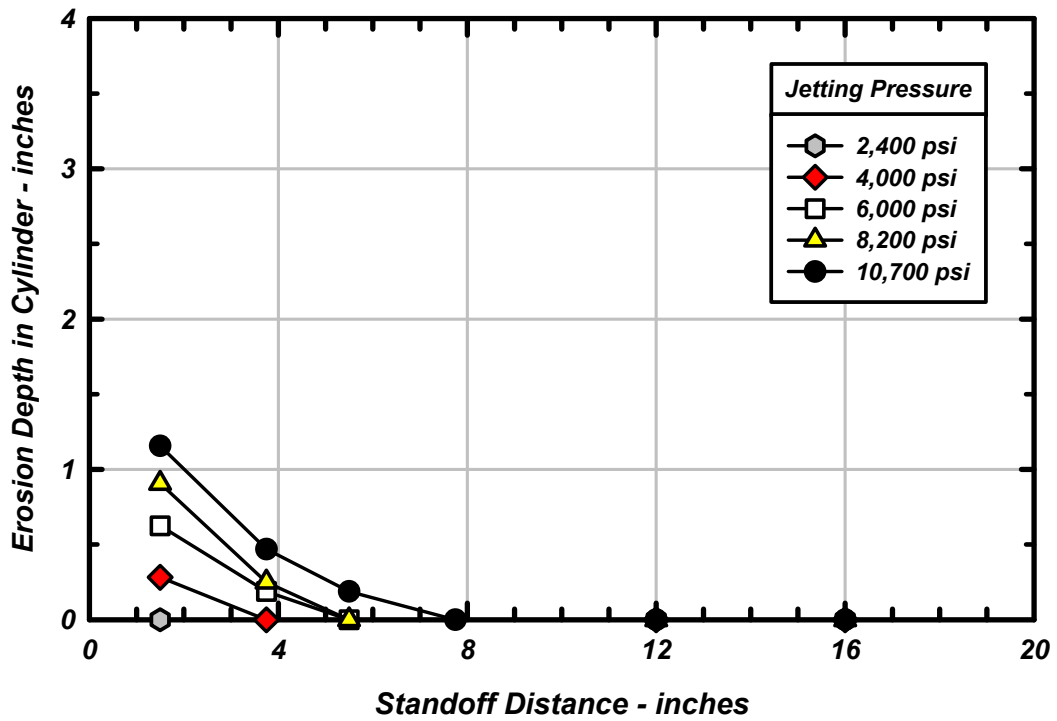


Figure 4.15 - Cylinder Erosion Depth as a Function of Jetting Pressure and Standoff Distance for CON-06 (compressive strength = 3,600 psi)

Figure 4.16 shows the cylinder test results in terms of maximum jetting distance as a function of water jetting pressure, with maximum jetting distance defined as the sum of the standoff distance of the farthest affected cylinder and its corresponding erosion depth. Data are shown on this graph for test series SCM-06 and CON-06. The points on Figure 4.16 identify how far the water jet can effectively act for different jetting pressures. These results likely bracket the jetting behavior expected for many deleterious materials encountered in drilled shafts, given the wide range in compressive strength.

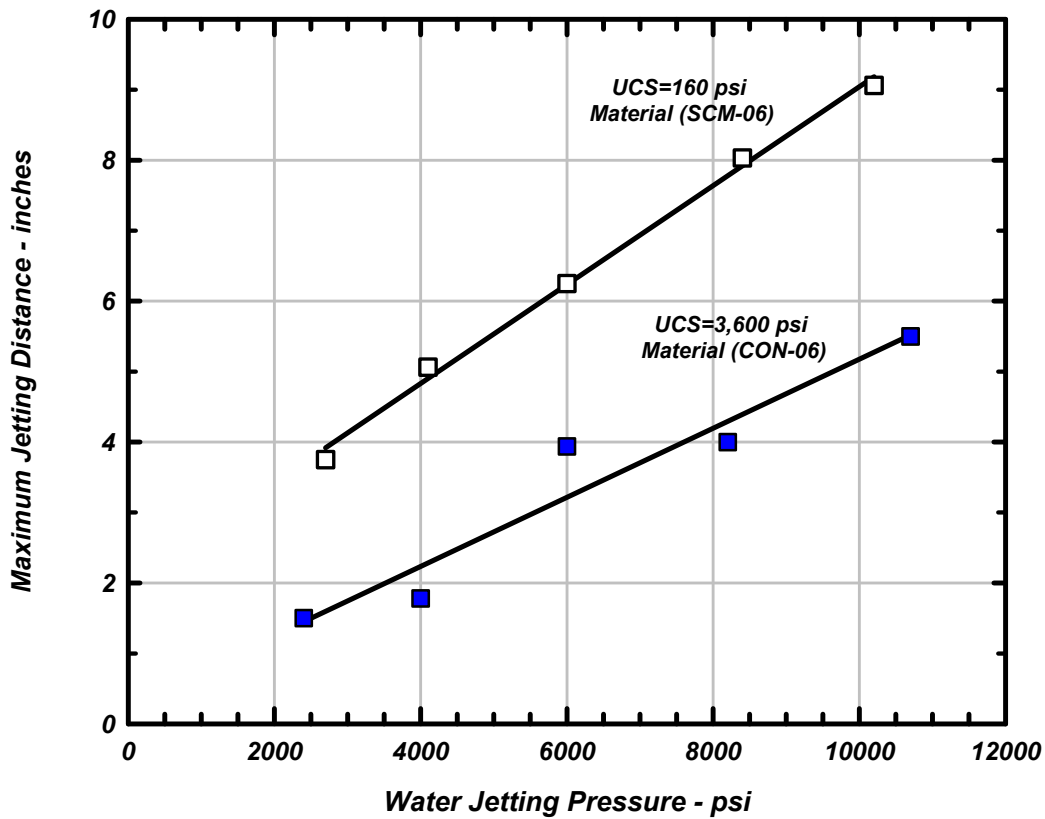


Figure 4.16 - Maximum Jetting Distance as a Function of Jetting Pressure for the 160 psi (SCM-06) and 3,600 psi (CON-06) Cylinder Tests

As evident from Figure 4.16, the water jet effectively acted over a maximum distance of approximately 9 inches for the 160 psi material at a jetting pressure of 10,200 psi. For the 3,600 psi material, an effective distance of approximately 5.5 inches was measured for a jetting pressure of 10,700 psi. These results compare favorably with the results shown on Figure 4.8. Maximum jetting distances of 9 and 5.5 inches equate to effective eroded diameters of about 20 and 13 inches, respectively, when considering the fact that the water jet housing has a diameter of about 2 inches.

These diameters (and their corresponding compressive strengths) plot at the upper range of erosion observed during the ring sample tests. It is likely that ring samples would exhibit less erosion than solid cylindrical samples (for a given jetting pressure and standoff distance) as a result of increased turbulence within the ring due to the presence of cuttings within a confined space.

4.3 WATER JETTING OF PVC ACCESS TUBES

The research team tested the PVC tube specimens following a procedure similar to that used during the concrete cylinder tests. This procedure is describe in Chapter 3. The research team tested tube specimens at jetting pressures of 2400, 4200, 6000, 8000, and 10400 psi and standoff distances equal to approximately 0.20 and 0.44 inches. Figure 4.17 shows post-test photographs for the 4200, 6000, and 8000 psi tests. The team did not observe erosion on the tube for the 2,400 psi jetting pressure at both standoff distances. At the 10,400 psi pressure, tubes at both standoff distances were completely cut in half after a minute of water jetting.

The photographs on Figure 4.17 illustrate two lines of erosion due to the angled orientation of the nozzles on the water jet. The water jet was held stationary in the vertical direction during testing, and the jet nozzles cut narrow slits in the tubing, as shown on the figure. The tubes positioned about 0.20 inches from the water jet showed slightly more erosion at each jetting pressure when compared with the tubes positioned about 0.44 inches from the water jet. Higher jetting pressures allowed the water jet to cut deeper into the PVC tubes. The water jet cut only partially through the tube at 4,200 psi for both standoff distances. The water jet cut completely through the tube at the 6,000 and 8,000 psi jetting pressure for both standoff distances.

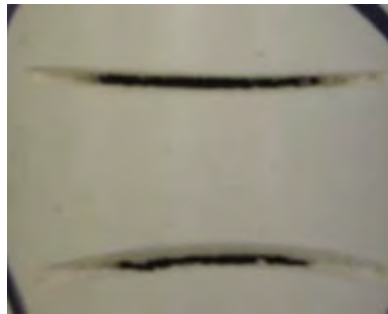
The results presented on Figure 4.17 show that PVC access tubes can be cut efficiently at jetting pressures less than 10,000 psi. In cases where a relatively weak deleterious material surrounds a PVC access tube, lower jetting pressures may be preferred when cutting and removing the tube during initial water jetting. A low jetting pressure (e.g. 6,000 psi) would cut the tube and have less of an impact on the surrounding deleterious material. A high jetting pressure (e.g. 10,000 psi) would certainly cut the tube; however, deleterious material surrounding the tube would also be eroded during this process. Erosion of weaker deleterious material would likely lead to a significant amount of cuttings, which could potentially clog the access tube and inhibit the removal of the PVC. The research team observed this situation during an initial series of ring tests (see Section 3.2.1).



(a) 4,200 psi at 0.20 inches



(b) 4,200 psi at 0.44 inches



(c) 6,000 psi at 0.20 inches



(d) 6,000 psi at 0.44 inches



(e) 8,000 psi at 0.20 inches



(f) 8,000 psi at 0.44 inches

Figure 4.17 - Front View Post-Test Photographs of PVC Tubing

4.4 SUMMARY OF WATER JETTING RESULTS

Average final effective eroded diameters are re-plotted on Figure 4.18 as a function of compressive strength. This figure is similar to Figure 4.8 except that data from the SCM-01, SCM-04, SCM-05, SMC-6, and CON-06 test series are now included. The new data from the reinforcing steel and cylindrical sample tests are specifically noted on the figure. These data are consistent with the ring test data originally presented on Figure 4.8. The results show that water jetting effectiveness is strongly influenced by material compressive strength.

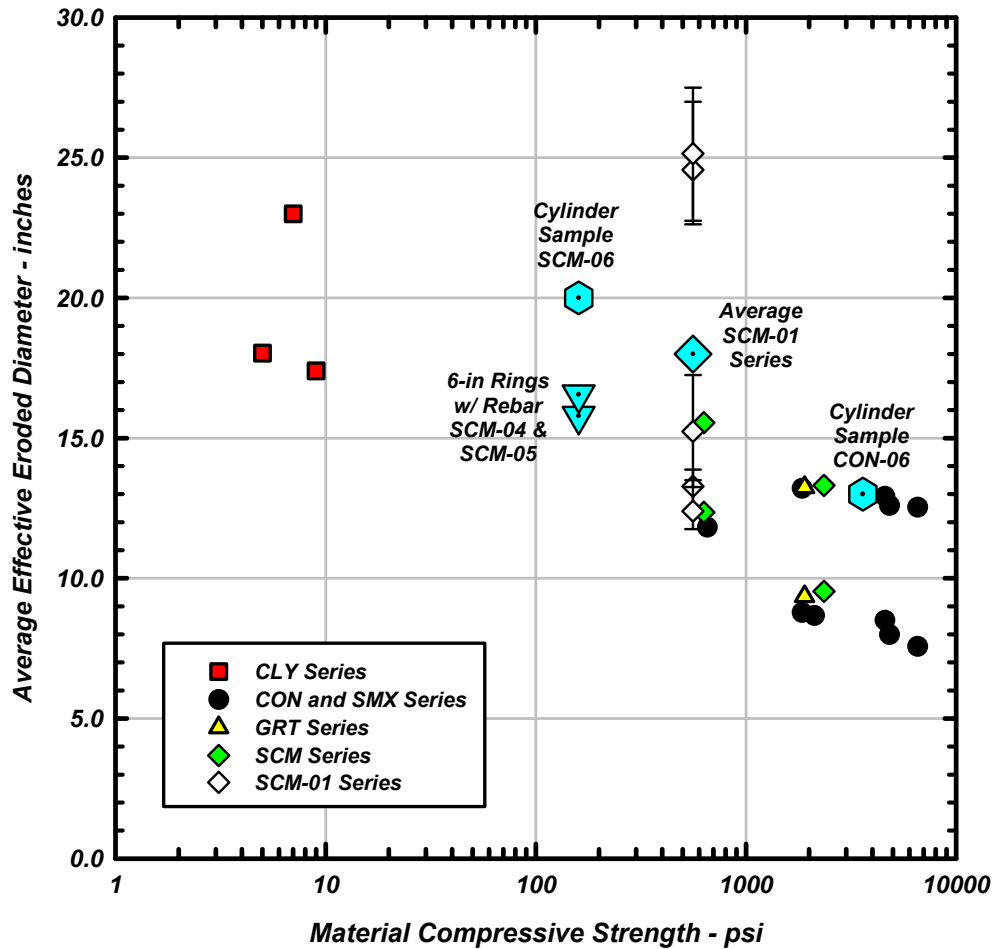


Figure 4.18 - Average Effective Eroded Diameter for all Material Samples

CHAPTER 5

SUMMARY AND RECOMMENDATIONS

5.1 SUMMARY

The primary objective of this research project was to establish an empirical relationship between water jetting pressure and the removal of deleterious materials from drilled shaft defects (e.g. low strength concrete, slurry mix concrete, semi-cemented sand, loose soil, etc.). The principal research activities conducted as part of this study included: (1) a search of the existing literature and interviews with foundation contractors to identify the current state of water jet technology; and (2) a parametric laboratory investigation to examine water jetting effectiveness in relation to jetting pressure, standoff distance, jetting time, and characteristics of deleterious materials.

The research team conducted the laboratory investigation by water jetting ring samples, ring samples cast with longitudinal and transverse reinforcing steel bars, and cylindrical samples. Materials tested as part of this investigation included concrete, low strength concrete, slurry mix concrete, sand-cement grout, and bentonite-cement grout. Compressive strengths for these materials ranged between 5 psi (bentonite-cement grout) and 6,600 pounds psi (concrete). The research team employed different water jetting techniques and jetting pressures during the laboratory investigation to study their influence on erosion levels and rates. Standoff distances were also varied to study the effect on erosion level. Reinforcing steel bars were cast in several of the test specimens to assess the degree to which these bars interfere with water jetting, erosion rates, and erosion levels.

Thirty (30) separate water jetting experiments were completed as part of the laboratory investigation. The results of these experiments were consistent with one another and generally repeatable. The results show that standoff distance, jetting pressure, and material compressive strength primarily influence erosion levels and rates during water jetting.

5.2 PRINCIPAL FINDINGS

Water jetting effectiveness was found to be controlled primarily by the compressive strength of the deleterious material, standoff distance, and jetting pressure. Aggregate characteristics of deleterious materials such as particle size and angularity did not noticeably influence water jetting effectiveness. These results were confirmed through two different types of water jetting experiments designed and conducted by the investigators.

The research team used three different approaches when water jetting the ring and cylindrical test samples. During separate experiments, the water jet was held stationary, cycled up and down, and moved slowly upward within (or adjacent to) the test specimens. In practice, a water jet is typically moved slowly upward within a drilled shaft during the repair of a defect. The research team found that the water jetting approach slightly affected the erosion rates measured during the experiments. However, overall erosion levels were found to be similar for similar compressive strength materials, regardless of the jetting approach utilized.

Using typical water jetting equipment and jetting pressures between 10,000 and 11,000 psi, the research team observed significant material erosion up to 13 inches from the axis of the water jet. Materials with the lowest compressive strengths exhibited the greatest tendency to erode. The erosion distances observed during the experiments are less than half the maximum design spacing for drilled shaft access tubes, as specified by Caltrans. This finding suggests that it may be difficult, if not impossible, to overlap water jetting influence areas between access tubes when using typical procedures and pressures to water jet deleterious materials. The inability to overlap water jetting influence areas for such cases would likely necessitate the coring of additional access holes from the top of the drilled shaft.

When examining jetted surfaces in the concrete samples, the research team observed that larger aggregates often created small shadow zones where jetting effectiveness was reduced and binder materials were less easily eroded. These shadow zones have been observed adjacent to reinforcing steel bars during water jetting of drilled shafts in the field. In specially designed experiments conducted as part of this study, shadow zones of deleterious material were observed behind reinforcing steel bars. Rebar were found to influence erosion levels and water jetting effectiveness by interfering with the jet path. The most pronounced shadow effects occurred behind bars with larger diameters and behind longitudinal-transverse bar arrangements with tight spacings. Shadow effects were more prominent the farther the rebar were positioned from the water jet. With the limited number of access tubes required for drilled shafts, it may be difficult in certain design configurations to adequately water jet shadow materials from behind reinforcing steel bars, unless additional access holes are cored from the top of the drilled shaft.

When water jetting weaker materials with compressive strengths less than approximately 1,000 psi, the potential exists to quickly generate significant cuttings, especially during the initial stages of water jetting. In the confined space of a PVC access tube, these cuttings can potentially clog the hole and the water jet, which can interfere with nozzle performance and cause a rotating water jet to seize. This phenomenon was observed numerous times during experiments completed as part of this study.

The clogging of a water jet can greatly reduce its efficiency and effectiveness. When relatively weak deleterious materials are encountered in drilled shafts, it may be advisable to initially water jet at lower pressures so that the materials are removed at a slower rate and the potential for clogging is reduced. As the materials are removed and the eroded cavity becomes larger, higher jetting pressures can be used to increase the effective jetting distance. Results from this study show that PVC access tubes can be effectively cut at jetting pressures between 4,000 and 6,000 psi. So, it is conceivable that a field jetting program could begin at lower jetting pressures (e.g. 5,000 psi) and eventually ramp to pressures typical of those used in practice (e.g. 10,000 psi or above).

Although not a focus of this investigation, the team discovered that removal of the PVC access tube can be one of the more difficult aspects of a water jetting operation. Removal of the access tube is especially difficult if the surrounding deleterious material is relatively weak. In such cases, cuttings (aggregates and cut binder material) can enter the access tube through incised sections of the PVC, potentially clogging the tube and restricting the rotation of the water jet swivel. Such an incident can prevent the efficient and complete removal of the PVC tube, which can delay water jetting operations. Once the PVC tube is removed, water jetting of the deleterious materials can commence under conditions similar to those modeled in the ring samples of this study. One would then expect to observe erosion levels similar to those measured during this investigation. However, cutting through and removing the PVC access tube represents a difficult first step.

5.3 RECOMMENDATIONS FOR ADDITIONAL RESEARCH

The outcomes of this research investigation suggest that further research is warranted in several different areas:

- Investigate water jetting effectiveness, erosion rates, and erosion levels for low and moderate compressive strength deleterious materials subject to water jetting pressures higher than those typically used in practice (i.e. 15,000 to 20,000 psi);
- Investigate water jetting effectiveness for single-nozzle, non-rotating water jets that can be controlled by hand and directed toward specific areas within a drilled shaft. Such a water jet may reduce the potential for clogging and may be more appropriate for repairing defects near the outer edges of drilled shafts;
- Investigate "staged" techniques for removing PVC access tubes and deleterious materials from drilled shafts whereby water jetting is initiated using lower pressures and eventually ramped to pressures of 10,000 psi or above;

- Investigate the development of a more efficient technique for removing PVC access tube sections from drilled shafts prior to the water jetting of deleterious materials; and
- Investigate improved methods for defining the size and shape of drilled shafts defects, evaluating the material characteristics and compressive strengths of deleterious materials found in drilled shaft defects, and evaluating (post-repair) the extent and quality of water jetting carried-out within a drilled shaft.

REFERENCES

- ADSC West Coast Chapter (2007). "Standard CIDH Pile Anomaly Mitigation Plans A and B." <http://www.dot.ca.gov/hq/esc/geotech/requests/adscstandardmitigationplan04302007.pdf>. Caltrans, Sacramento. File accessed on August 1, 2012.
- Atmatzidis, D., and F. Ferrin (1983). "Laboratory Investigation of Soil Cutting with a Water Jet." Proceedings, Second U.S. Water Jet Conference. Water Jet Technology Association, 121-135.
- Branagan, P., W. Vanderpool, H. Murvosh, and M. Klein (2000). "CSL Defines CIDH Defects: Coring Confirms Results." Proceedings, New Technological and Design Developments in Deep Foundations. Geotechnical Special Publication #100, ASCE, 110-124.
- Brown, D.A., J.P. Turner, and R.J. Castelli (2010). "Drilled Shafts: Construction Procedures and LRFD Design Methods." Geotechnical Engineering Circular No. 10, Publication FHWA NHI-10-016, Federal Highway Administration, Washington, D.C.
- Caltrans (2005). "California Test 233: Method of Ascertaining the Homogeneity of Concrete in Cast-in-Drilled Hole (CIDH) Piles using the Gamma-Gamma Test Method. Department of Transportation, Division of Engineering Services, November.
- Caltrans (2008). "Foundation Manual." Department of Transportation, Engineering Services, <http://www.dot.ca.gov/hq/esc/construction/manuals/OSCCompleteManuals/Foundation.pdf> Offices of Structure Construction, Sacramento. File accessed on August 1, 2012.
- Caltrans (2009). "Gamma-Gamma Logging and Crosshole Sonic Logging Test Results: West Sylmar OH (Widen)." Foundation Testing Branch Report, June, provided by J. Wahleithner.
- Caltrans (2010). "Standard Specifications." Department of Transportation, Sacramento, http://www.dot.ca.gov/hq/esc/oe/specifications/std_specs/2010_StdSpecs/2010_StdSpecs.pdf File accessed on August 1, 2012.
- Goodwin, J. (2007). "Hydro-Blasting Technique for Drilled Shaft Remediation." Foundation Drilling. International Association of Foundation Drilling (ADSC), November, 61-62.
- Heavin, J.C. (2010). "Influence of Material Type, Aggregate Size, and Unconfined Compressive Strength on Water Jetting of CIDH Pile Anomalies." M.S. Thesis, Civil Engineering, California Polytechnic State University, San Luis Obispo.
- Liebich, B.A. (2004). "Acceptance Testing of Drilled Shafts by Gamma-Gamma Logging." Proceedings., Geotechnical Engineering for Transportation Projects. Geotechnical Special Publication #126, ASCE, 1200-1208.
- Liebich, B.A. (2008). Personal communication, California Department of Transportation, Foundation Testing Branch, Sacramento, December.
- Liebich, B., and M. Bonala (2007). "Efficient Repair of Bridge Foundations, Phase I Study: Water Jetting of CIDH Pile Anomalies." Unpublished Research Problem Statement, Caltrans, Sacramento.

- Likins, G., F. Rausche, K. Webster, and A. Klesney (2007). "Defect Analysis for CSL Testing." Proceedings, Contemporary Issues in Deep Foundations, Geotechnical Special Publication #158, ASCE, 23-32.
- Mikkelsen, P. (2002). "Cement-Bentonite Grout Backfill for Borehole Instruments." Geotechnical News, December, 38-42.
- Momber, A. (2005). "Hydrodemolition of Concrete Surfaces and Reinforced Concrete." Elsevier, New York, NY.
- O'Neill, M., and L. Reese (1999). "Drilled Shafts: Construction Procedures and Design Methods." Publication FHWA-IF-99-025, Federal Highway Administration, Washington, D.C.
- O'Neill, M., and H. Sarhan (2004). "Structural Resistance Factors for Drilled Shafts Considering Construction Flaws." Proceedings, Current Practices and Future Trends in Deep Foundations, Geotechnical Special Publication #125, ASCE, 167-185.
- O'Neill, M. (2005). "Construction Practices and Defects in Drilled Shafts." Transportation Research Record: Journal of the Transportation Research Board, No. 1331, Transportation Research Board of the National Academies, Washington, D.C., 39-47.
- Rockwell, P. (1981). "Water Jet Trenching in Submerged Clays." Proceedings, First U.S. Water Jet Conference. Water Jet Technology Association, 195-206.
- Schaffer, M.J. (2011). "Influence of Nozzle Pressure, Standoff Distance, and Reinforcing Steel Cage on Water Jetting of CIDH Pile Anomalies." M.S. Thesis, Civil Engineering, California Polytechnic State University, San Luis Obispo.
- Skeen, S., and B. Liebich (2004). "Trabuco Creek: Drilled Shaft Defect Identification and Mitigation." Proceedings., Geotechnical Engineering for Transportation Projects. Geotechnical Special Publication #126, ASCE, 1248-1257.
- Sykes, A. (2009). Personal communication, Pacific Coast Drilling Company, Santa Rosa, California, November.
- Wahleithner, J. (2009). Personal communication, California Department of Transportation, Foundation Testing Branch, Sacramento, November.
- Wolgamott, J., and G. Zink (1999). "Self Rotating Nozzle Heads." Proceedings, Sixth American Water Jet Conference. Water Jet Technology Association, 603-612.
- Wright, D., J. Wolgamott, and G. Zink (1997). "A Study of Rotary Jets for Material Removal." Proceedings, Ninth American Water Jet Conference. Water Jet Technology Association.

APPENDIX A

DATA SHEET FOR SELF-ROTARY SWIVEL WATER JET

Gopher™ 22 kpsi Self-Rotary Swivel (GO-M9)

US Pat. No. 5,909,848 and 6,059,202
European Patent 1068021

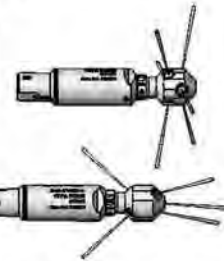
Description:

The **Gopher** is a self-rotating swivel designed for tube and pipe cleaning. It has an outside diameter of 1.62 inches (42mm). The tool can be used at operating pressures from 5,000 to 22,000 psi (345 to 1500 bar) and flow rates from 8 to 25 gpm. The tool has a 9/16 medium pressure cone and thread female inlet, and can be supplied with inlet adapter fittings for 1/2 or 3/8 npt female pipe thread. The swivel is filled with 10W-40 for lubrication; it also affects rotation speed. The swivel rotation can be slowed with a heavier oil such as 80W-90.

Two standard heads are available for the Gopher; both have 1/8 npt pipe threads. When installing nozzles, use Parker Thread Mate and Teflon tape for best results. The **Polisher Head (GO 042)** is intended for removing scale. The **Unplugging Head (GO 043)** is intended for use in plugged tubes. Stamped on the head is an R17 or R.14; this is the offset that makes the head rotate. If less flow is used than the range shown, the swivel will not rotate. If more flow is used than shown in the range, the tool will rotate too fast, damaging the bearings and using up the high pressure seal. Consult the table for the correct flow range for each head offset.

Offset	R17	R14	R08	R07
Flow (Polisher)	-	7 to 13 gpm	-	14 to 25 gpm
Flow (Unplugging)	8 to 14 gpm	-	15 to 25 gpm	-

The next step is to determine where the jets should go in the head. The thrust of the jets can be used to pull the tool thru a pipe or tube. Little or no pull is needed for cleaning vertically downward, but more pull is needed if cleaning horizontally or climbing upward. The jet sizes should be selected based on proportioning the total flow rate between the forward and backward jets to achieve the pulling force needed, but still applying enough power to the material being removed ahead of the tool.



**Polisher Head
GO 042**
3 jets @ 80°
3 jets @ 100°

**Unplugging Head
GO 043**
3 Forward Ports
2 Back Ports

Operation:

Make sure there is an operator controlled dump in the system, operated by the person closest to the cleaning job. Flush out the high pressure hoses before connecting Gopher to hose and or stinger. When pipe cleaning, it is recommended that the hose be marked a few feet from the end with a piece of tape so the operator knows when to stop on the way back out. When tube cleaning, a stinger is recommended; a stinger is a rigid piece of pipe or tubing used between the end of the hose and the nozzle. It is typically 2 feet in length, and is primarily a safety device for hand flex lancing. Install tool on hose, position it in a tube or the pipe while the pressure is being set. The high pressure seal may leak initially; it should stop when pressure is increased and rotation begins. Close the dump and slowly bring up to pressure the first time, to make sure no nozzles are plugged and that the jet thrust is correct. The swivel should begin to slowly rotate. Once operating pressure is reached, feed the tool into the tube or pipe to begin the cleaning job. When using rotating nozzles in plugged tubes, the head must not be forced into the deposit, as this will stop the rotation of the tool and impede the cutting ability. When the tool contacts the deposit, allow it to cut away the material and advance at its own rate. If it stops advancing, pull back slightly on the hose to pull the head slightly away from the deposit, in case it is being stopped from rotating by the deposit. This also allows the angled jets to attack the deposit at different places. When polishing tubes with scale, it is possible to allow the nozzle to pass through the tube at incredibly fast rates, unless the deposit is very easy to remove, this will not completely remove the scale. The operator needs to be trained to feed the nozzle through the tube at a rate sufficient to clean the tube. Once the work is complete and the tool is disconnected from the hose, blow out all water to prolong the life of the tool. A small amount of oil can be blown into the inlet nut as well.

Troubleshooting:

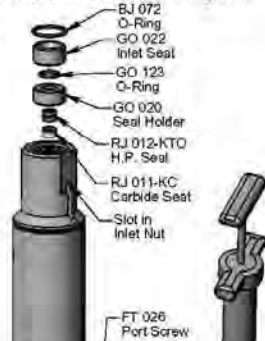
Head will not rotate: First by rotating head by hand and see if it feels rough or gritty to turn. If it does, the tool must be disassembled and repaired. If the tool has just been repaired and the head starts to rotate but slows down and stops as pressure is increased, the front bearing (RJ 007) is installed backwards. If the tool feels okay, check to see if any nozzles are plugged; even if a nozzle is only partially blocked it can keep the head from rotating. Nozzles must be removed from the head to properly clean them. Refer to the above description about the head offset and double check the nozzle sizes to make sure they are correct for the expected flow rate.
Head spins too fast: if the swivel is low on oil, or the oil has water in it. Add a full syringe of oil; check that the shaft seals are still good and will keep the fluid from leaking out. Finally, if it is rotating extremely fast and failing high pressure seals in a few minutes, the spring that controls the speed is broken or disconnected.
Seal Leak: The seal may leak initially up to several thousand psi, but should pop closed as pressure is increased. If operating pressure is reached and the seal is leaking continuously, the high pressure seal may need to be replaced. Refer to the maintenance below. If the seal and seat are replaced and the tool still leaks, inspect the shaft end face for damage such as dents, nicks or erosion.
Seals wear out quickly: The tool must be disassembled and inspected. The carbide seat should be checked for being installed in the right direction, and it should not have any chips or erosion marks on it. The seal holder (GO 020) should be replaced if it has any groove in the bore where the seal fits.

Maintenance: *Blow out all water with compressed air before storing tool!

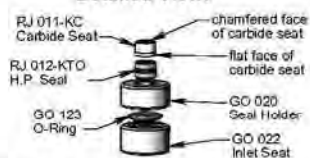
The Gopher uses 10W-40 Oil for lubrication. It is recommended that a full syringe of fresh oil be added to the swivel after every 20 to 40 hours of use. If faster rotation speed is desired, use oil with lower viscosity. If slower rotation speed is desired, use oil with higher viscosity.

To fill the Gopher with oil:

1. Fill the syringe (FT 110) with oil.
2. Remove the Port Screw (FT 026) and thread the syringe into the port.
3. Squeeze fresh oil into the swivel; excess will come out the slots.
4. Remove Syringe and install Port Screw. Make sure the Port Screw has the washer on it.

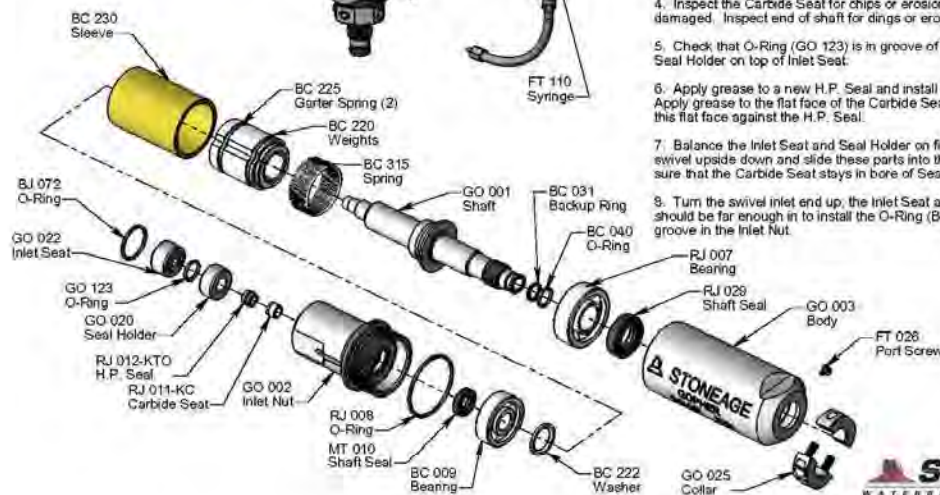


Detailed View:



To replace the high pressure seal:

1. Remove the O-Ring (BJ 072) from groove in Inlet Nut. It is easiest to push it inward from the top of the slot.
2. Use two picks inserted thru the slots to pry the Seal Holder (GO 020) and Inlet Seat (GO 022) up and out.
3. Remove the Carbide Seat (RJ 011-KC) and H.P. Seal (RJ 012-KTO). Inspect the Seal Holder for grooves. If it is badly grooved, it can be flipped over or replaced.
4. Inspect the Carbide Seat for chips or erosion. Replace if damaged. Inspect end of shaft for dings or erosion.
5. Check that O-Ring (GO 123) is in groove of Inlet Seat. Place Seal Holder on top of Inlet Seat.
6. Apply grease to a new H.P. Seal and install in Seal Holder. Apply grease to the flat face of the Carbide Seat and install with this flat face against the H.P. Seal.
7. Balance the Inlet Seat and Seal Holder on fingertip; turn swivel upside down and slide these parts into the Inlet Nut. Make sure that the Carbide Seat stays in bore of Seal Holder.
8. Turn the swivel inlet end up; the Inlet Seat and Seal Holder should be far enough in to install the O-Ring (BJ 072) into the groove in the Inlet Nut.



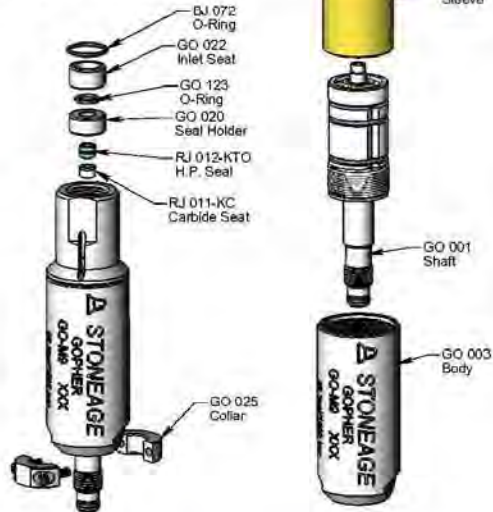
STONEAGE
WATERBLAST TOOLS
© 2009 StoneAge. All Rights Reserved

Gopher™ 22 kpsi Self-Rotary Swivel (GO-M9)

US Pat. No. 5,909,848 and 6,059,202
European Patent 1068021

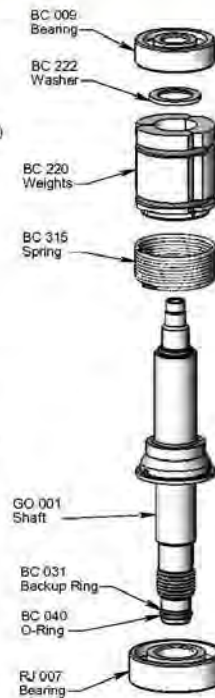
Disassembly:

1. Remove O-Ring (BJ 072) from Inlet Nut. Pry out the Seal Holder (GO 020) and Inlet Seat (GO 022) as explained in the Maintenance Section.
2. Remove the Collar (GO 025) from the Shaft.
3. Unscrew the Inlet Nut (GO 002) from the Body (GO 003).
4. Push Shaft (GO 001) and all attached parts up and out of Body.
5. Slide the Sleeve (BC 230) off of the Shaft.



6. If the Shaft Seals (MT 010, RJ 029) in the Inlet Nut and Body appear damaged, pry them out and replace them.
7. Pull the Bearing (BC 009) off of the top of the Shaft; remove the Washer (BC 222).

8. Unhook the Spring (BC 315) from the hole in the Shaft; remove the Weights (BC 220) and Spring (BC 315) from the Shaft. Leave the Weights together.
9. Inspect the O-Ring (BC 040) and Backup Ring (BC 031) on the Shaft end. Replace them if they are cut or damaged.

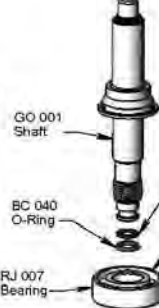


Assembly:

1. Install O-Ring (RJ 008) over the threads of the Inlet Nut (GO 002). Install Shaft Seal (MT 010) into the Inlet Nut; the lip with the spring faces down in this view.
2. Install Shaft Seal (RJ 029) into Body (GO 003); the lip with the spring faces up in this view. Apply grease or Armour-All to the lips of the seals.



3. Install Bearing (RJ 007) on Shaft (GO 001); this is a thrust bearing and must be installed with the wide inner race facing toward shoulder on Shaft.
4. If O-Ring and Backup Ring were removed, install new ones in the correct order.
5. Insert Spring (BC 315) and into hole in Weights (BC 220), then slide Weights and Spring onto Shaft and insert other spring end into hole in Shaft.



6. Place Washer (BC 222) on top of Weights, with the chamfered side facing toward the Weights.
7. Slide Bearing (BC 009) onto Shaft. Slide Sleeve (BC 230) over the assembly.
8. Carefully insert shaft assembly into the Body.
9. Thread Inlet Nut into Body; tighten to 40 ft-lb.



10. Install the Collar (GO 025) onto the Shaft end.
11. Install the high pressure seal components as described in the Maintenance Section.
12. Fill the swivel with oil as shown in the Maintenance Section. Install the Port Screw (FT 026).



STONEAGE
WATERBLAST TOOLS
© 2009 StoneAge. All Rights Reserved